

# Microbubble stability and applications in food

Tijs A.M. Rovers

## **Thesis committee**

### **Promotor**

Prof. Dr E. van der Linden

Professor of Physic and Physical Chemistry of Foods

Wageningen University

### **Co-promotors**

Dr M.B.J. Meinders

Senior Researcher

Wageningen UR, Food and Biobased Research

Dr G. Sala

Researcher

Wageningen UR, Food and Biobased Research

### **Other members**

Prof. Dr C.G.P.H. Schroen, Wageningen University

Prof. Dr M. Edirisinghe, University College London, United Kingdom

Prof. Dr M. Postema, University of Bergen, Norway

Dr R. Miller, Max Planck Institute of Colloids and Interfaces, Potsdam, Germany

This research was conducted under the auspices of the Graduate School VLAG  
(Advanced studies in Food Technology, Agrobiotechnology, Nutrition and Health  
Sciences)

# Microbubble stability and applications in food

Tijs A.M. Rovers

## **Thesis**

submitted in fulfilment of the requirements for the degree of doctor

at Wageningen University

by the authority of the Rector Magnificus

Prof. Dr A.P.J. Mol

in the presence of the

Thesis Committee appointed by the Academic Board

to be defended in public

on Friday 16 October 2015

at 1.30 p.m. in the Aula.

Tijs A.M. Rovers

Microbubble stability and applications in food

138 pages

PhD thesis, Wageningen University, Wageningen, NL (2015)

With references, with summary in English

ISBN 978-94-6257-475-5

## Table of content

Chapter 1	General Introduction	1
Chapter 2	Temperature is key to yield and stability of BSA stabilized microbubbles	15
Chapter 3	Disintegration of protein microbubbles in presence of acid and surfactants: a multi-step process	41
Chapter 4	Effect of temperature and pressure on the stability of protein microbubbles	63
Chapter 5	Effect of microbubbles on rheological, tribological and sensorial properties of model food systems	83
Chapter 6	General Discussion	105
	Summary	125
	Acknowledgements	131
	List of publications	135
	Curriculum vitae	136
	Overview of completed training activities	137



# Chapter 1:

## General Introduction

---

## Introduction

Aerated foods are often perceived as creamy, an attribute that most consumers prefer <sup>1-3</sup>. Therefore, air bubbles are seen as an appropriate ingredient to obtain a desirable mouthfeel <sup>2</sup>. However, traditional wet foams are not stable for a prolonged time. Microbubbles are micron-sized air bubbles that are stable for longer time than air bubbles in a foam. That is why food researchers have recently become interested in microbubbles as a promising new ingredient to replace fat, to create new textures, and to improve the sensorial properties of foods <sup>4-6</sup>. The use of food proteins as material to produce microbubbles and the application of such microbubbles in food is still a topic to be explored further. This topic is the subject of this thesis. The aim of this thesis was to investigate the key parameters for applications of microbubbles in food systems. In particular, this thesis describes the effect of preparation parameters on microbubble characteristics, the effect of food components and conditions on the microbubble stability, and the possibilities of using microbubbles in food systems. In this introductory chapter the relevant topics for this investigation are shortly introduced. First, we will introduce microbubbles, the formation of microbubbles, and the proteins we used to obtain microbubbles. Subsequently, we discuss the current status of the research on the interactions of the proteins within the shell, and the stability of microbubbles. Then we introduce the current knowledge on microbubble in foods. Finally, the aim and the outline of the thesis are given.

## Microbubbles

Microbubbles are gas bubbles covered with a shell that ensures a slowing down of disproportionation and preventing coalescence. Microbubbles are currently used, among others things, as delivery system of therapeutic components and as contrast agent for echo-imaging <sup>7-12</sup>. The shell can be made of lipids <sup>13, 14</sup>, phospholipids <sup>15-17</sup>, polymers <sup>18, 19</sup>, particles <sup>20, 21</sup>, proteins and combinations thereof <sup>22-26</sup>. Proteins that are used include hydrophobins <sup>6, 27, 28</sup>, egg white protein <sup>4, 5, 29</sup>, poly-glutamate <sup>30</sup>, lysozyme <sup>8, 31, 32</sup> and bovine serum albumin <sup>4, 5, 9, 12, 29, 33</sup>. Besides air <sup>8, 9, 12, 13, 23, 32</sup>, microbubbles that are used as contrast agents contain poorly water-soluble gasses



like perfluorocarbon, octafluoropropane, perfluorobutane and sulphur hexafluoride <sup>11, 26, 34, 35</sup>. A wide variety of methods to produce microbubbles is available, among which sonication, high shear mixing, template-layer-by-layer deposition and membrane emulsification are commonly used <sup>4, 10, 11, 36, 37</sup>. Several new technologies to produce microbubbles have been developed recently, among which microfluidic devices, coaxial electrohydrodynamic atomization and pressurized gyration <sup>33, 38-42</sup>. In thesis, we study air-filled microbubbles made from bovine serum albumin (BSA) and egg white protein (EWP), using sonication.

## Formation of microbubbles by sonication

Sonication is a method to produce microbubbles by using high intensity ultrasound that causes ultrasonic wave fronts <sup>7, 43</sup>. For our investigations, microbubbles were prepared by sonication with the tip of the ultrasound horn being placed at the air-liquid interface. Thus, air bubbles were introduced from the air in the head space above the solution. This has been visualized in Fig. 1.1.

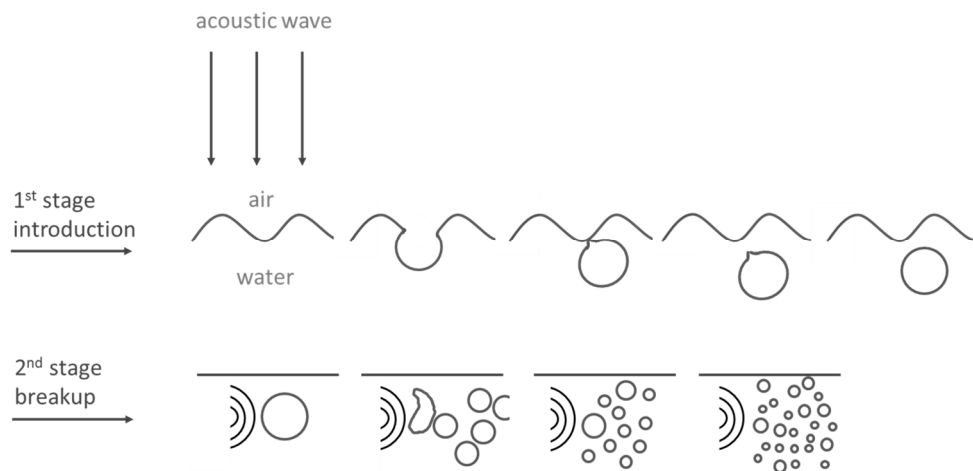


Fig 1.1 Schematic representation of the introduction and break-up of air bubbles, modified after Feshitan et al. <sup>34</sup>

After introduction of air from the headspace <sup>34</sup> (as shown in the top of Fig. 1.1), high intensity sound waves are applied to the liquid, which implies a high intensity oscillating pressure. This oscillating pressure causes the air bubble to

expand and compress<sup>7, 44</sup>. During these continuous cycles the bubbles grow a little bit more during expansion than they shrink during compression, until they reach a critical size<sup>44</sup>. Above this critical size the bubble violently collapses, resulting in a local increase in heat<sup>7, 34, 43, 44</sup>. The described phenomenon ends with the formation of multiple micron- sized gas bubbles in the liquid<sup>7, 34, 43, 44</sup> (shown in the lower part of Fig 1.1). It has been reported that the temperature and pressure inside the micron-sized air bubbles can be at very high<sup>7</sup>. Since the liquid is at much lower temperature and pressure, a transition zone exists at the interface. This transition zone may cause heat induced interactions among molecules near the bubble surface<sup>45</sup>. The nature of the interactions in the resulting microbubble shell has been subject of debate (see below in section “Interactions in the microbubble shell”) and this has been investigated in *Chapter 3* of this thesis. When the micron-sized air bubbles are sufficiently stabilised, they remain in the liquid, resulting in a microbubble dispersion. These stable microbubbles are all observed to be covered by a multi-layer of protein<sup>8, 45</sup>. Shells made from BSA have thicknesses of around 50 nm, corresponding to approximately 6 layers of BSA molecules<sup>45</sup>, while shells made from lysozyme have thicknesses of around 130 nm, corresponding to layers of 26 molecules thick<sup>8</sup>. The first layer of molecules is adsorbed at the air-water interface. During the expansion of the microbubble more proteins might adsorb to this protein layer, while during compression this layer is thickened<sup>8, 10, 44</sup>. Assuming the interactions in the shell are heat induced protein-protein interactions, the absorbed protein will interact with the protein layer as long as the temperature is high enough.

It has been reported that sonication parameters, like frequency, sonication power and sonication time, affect the microbubble characteristics<sup>8, 23, 32, 43</sup>. Higher ultrasound frequency results in microbubbles with a smaller average size and a more narrow size distribution<sup>43</sup>. The effect of sonication time on the microbubbles size is unclear, since some authors claim that the average size decreases with increasing sonication time<sup>8, 23</sup>, while others claim that the average size increases<sup>32</sup>. Furthermore, higher sonication time and sonication power were found to result in higher microbubble stability<sup>23</sup>. Regarding the yield, an optimum sonication time

and sonication power was found. At too low powers and times no microbubbles are formed, at too high powers only protein aggregates are formed, while microbubbles are formed within a narrow range of sonication powers and time <sup>32</sup>. Whereas most of these parameters influence the temperature of the microbubble solution we aim to have an insight on the effect of temperature of the solution on the formation of a microbubble. We initially kept all sonication parameters constant. Later on we changed the duty cycle, i.e. the fraction of the time that no ultrasound pulses are generated. When ultrasound is not applied continuously but is applied in pulses, a certain amount number of air bubbles can dissolve in the time between the pulses <sup>7, 46</sup>. Consequently, less air bubbles will be broken down and less heat is generated.

## **Proteins**

Bovine serum albumin (BSA) <sup>4, 6, 9, 10, 12, 23, 29, 33</sup> and egg white protein (EWP) <sup>4, 5, 29</sup> have been used extensively as shell material in microbubbles. Therefore in this thesis BSA and EWP are used for microbubble production. BSA accounts for approximately 10% of the protein in whey and it is the most abundant protein in bovine blood <sup>47-49</sup>. It is a globular protein, it consists of 583 amino acids and has a molecular weight of 66.4 kDa <sup>47, 48</sup>. It contains 17 disulphate bonds and 1 free cysteine group <sup>48, 49</sup>. The denaturation temperature is 63°C <sup>47, 50-52</sup>. The configuration of BSA depends on temperature and in pH <sup>53-55</sup>. The conformation changes at pH below the isoelectric point are more investigated than the changes above the isoelectric point. When lowering the pH to 4.3 the configuration changes from a compact native (N) configuration to a more elongated configuration (so-called fast (F) configuration) . The change into an even more extended (E) configuration occurs at a pH lower than 2.7 <sup>53-55</sup>. These configurations coincide with differences in surface activity. The equilibrium surface pressure and surface elasticity of the E configuration are lower than those of the F configuration, while the difference with that of the native configuration is even larger <sup>54, 55</sup>. These differences are ascribed to differences in surface coverage <sup>55</sup>. The above implies that changing the pH will affect the transient microbubble stability (i.e. during formation). It has been

reported that on liquid-solid interfaces BSA starts aggregating at lower temperatures compared to aggregation in bulk <sup>56</sup>. For other proteins, this lower aggregation temperature is also found at an air-water interface <sup>57</sup>. Although it has not been investigated, we assume that BSA starts aggregating at an air-water interface at lower temperatures compared to the temperatures for bulk aggregation. This may be an additional factor why BSA can aggregate at a specific temperature at the air-water interface (creating microbubbles) and not yet in the bulk at that specific temperature (creating protein aggregates)

Egg white is a mixture of about 40 different kinds of proteins. The major proteins are ovalbumin, ovotransferrin and ovomucoid, with protein concentrations of, respectively, 54%, 12% and 11% <sup>58</sup>. Some of the egg white proteins, like ovalbumin <sup>29</sup>, ovotransferrin <sup>29</sup>, lysozyme <sup>8, 32</sup> and streptavidin <sup>59</sup>, are used to make microbubbles.

## Interactions in the microbubble shell

During sonication proteins at the air bubble surface interact with each other, thereby forming a multi-layered protein shell <sup>8</sup>. The yield and stability of the microbubbles can be related to the nature and magnitude of the interactions. For example, covalent bonds are stronger than non-covalent interactions <sup>4,8</sup>. The nature of the interactions, and its role for the stability of the microbubbles, are subject to debate in literature. According to Suslick and coworkers <sup>9, 12</sup>, when bubbles collapse during sonication, the radicals  $\text{OH}\cdot$  and  $\text{H}\cdot$  are formed, which subsequently form  $\text{H}_2$ , peroxide and superoxide. The radicals, peroxide and superoxide were all found to be able to oxidize the cysteine residues of the BSA molecules, resulting in disulphide bond formation <sup>9,12</sup>. The creation of a disulphide bond through oxidation seems to be confirmed by the observation that no microcapsules could be produced when the sonication is applied under running nitrogen, argon or helium gas <sup>12</sup>. Furthermore, some authors specifically mention the use of cysteine-rich protein to form microbubbles <sup>4</sup>, while others deliberately made cysteine groups available in order to produce microbubbles <sup>8, 32</sup>. However, another study <sup>59</sup> shows that microbubbles also can be obtained with proteins that

have no cysteine residues and that microspheres can be obtained under argon. It was stated that hydrophobic or thermal denaturation of the protein is responsible for the formation and stability of microbubbles covered with these proteins<sup>59</sup>. For microspheres made with polyglutamate, it was mentioned that the interactions in the shell are non-covalent and could include hydrogen bonding, van der Waals, hydrophobic, and electrostatic interactions<sup>30</sup>. In the study in which cysteine groups deliberately were made available to produce microbubbles, it was claimed that initially hydrophobic interactions form a loose network that is further stabilized by disulphide crosslinking<sup>8</sup>. We aim to elucidate the nature of the interactions between the proteins in the microbubble shell for the proteins that we used.

## **Stability of microbubbles**

In order to obtain a better understanding of the underlying reasons for microbubble stability it is very important to obtain insights on the behaviour of microbubbles in different environments and at varying conditions. Furthermore, these insights will also provide a framework of the limits for the use of microbubbles in food systems.

To our knowledge, the effect on microbubble stability of specific components, that are representative of food components, has not been studied systematically. Some studies where microbubbles are added to food systems, hint on how a combination of ingredients can affect the microbubble stability. It has been described that microbubbles are stable for 2 months in an oil in water emulsion with the thickening agents iota-carrageenan and xanthan gum in the aqueous phase (where the oil droplets covered with the surfactant Tween 60)<sup>5</sup>. Microbubbles are reported to remain in the aqueous phase of a water-in-oil emulsion (having a 80% oil volume fraction)<sup>29</sup>. Addition of 1.5% (= 0.26 mol/l) salt to this water in oil emulsion did not affect the microbubbles<sup>29</sup>. Microbubbles that are prepared in a solution containing dextrose are reported to be stable up to one year<sup>23</sup>.

Besides the addition of food component, the microbubble stability might also be influenced by processes typical of the food industry, like heating and pressurizing, but also by variations of storage conditions like temperature. In studies it was

found that the yield decreased with increasing temperature, indicating a decrease in the microbubble stability <sup>29</sup>. In this study the yield of microbubbles was gauged in terms of the turbidity of the microbubble dispersion. The decrease in turbidity of dispersions of BSA coated microbubbles was 24% at 50°C and 85% at 75°C. For dispersions with whey protein coated microbubbles the decrease at those temperatures was 8% and 37%, respectively. In other words, in the reported study, microbubbles coated with whey protein are more stable against temperature increase than those covered with BSA <sup>29</sup>. Others report that BSA covered microbubbles stay intact and form a gel of microbubbles when subjected to a temperature of 121°C for 15 minutes <sup>4</sup>. Since the effect of heating on microbubble stability is so relevant for food industry processes, the effect of heating on the number of microbubbles was investigated in this thesis. This effect of temperature will also create a more fundamental understanding of microbubble stability.

With regard to effects of applied overpressure, it has been reported that human serum albumin covered microbubbles lost 40% of their original gas volume after 10 seconds at 1.37 bar overpressure <sup>60</sup> and that they lost their activity as contrast agent after 15 seconds at 0.25 bar overpressure <sup>61</sup>. Polyester covered microbubbles ruptured at overpressures around 1 bar <sup>62</sup>. The onset of instability as a result of pressure variations turned out to be mainly determined by the ratio between the shell thickness and the bubble radius ( $\frac{d}{R}$ ) and the Young's elastic modulus (E) of the microbubble shell <sup>62</sup>. Using a direct method to measure modulus by means of atomic force microscopy, it was found that the modulus was dependent on the material used for the shell. The reported values are around 0.6 MPa for lysozyme shells of air-filled microbubbles <sup>31</sup>, and 8- 40 MPa for phospholipid shells of fluorocarbon gas filled microbubbles <sup>15</sup>. The way how stability against air overpressure is dependent on the elastic modulus, bubble radius and shell thickness is a topic to be further investigated, together with ways to increase this stability. Part is addressed in this thesis.

With regard to storage temperatures, it has been reported that streptavidin covered microbubbles were stable for several hours when stored at room temperature, and for at least one month when stored at 4°C <sup>59</sup>. BSA stabilized microbubbles stored at

8°C showed a decrease in number after 14 days of storage <sup>4</sup>, while microbubbles with a shell composed of BSA and dextrose are reported to be stable for more than a year, when stored at 5°C <sup>23</sup>. These studies report microbubble stability at one or two storage times and at only one single storage temperature. A systematic study to the effect of various storage temperatures on the shelf life of protein stabilized microbubbles is missing in the literature. Such a study will give tools for the application with regard to storage conditions, and will give insight in the strength of the obtained interactions in the microbubble shell. This is also addressed in this thesis.

## **Applications of microbubbles in food**

It has been proposed that microbubble can be used in food systems. However, hardly any literature is available on incorporation of microbubbles in food systems. Since it has been proposed that aerated foods are considered creamy, a sensory attribute mostly related to oil containing products, Tcheunbou-Magaia et al. <sup>5</sup> investigated the microbubbles in combination with emulsion droplets. They mixed a microbubble dispersion with an oil-in-water emulsion and measured the friction force of the mixture and the pure emulsion. This showed that addition of microbubbles to an emulsion did not affect the lubricative properties of the emulsion <sup>5</sup>. As a next step, the effect of microbubbles as potential fat replacers should be investigated. This investigation should focus on the sensorial effect of microbubbles in food systems, which should be compared with the sensorial effect of emulsion droplets in food systems. Benjamins et al. <sup>29</sup> filed a patent in which microbubbles are incorporated in a water-in-oil emulsion. They claim that the microbubbles limit the degree of spattering when this water-in-oil emulsion is heated <sup>29</sup>. So far, this margarine-like product is the only food product in which the effect of microbubbles has been tested. In this thesis we aim to explore other food products to incorporate microbubbles.

## Aim and outline of the thesis

The aim of this thesis was to investigate the key parameters for applications of microbubbles in food systems. Therefore we investigated the effect of production parameters, the stability of microbubble under several conditions and the behaviour of food systems with incorporated microbubbles. In Fig 1.2 a schematic overview of the thesis is shown.

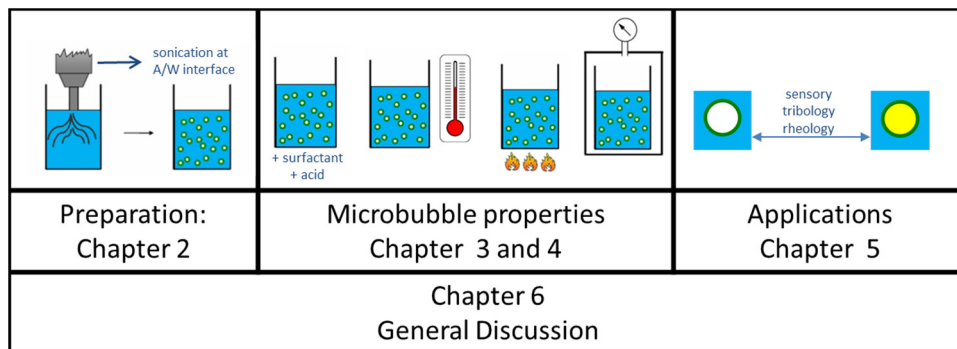


Fig. 1.2 Schematic overview of the thesis

In *Chapter 2*, we describe the effect of the microbubble preparation parameters on the microbubble characteristics, like the microbubble yield, size and stability

In *Chapter 3*, we investigated the microbubble stability upon addition of surfactants and acid, while in *Chapter 4* the stability of the microbubbles upon pressure or heating/cooling treatment and after storage is studied. In these chapters, we related the microbubble stability to microbubble properties, such as the interactions between protein within the microbubble shell, and the elastic modulus of the shell.

In *Chapter 5*, we investigated the effect of microbubbles on the rheological, tribological sensorial properties of model food systems. We compared this to the effect of emulsion droplets on the rheological, tribological sensorial properties.

Finally, in *Chapter 6*, the findings of this thesis are discussed and possible directions for future work are presented.



## References

1. D. Kilcast and S. Clegg, *Food Quality and Preference*, 2002, **13**, 609-623.
2. M. Minor, M. H. Vingerhoeds, F. D. Zoet, R. De Wijk and G. A. Van Aken, *International Journal of Food Science & Technology*, 2009, **44**, 735-747.
3. H. Wildmoser, J. Scheiwiller and E. J. Windhab, *LWT - Food Science and Technology*, 2004, **37**, 881-891.
4. F. L. Tchienbou-Magaia, N. Al-Rifai, N. E. M. Ishak, I. T. Norton and P. W. Cox, *Journal of Cellular Plastics*, 2011, **47**, 217-232.
5. F. L. Tchienbou-Magaia and P. W. Cox, *Journal of Texture Studies*, 2011, **42**, 185-196.
6. F. L. Tchienbou-Magaia, I. T. Norton and P. W. Cox, *Microbubbles with protein coats for healthy food air filled emulsions*, Royal Soc Chemistry, Cambridge, 2010.
7. M. Ashokkumar, *Ultrasonics Sonochemistry*, 2011, **18**, 864-872.
8. F. Cavalieri, M. Ashokkumar, F. Grieser and F. Caruso, *Langmuir*, 2008, **24**, 10078-10083.
9. M. W. Grinstaff and K. S. Suslick, *Proceedings of the National Academy of Sciences of the United States of America*, 1991, **88**, 7708-7710.
10. M. Lee, E. Y. Lee, D. Lee and B. J. Park, *Soft matter*, 2015, **11**, 2067-2079.
11. E. Stride and M. Edirisinghe, *Soft Matter*, 2008, **4**, 2350-2359.
12. K. S. Suslick, M. W. Grinstaff, K. J. Kolbeck and M. Wong, *Ultrasonics Sonochemistry*, 1994, **1**, S65-S68.
13. M. A. Borden and M. L. Longo, *Langmuir*, 2002, **18**, 9225-9233.
14. J. S. D'Arrigo and T. Imae, *Journal of Colloid and Interface Science*, 1992, **149**, 592-595.
15. E. Buchner Santos, J. K. Morris, E. Glynos, V. Sboros and V. Koutsos, *Langmuir : the ACS journal of surfaces and colloids*, 2012, **28**, 5753-5760.
16. M. J. Hasik, D. H. Kim, L. E. Howle, D. Needham and D. P. Prush, *Ultrasonics*, 2002, **40**, 973-982.
17. A. K. Thompson, J. P. Hindmarsh, D. Haisman, T. Rades and H. Singh, *Journal of Agricultural and Food Chemistry*, 2006, **54**, 3704-3711.
18. K. Bjerknes, P. C. Sontum, G. Smistad and I. Agerkvist, *International Journal of Pharmaceutics*, 1997, **158**, 129-136.
19. D. Lensen, E. C. Gelderblom, D. M. Vriezema, P. Marmottant, N. Verdonschot, M. Versluis, N. de Jong and J. C. M. van Hest, *Soft Matter*, 2011, **7**, 5417-5422.
20. D. Grigoriev, R. Miller, D. Shchukin and H. Mohwald, *Small*, 2007, **3**, 665-671.
21. G. Mohamedi, M. Azmin, I. Pastoriza-Santos, V. Huang, J. Pérez-Juste, L. M. Liz-Marzán, M. Edirisinghe and E. Stride, *Langmuir*, 2012, **28**, 13808-13815.
22. M. A. Borden, G. Pu, G. J. Runner and M. L. Longo, *Colloids and Surfaces B-Biointerfaces*, 2004, **35**, 209-223.
23. M. J. Borrelli, W. D. O'Brien, L. J. Bernock, H. R. Williams, E. Hamilton, J. N. Wu, M. L. Oelze and W. C. Culp, *Ultrasonics Sonochemistry*, 2012, **19**, 198-208.
24. M. M. Lozano and M. L. Longo, *Langmuir*, 2009, **25**, 3705-3712.
25. Y. Shen, R. L. Powell and M. L. Longo, *Journal of Colloid and Interface Science*, 2008, **321**, 186-194.

26. S. Sirsi, C. Pae, D. K. T. Oh, H. Blomback, A. Koubaa, B. Papahadjopoulos-Sternberg and M. Borden, *Soft Matter*, 2009, **5**, 4835-4842.
27. F. L. Tchuente-Magaia, I. T. Norton and P. W. Cox, *Food Hydrocolloids*, 2009, **23**, 1877-1885.
28. A. Watanabe, H. Larsson and A. C. Eliasson, *Cereal Chemistry*, 2002, **79**, 203-209.
29. J. Benjamins, A. Sein, and C. van Vliet *United States of America Pat.*, 2002, patent nr US2002/0155208.
30. E. M. Dibbern, F. J. J. Toublan and K. S. Suslick, *Journal of the American Chemical Society*, 2006, **128**, 6540-6541.
31. F. Cavalieri, J. P. Best, C. Perez, J. Tu, F. Caruso, T. J. Matula and M. Ashokkumar, *Acs Applied Materials & Interfaces*, 2013, **5**, 10920-10925.
32. M. F. Zhou, F. Cavalieri and M. Ashokkumar, *Soft Matter*, 2011, **7**, 623-630.
33. S. Mahalingam, M. B. J. Meinders and M. Edirisinghe, *Langmuir*, 2014, **30**, 6694-6703.
34. J. A. Feshitan, C. C. Chen, J. J. Kwan and M. A. Borden, *Journal of Colloid and Interface Science*, 2009, **329**, 316-324.
35. Z. W. Xing, H. T. Ke, J. R. Wang, B. Zhao, X. L. Yue, Z. F. Dai and J. B. Liu, *Acta Biomaterialia*, 2010, **6**, 3542-3549.
36. M. Kukizaki and M. Goto, *Journal of Membrane Science*, 2006, **281**, 386-396.
37. Q. Y. Xu, M. Nakajima, S. Ichikawa, N. Nakamura and T. Shiina, *Innovative Food Science & Emerging Technologies*, 2008, **9**, 489-494.
38. Z. Ekemen, Z. Ahmad, M. Edirisinghe and E. Stride, *Macromolecular Materials and Engineering*, 2011, **296**, 8-13.
39. M. Lee, E. Y. Lee, D. Lee and B. J. Park, *Soft Matter*, 2015, **11**, 2067-2079.
40. S. Mahalingam, B. T. Raimi-Abraham, D. Q. M. Craig and M. Edirisinghe, *Langmuir*, 2015, **31**, 659-666.
41. E. Stride and M. Edirisinghe, *Medical & Biological Engineering & Computing*, 2009, **47**, 883-892.
42. E. Talu, K. Hettiarachchi, R. L. Powell, A. P. Lee, P. A. Dayton and M. L. Longo, *Langmuir*, 2008, **24**, 1745-1749.
43. A. Brotchie, F. Grieser and M. Ashokkumar, *Physical Review Letters*, 2009, **102**.
44. T. Leong, M. Ashokkumar and S. Kentish, *Acoustics Australia*, 2011, **39**, 54-63.
45. D. G. Shchukin and H. Mohwald, *Physical Chemistry Chemical Physics*, 2006, **8**, 3496-3506.
46. J. Lee, M. Ashokkumar, S. Kentish and F. Grieser, *Journal of the American Chemical Society*, 2005, **127**, 16810-16811.
47. J. I. Boye, I. Alli and A. A. Ismail, *Journal of Agricultural and Food Chemistry*, 1996, **44**, 996-1004.
48. N. El Kadi, N. Taulier, J. Y. Le Huerou, M. Gindre, W. Urbach, I. Nwigwe, P. C. Kahn and M. Waks, *Biophysical Journal*, 2006, **91**, 3397-3404.
49. R. X. Su, W. Qi, Z. M. He, Y. B. Zhang and F. M. Jin, *Food Hydrocolloids*, 2008, **22**, 995-1005.
50. B. Jachimska, M. Wasilewska and Z. Adamczyk, *Langmuir*, 2008, **24**, 6866-6872.

51. P. L. San Biagio, V. Martorana, A. Emanuele, S. M. Vaiana, M. Manno, D. Bulone, M. B. Palma-Vittorelli and M. U. Palma, *Proteins-Structure Function and Genetics*, 1999, **37**, 116-120.
52. A. Tobitani and S. B. Ross-Murphy, *Macromolecules*, 1997, **30**, 4845-4854.
53. J. T. Foster, in *Albumin: Structure, Function and Uses*, eds. V. M. Rosenoer, M. Oratz and M. A. Rothschild, Pergamon Press, Oxford, 1977, pp. 53-84.
54. B. A. Noskov, A. A. Mikhailovskaya, S. Y. Lin, G. Loglio and R. Miller, *Langmuir*, 2010, **26**, 17225-17231.
55. L. G. C. Pereira, O. Theodoly, H. W. Blanch and C. J. Radke, *Langmuir*, 2003, **19**, 2349-2356.
56. R. J. Green, I. Hopkinson and R. A. L. Jones, *Langmuir*, 1999, **15**, 5102-5110.
57. S. A. Holt, M. J. Henderson and J. W. White, *Australian Journal of Chemistry*, 2002, **55**, 449-459.
58. H. Sugino, T. Nitodo and L. R. Juneja, in *Hen eggs: Basic and applied science*, eds. T. Yamamoto, L. R. Juneja, H. Hatta and M. Kim, CRC printing, Boca Raton, USA, 1997, pp. 13-24.
59. S. Avivi and A. Gedanken, *Biochemical Journal*, 2002, **366**, 705-707.
60. S. Podell, C. Burrascano, M. Gaal, B. Golec, J. Maniquis and P. Mehlhaff, *Biotechnology and Applied Biochemistry*, 1999, **30**, 213-223.
61. C. Vuille, M. Nidorf, R. L. Morrissey, J. B. Newell, A. E. Weyman and M. H. Picard, *Journal of the American Society of Echocardiography : official publication of the American Society of Echocardiography*, 1994, **7**, 347-354.
62. P. V. Chitnis, P. Lee, J. Mamou, J. S. Allen, M. Böhmer and J. A. Ketterling, *Journal of applied physics*, 2011, **109**, 084906.



## Chapter 2:

### Temperature is key to yield and stability of BSA stabilized microbubbles

---

The effect of preparation and storage parameters on the number, size and stability of microbubbles covered with bovine serum albumin (BSA) was investigated. A large number of microbubbles with a high stability was obtained at protein concentration of 7.5% or higher, at pH between 5 and 6, at an ionic strength of 1.0 M and at a preheating temperature of 55-60°C. Microbubbles stored at 4°C were more stable than those stored at room temperature. This was observed for a specific commercial BSA batch. We found that optimal preparation parameters strongly depend on the batch. Certain BSA batches were found not to lead to microbubbles at all. Microbubbles made with different protein concentration and preheating temperatures shrunk in time to a radius between 300 nm and 350 nm, after which the size remained constant during further storage. We argue that the constant final size can be explained by a thickening of the microbubble shell as a result of the microbubble shrinkage, thereby withstanding the Laplace pressure. The effects of protein concentration, pH and ionic strength on the number of microbubbles directly after sonication can be ascribed to the influence of these parameters on the adsorption speed and ability to cover the surface of air bubbles formed during sonication with enough protein to stabilize the bubble against coalescence and dissolution. We suggest that the effect of temperature during sonication on the formation of microbubbles can be related to thermally induced protein-protein interaction at the air-water interface.

This chapter is published as:

T.A.M. Rovers, G. Sala, E. van der Linden and M. B.J. Meinders (2016) Temperature is key to yield and stability of BSA stabilized microbubbles, *Food Hydrocolloids*, 52, 106-115

## Introduction

Microbubbles are commonly applied in clinical and diagnostic research <sup>1, 2</sup>. Recently, food researchers have become interested in microbubbles as a promising new ingredient for encapsulation, to replace fat, to create new textures, and to improve the sensorial properties of foods. <sup>3-5</sup>. Therefore, microbubbles might be important food hydrocolloids to allow the food industry to produce healthy and appealing foods. All existing definitions of a microbubble have in common that a microbubble is a small gas bubble covered by a shell of a specific material. Microbubbles have been produced with different methods, included gasses and shell materials. They vary in size, shell thickness and stability. Commonly used production methods include sonication, high shear emulsification and microfluidic systems <sup>6, 7</sup>. Commonly used materials are proteins, phospholipids and surfactants <sup>7</sup>.

For applications in food systems, protein covered microbubbles are claimed to be promising <sup>3, 4</sup>. Sonication is normally used for the production of these microbubbles <sup>3, 5, 8-10</sup>. In the cited studies the microbubble diameters ranged from 0.5  $\mu\text{m}$  to 10  $\mu\text{m}$ , the shell thickness varied between 20 nm and 130 nm and the number of the obtained microbubbles was in the order of  $10^9$  microbubbles (per ml).

In a review, several studies on the production of protein stabilized microbubble by sonication were summarized <sup>7</sup>. In general, sonication is claimed to occur via a two step process. Firstly, air is introduced in the liquid and broken down into bubbles, while proteins are adsorbed at the bubble surface. Secondly, under the influence of the sound waves, gas bubbles will oscillate in a repeated cycle of expansion and contraction. According to Ashokkumar <sup>11</sup>, these gas bubbles will grow up to a certain size and subsequently collapse, resulting, locally, in extremely high temperatures and pressures. This leads to modification of the protein and to protein crosslinking at the air-water interface <sup>7</sup>. The yield and stability of the microbubbles can be related to the interactions that are formed between BSA molecules at the microbubble surface during sonication <sup>3, 9</sup>. These interactions and their role for the stability of the microbubbles are actually subject of debate in literature. Suslick et al. <sup>2</sup> claimed that covalent disulfide bonds between the

cysteine residues of BSA molecules are responsible for the interactions in the shell. However, another study <sup>12</sup> showed that microbubbles can also be obtained with proteins that have no cysteine residues implying that hydrophobic interactions are responsible for the formation and stability of microbubbles covered with these proteins. More recently, microbubbles were formed from lysozyme with additional available thiol groups. For microbubbles prepared with this protein, it is claimed that initially hydrophobic interactions form a loose network that is further stabilized by disulphide crosslinking <sup>9</sup>.

The microbubble characteristics (number, size and stability) can be influenced by several parameters. The initial protein concentration, the pH and ionic strength of the solution, the preheating temperature, the sonication time, sonication intensity and the storage temperature are claimed to play a role <sup>3, 5, 8-10</sup>.

Tchuenbou-Magaia et al.<sup>3</sup> reported that an increase in protein concentration from 0.5% (w/v) to 5.0% (w/v) resulted in an increase in microbubble yield and stability after 14 days. According to Borrelli et al. <sup>8</sup>, the protein concentration influences the size of the microbubble, with a constant diameter for concentrations between the 3% and 10% and a larger diameter at higher protein concentrations (without specification of the sizes obtained under these conditions). Furthermore, Borrelli et al. <sup>8</sup> claimed that an increase in protein concentration results in higher storage stability. According to Tchuenbou-Magaia et al. <sup>3</sup>, the highest number of microbubbles, when using BSA as shell material, can be obtained at pH 5. Benjamins et al. <sup>13</sup> reported that with this protein the highest number of microbubbles is obtained at pH 3. However, the stability of these microbubbles was very low <sup>13</sup>. In literature the effect of preheating and ionic strength on microbubble yield and stability is only marginally described. Avivi & Gedanken <sup>12</sup> found that at room temperature the microbubbles were stable for several hours, while at 4°C the microbubbles were stable for at least one month. Tchuenbou-Magaia et al. <sup>3</sup> showed micrographs of microbubble dispersions that were stored at 8°C for 2 days and for 14 days. In these micrographs, it can be seen that in time the number of microbubbles decreased. Borrelli et al. <sup>8</sup> showed that also the size of microbubbles decreased in time, when stored at 5°C.

The above mentioned studies give an insight on the effect of preparation parameters on either the number of microbubbles or their stability. In this study we aim to describe the effect of preparation and storage conditions on both the characteristics directly after sonication (number and size of microbubbles) and the stability of the microbubbles. Furthermore, we aim to explain these effects in relation to a comprehensive description of the different processes during sonication. The number of obtained microbubbles, their size and their stability in time were studied as function of protein concentration, pH, ionic strength, preheating temperature and storage temperature. It was tested if microbubbles could be formed using BSA from different commercial batches. Furthermore, we studied the shell morphology and estimated the shell thickness using electron microscopy. Finally, the ability to freeze-dry BSA covered microbubbles and redisperse the obtained powder was tested. Based on our findings, relevant mechanisms that play a role in forming and stabilizing microbubbles are discussed.

## **Materials and methods**

### **Materials**

Bovine serum albumin (BSA, Fraction V, lot nr: 100M1900V), sodium hydroxide (NaOH), hydrochloric acid (HCl) and sodium chloride (NaCl) were purchased from Sigma-Aldrich (St Louis, MO, USA). For all experiments, demineralized water was used. To study the effect of different protein batches, we also performed some experiments using other batches of BSA from Sigma-Aldrich (St Louis, MO, USA): SLBB6871V, 061M1804V, SLBC8307V, 110M1310V, SLBB2450V, SLBF0550V, 100M1779V.

### **Preparation of microbubbles with different preparation parameters**

BSA was dissolved in demineralized water at different BSA concentrations, 2.5%, 5.0, 7.5% and 10% (w/w), and the solutions were stirred for at least 2 hours. Subsequently, the pH was set (between pH 3.0 and pH 9.0) by addition of hydrochloric acid (2 M HCl and 0.2 M HCl, for pH from 7.0 till 3.0) or sodium



hydroxide (2 M NaOH and 0.2 M NaOH for pH 8 and 9). The ionic strength was set to 0.05 M, 0.20 M and 1.00 M, using NaCl. The solutions were subdivided in portions of 25 ml, which were transferred into 50 ml beakers. The solutions were preheated for 10 minutes in a water bath. The preheating temperatures were set to 40°C, 50°C, 55°C, 60°C and 70°C. The samples were sonicated for 3 minutes at power level 8 and duty cycle 30%, using a Branson 450 sonicator (Branson Ultrasonics Corporation, Danbury, CT, USA). The sonicator was equipped with a 20 kHz, 12.7 mm probe, which was placed just below the air-water interface of the BSA solution. When a certain preparation parameter was varied, the others were kept constant, being 5% BSA, pH 6, ionic strength 0.05 M and a preheating temperature of 55°C. After preparation, the microbubble dispersions were transferred into closed glass vials and stored at 4°C and at room temperature (20°C-25°C).

### **Determination of number and size of microbubbles**

For each microbubble dispersion, 8 images were taken using a microscope (Axioskop, Carl Zeiss AG, Oberkochen, Germany) equipped with a camera (Axiocam HRc, Carl Zeiss AG, Oberkochen, Germany). The number of microbubbles was estimated by image analysis using ImageJ (1.44n, National Institutes of Health, Bethesda, MD, USA). The grid of an Improved Neubauer counting chamber (Paul Marienfeld GmbH & Co. KG, Lauda-Königshofen, Germany) was used to calibrate the scale. Using this scale, the dimension of the visual volume was determined to be  $3.52 \cdot 10^{-7}$  ml.

The size distribution of the microbubbles was determined by dynamic light scattering, using a ZetaNanosizer (Malvern Instruments Ltd, Malvern, United Kingdom).

### **Washing and freeze-drying of the samples**

After preparation, the microbubble dispersion was dialysed to remove most of the protein in solution using a porous dialysis membrane with a pore size of 100 kDa (Spectrum Laboratories, Inc., Rancho Dominguez, CA, USA). The membrane tubes

were filled with the microbubble dispersion and placed in a bucket with demineralised water, which was put in a cold room (4°C) and stirred slowly with a magnetic stirrer. After 3 hours the water was refreshed. This procedure was repeated 5 times.

Subsequently, the dialysed microbubble dispersion was freeze-dried using a Christ 1-4 LD Plus freeze-drier (Martin Christ Gefriertrocknungsanlagen GmbH, Osterode am Harz, Germany) for 1.5 days at a temperature of - 55°C and a pressure of 0.080 mbar.

### **Scanning Electron Microscope observations**

Scanning Electron Microscopy (SEM) was used to observe the morphology of the microbubble and to estimate the thickness of the shell. SEM images were made of both freeze-dried microbubbles and microbubbles in dispersion.

The freeze-dried microbubbles were glued onto silver tape that was placed on an aluminium holder with conductive carbon tape. Then the sample was placed under vacuum to dry. The microbubbles in dispersion were allowed to adhere on the surface of poly-lysine coated glass and were subsequently submerged in glutaraldehyde to increase fixation to the glass. Thereafter, the samples were put in acetone and air-dried. All the samples were sputtered with platinum or iridium to form a layer of approximately 10 nm. The samples were examined with an FEI Maggala 400 (Hillsboro, OR, USA) electron microscope at room temperature, operating at 2 kHz. Some samples were sanded before sputtering using sandpaper in order to break some microbubbles, enabling the determination of the shell thickness of the microbubbles.

## **Results and discussion**

### **Production and characterization of microbubbles**

We investigated the possibility of manufacturing microbubbles from different batches of BSA. Using the following conditions: 5% BSA, pH 6, ionic strength 0.05 M, preheating to 55°C, sonication power level 8, duty cycle 30% and sonication

time 3 minutes, best results were obtained for one specific batch of BSA (batch number 100M1900V). With these settings no microbubbles could be formed using other batches, purchased from the same supplier. When the duty cycle of sonication was increased from 30% to 90%, microbubbles could also be formed with the other investigated BSA batches. However, a detrimental side effect of the increased duty cycle was the formation of a large amount of protein aggregates. In the rest of this paper we will discuss the effects of microbubbles, made from BSA batch 100M1900V, using a 30% duty cycle, which only contained microbubbles and no protein aggregates. Furthermore, we attempted the use of air and nitrogen sparging. Since this led to enormous volumes of foam and hardly any microbubbles, the use of sparging was cancelled.

The morphology and shell thickness of the microbubbles were determined using SEM. We analysed microbubbles before as well as after freeze-drying. Before placing the sample in the SEM apparatus, some of the freeze-dried microbubbles were broken by the use of sandpaper. In Fig. 2.1 typical SEM pictures of intact and broken microbubbles are shown.

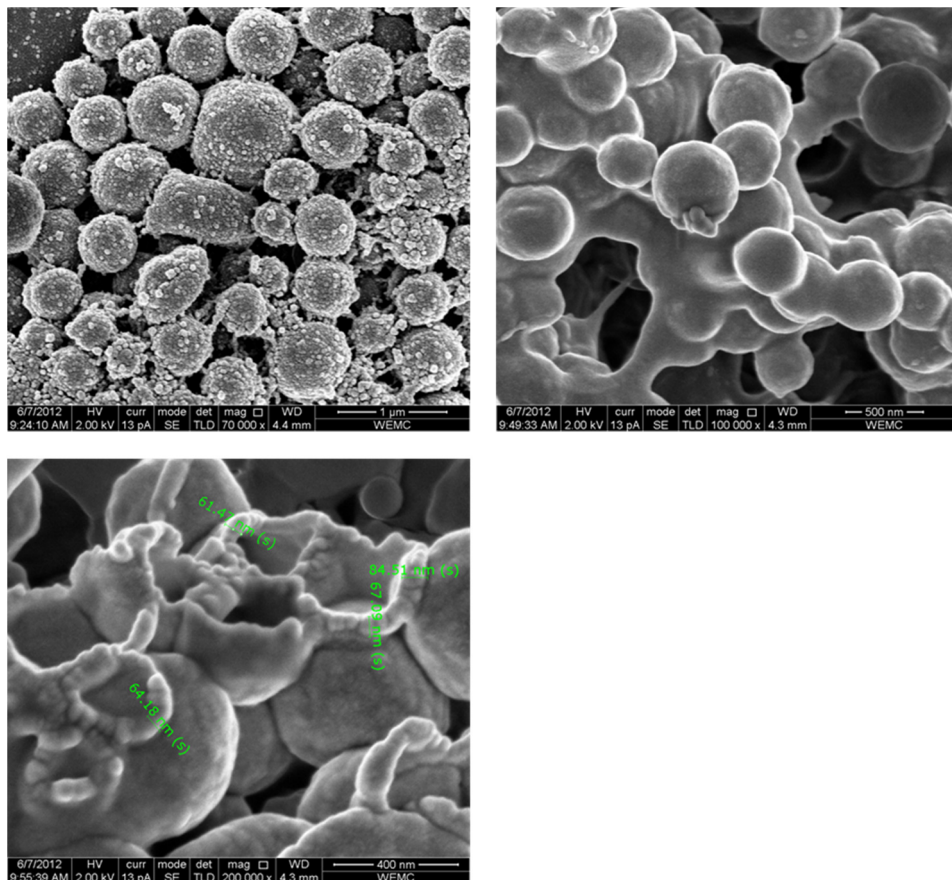


Fig.2.1. SEM pictures of microbubbles made with 5% BSA at pH 4: microbubbles before freeze-drying (top left), intact freeze-dried microbubbles (top right), and broken freeze-dried microbubbles with indicated shell thicknesses (bottom left). The numbers on the picture at the bottom left indicate the shell thickness

The morphology of the microbubbles before freeze-drying was different from that of the freeze-dried microbubbles. Before freeze-drying the microbubbles had a much rougher surface. Furthermore, the SEM pictures of the microbubbles before freeze-drying show all separate bubbles, while the freeze-dried microbubbles seemed to be aggregated. The smoother appearance can be explained by the deposition of BSA molecules, present in the water phase of the dispersion, on the surface of the microbubbles. This results in a homogeneous layer, which covers the

irregularities on the surface of the microbubbles. Furthermore, the deposition of protein on the bubbles forms the connections between neighbouring microbubbles. Freeze-dried microbubbles could be redispersed in water. In comparison with freshly prepared microbubbles, the redispersed microbubbles had the same morphology and the same size. Furthermore, like the microbubbles before freeze-drying, they creamed, indicating that they still contained air. All shells appeared to have a thickness of 40 to 70 nm. The shell thickness is comparable to that described by other authors<sup>10</sup>, and represents a layer of around 6 BSA molecules thick<sup>9,14</sup>. The creation of this multilayer shell was attributed to thermally induced crosslinking of the BSA molecules at the air-water interface, thereby forming a network of interacting proteins. The nature of this interactions are further discussed in *Chapter 3*.

SEM micrographs of microbubbles made from BSA solutions at pH 4, 6 and 8, and with BSA concentrations of 5% and 10% showed similar morphology and shell thickness.

### **Effect of storage temperature on the stability of microbubbles**

All samples were stored at 4°C and at room temperature. Regardless of the preparation parameters, it was seen that the microbubbles stored at room temperature were less stable than those stored at 4°C. In Fig. 2.2 micrographs are shown of dispersions stored for 43 days at 4°C and for 36 days at room temperature. In Fig. 2.3 the relative number of microbubbles (compared to day 0) is shown for microbubbles that were stored at 4°C and at room temperature.

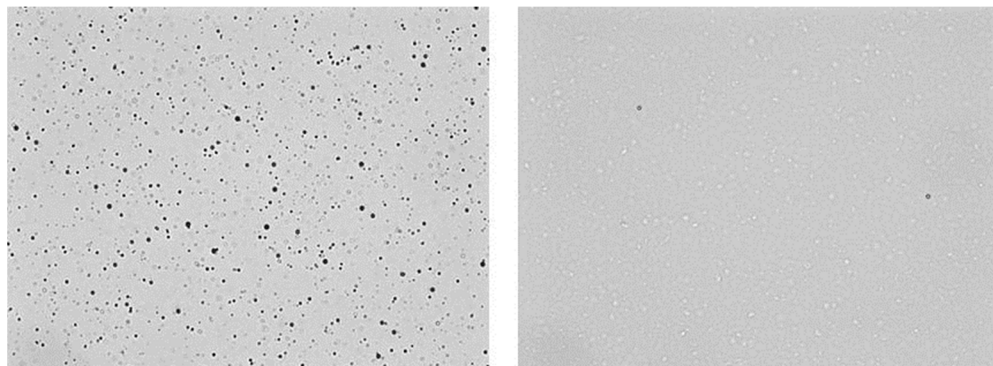


Fig. 2.2. Micrographs of microbubbles (5% BSA, pH 6, ionic strength 0.05 M and preheating temperature of 55°C), stored at 4°C after 43 days (left) and stored at room temperature after 36 days (right). The black spots correspond to the microbubbles, the white spots (mainly seen on the right frame) correspond to the remainders of the shells after air has left the microbubble.

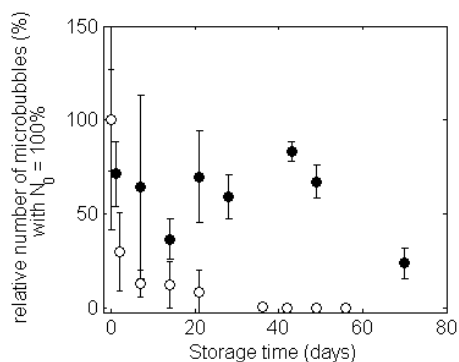


Fig. 2.3. Relative number of microbubbles, compared to the number of microbubbles at day 0, stored at 4°C (closed symbols) and room temperature (open symbols)

As can be seen in Fig. 2.2 and 2.3, the number of microbubbles that disappeared in time from the dispersion stored at 4°C is clearly smaller than the number that disappeared in the dispersion stored at room temperature. This finding is comparable to that of Avivi & Gedanken<sup>12</sup>, who showed that streptavidin covered microspheres stored at room temperature were less stable than those stored at 4°C. In the rest of this manuscript, when the stability of microbubbles will be discussed

as function of one of the preparation parameters, the reported stability will refer to the stability of microbubbles stored at 4°C.

The temperature dependency of the stability of the microbubbles can be explained by the fact that with increasing temperature the rigidity of the gels is decreases due to relaxation or creep. This temperature dependency of protein gels is further supported by studies that reported for whey protein gels a lower elastic modulus, a lower viscosity <sup>15</sup> and lower tangent  $\delta$  <sup>16</sup> with increasing temperature.

### Effect of BSA concentration on formation and stability of microbubbles

We investigated the effect of protein concentration in a range from 2.5% to 10% (wt/wt) on the initial number and initial size of produced microbubbles (Fig. 2.4).

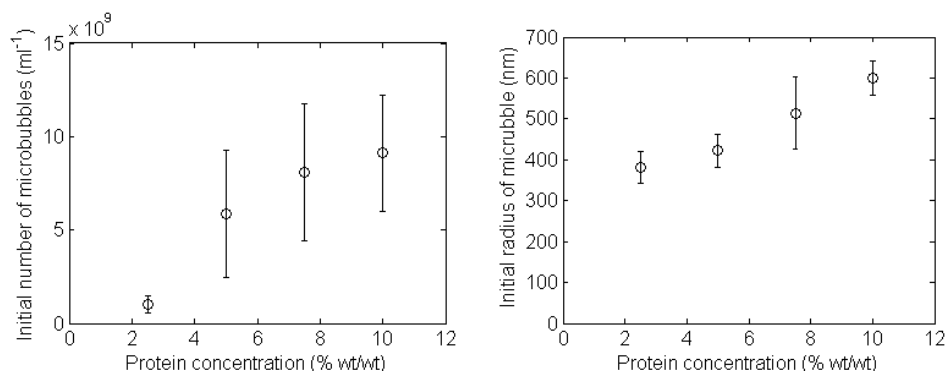


Fig. 2.4. Number (per ml) of microbubbles (left) and size of microbubbles (right) immediately after preparation as a function of the BSA concentration.

It can be seen that with increasing protein concentration the number of microbubbles increased. Above 7.5% BSA the effect of a further increase in BSA concentration seems marginal. Tchuenbou-Magaia et al. <sup>3</sup> also found a relative small difference in the number of obtained microbubbles with additional amount of protein above a certain protein concentration. For Tchuenbou-Magaia et al. <sup>3</sup>, this concentration was 3%, which is significantly lower than what was found in our study. As can be seen in Fig. 2.4, the maximum number of microbubbles produced

per millilitre was around 10 billion, which is an order of magnitude higher than described in studies of Tchuenbou-Magaia et al.<sup>3</sup> and Borrelli et al.<sup>8</sup>.

The effect of protein concentration on the initial average size of the microbubbles is shown in the right part of Fig. 2.4. A higher protein concentration led to the formation of larger microbubbles. Comparably, a study on BSA/dextrose microbubbles<sup>8</sup> found that an increase from 5% to 15% in BSA concentration led to an increase in microbubble size from 1.3  $\mu\text{m}$  to 1.6  $\mu\text{m}$ .

From the number of obtained microbubbles, their average radius and shell thickness, an estimation was made of the ratio between the protein in the microbubbles and the protein still in solution. This yielded that only less than 5% of the protein in the initial the solution was present in the shell. Furthermore, it turned out that microbubbles still could be made with the protein solution obtained after removal of microbubbles from a sonicated dispersion. This is in line with an earlier study<sup>13</sup>. Also the volume fraction of gas was estimated, which turned out to be maximally 1%.

As mentioned in the introduction, in the first stage of sonication protein is adsorbed at the air-water interface. The relation between protein concentration and surface properties of the sonicated solutions could affect protein adsorption of protein at the air-water interface, and, consequently, the microbubble yield. It has been reported that coalescence can be largely prevented when the surface coverage (the amount of protein at the interface) has reached a critical value which is 50% for beta-lactoglobulin<sup>17</sup>. The flux of proteins to the interface is proportional to protein concentration. Therefore, the probability to cover the surface to such an extent that coalescence is prevented is proportional to the protein concentration. This implies also that the number of microbubbles is proportional to the protein concentration. In the rest of the manuscript, we will refer to these air bubbles as 'sufficiently covered bubbles'.

To study the effect of the protein concentration on stability, the number of microbubbles was determined once a week for the first seven weeks, and once more ten weeks after preparation for every sample. Visual observation showed that during the first seven weeks the number of microbubbles was rather stable



and no microbubble shell debris was observed. After ten weeks a clear decrease in the number of microbubbles was observed.

In Fig. 2.5 the effect of protein concentration on the size of microbubbles in time is shown.

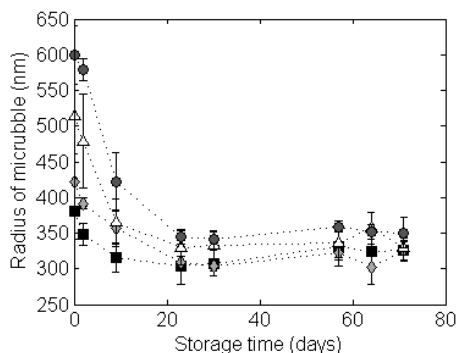


Fig. 2.5. Average radius of microbubbles as a function of storage time for different BSA concentrations of the sonicated solutions: 2.5% (squares), 5.0% (diamonds), 7.5% (triangles) and 10% (circles).

The microbubbles shrunk within 23 days to a radius of about 320-350 nm, with the highest final radius for the microbubbles that also had the highest initial radius. Thereafter, the size remained more or less constant. The microbubbles with larger initial size shrunk relatively more. Likewise, Borrelli et al. <sup>8</sup> reported that the size of small microbubbles (< 1  $\mu\text{m}$  diameter) hardly changed in time, while larger microbubbles (2  $\mu\text{m}$  to 3  $\mu\text{m}$ ) decreased in size.

A probable driving force for the reduction of the size of microbubbles is the Laplace pressure, resulting in a flux of air from the bubbles into the solution, in equilibrium with the headspace of the dispersion. Shrinkage of microbubbles as a result of Laplace overpressure in the bubbles has been reported before for lipid covered microbubbles <sup>18</sup>. When air is diffusing out, stress is build up in the bubble surrounding shell. When the shell behaves purely elastically and does not show relaxation or creep, disproportionation can be stopped <sup>19</sup>. One finds as stability condition that  $E_B > \frac{3}{2} \frac{\sigma R}{d^2}$ , in which  $E_B$  is the bulk modulus of the shell material,  $R$  is the bubble radius,  $\sigma$  is the interfacial tension of the interface between air and the

solution, and  $d$  is the layer thickness <sup>19</sup>. In our case the surface tension is about 50 mNm<sup>-1</sup>, the microbubble final radius 350 nm and the layer 50 nm. This would imply that the modulus should be at least  $1.05 \cdot 10^7$  N/m<sup>2</sup>. According to a study of Hagiwara et al. <sup>20</sup>, the bulk modulus of BSA gels as a function of the BSA concentration can be approximated by  $E_B = (c_{BSA})^{4.28}$  (in  $10^5$  N/m<sup>2</sup>) in which  $c_{BSA}$  is the BSA concentration in  $10^2$  kg/m<sup>3</sup>. Consequently, we find that microbubbles are stabilized when the gelled microbubble layer has a BSA concentration of at least 300 kg/m<sup>3</sup>, corresponding to a packing density of 22% ( $\rho_{BSA} = 1360$  kg/m<sup>3</sup>). Furthermore, Borrelli et al. <sup>8</sup> suggested that during shrinking of the microbubble the microbubble shell would become thicker. Assuming that the microbubble upon shrinking would not lose shell material, the layer thickens with a factor  $\frac{R_0^2}{R_{end}^2}$  (with  $R_0$  being the radius at  $t=0$  and  $R_{end}$  the radius after 23 days), resulting in a factor ranging from 1.57 for the 2.5% BSA sample to 3.02 for the 10% BSA sample. This would mean that microbubbles can be stabilized if the microbubble layer has a BSA concentration as low as 240 kg/m<sup>3</sup> (packing density = 18%) for the sample with 2.5% initial BSA concentration and 180 kg/m<sup>3</sup> (packing density = 13%) for the 10% BSA sample.

### **Effect of pH and ionic strength on formation and stability of microbubbles**

In an earlier research Tchuénbou-Magaia et al. <sup>3</sup> found that pH had a major influence on the number of produced microbubbles. They showed that highest number of microbubbles could be formed at pH around the isoelectric point. Furthermore, they claimed that at pH 7 microbubbles could be formed at an ionic strength of 0.01 M, but could not be formed at an ionic strength of 0.2 M. Both pH and ionic strength seem to play an important role in the formation and stability of microbubbles. In our research we investigated the effect of pH on the number of obtained microbubbles (Fig. 2.6) and on microbubble stability (Fig. 2.7) in a wide range of ionic strength.

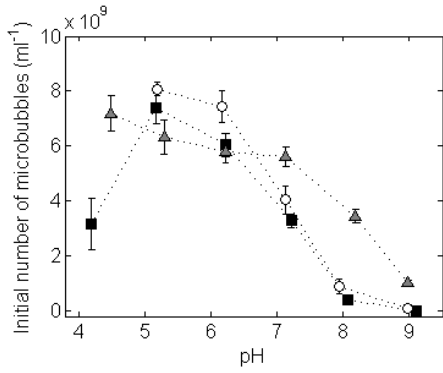


Fig. 2.6. Number of microbubbles immediately after preparation as a function of pH of the BSA solution for different ionic strengths: 0.05M (squares), 0.2M (circles) and 1M (triangles).

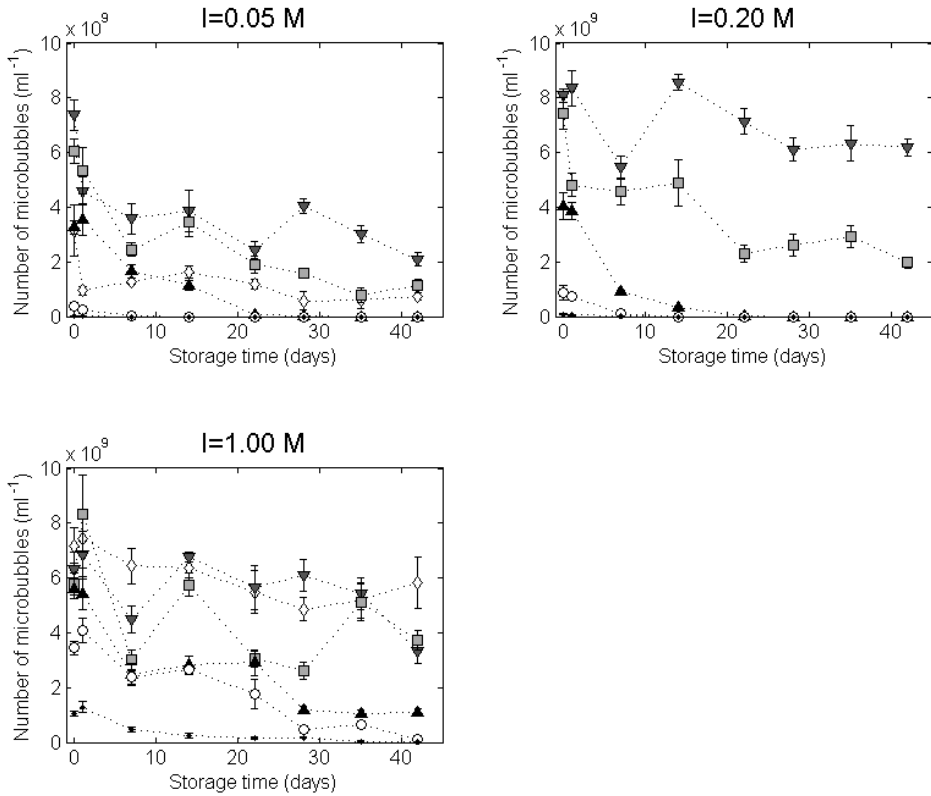


Fig. 2.7. Number of microbubbles as a function of storage time for different ionic strengths and different pH values: pH 4 (diamonds), pH 5 (downward triangles), pH 6 (squares), pH 7 (upward triangles), pH 8 (circles) and pH 9 (dots).

From the initial number of microbubbles (Fig. 2.6) and the evolution of the number of microbubbles in time (Fig. 2.7), it can be seen that the highest yield and stability were obtained at pH just above the isoelectric point ( $\sim 4.8$ ), which is in accordance to the findings of Tchuénbou-Magaia et al.<sup>3</sup> These authors propose that the high yield and stability of microbubbles at pH close to the isoelectric point can be explained by a high surface coverage at the air-water interface when the protein molecules have no net charge. In our experiments addition of salt led to a higher yield and stability, while other papers report lower yield and stability with increasing ionic strength. At ionic strength of 0.2 M Tchuénbou-Magaia et al.<sup>3</sup> could not form microbubbles, whereas at 0.01 M microbubbles were obtained. At ionic strength of 0.4 M and higher Dibbern et al.<sup>21</sup> observed a decrease in microbubble yield. It has been described in literature<sup>22, 23</sup> that a high surface coverage and a more rigid air-water interface at pH close the isoelectric point, or upon salt addition, can be attributed to both the charge and the conformation of the molecules. A decreased repulsion between molecules appears to result in a higher coverage at the air-water interface<sup>22</sup>. Furthermore, at pH around the isoelectric point and at high ionic strength BSA molecules are in a native, more compact conformation, allowing a more efficient filling of the available space<sup>23</sup>. This causes that during the first stage of sonication more bubbles are formed, with a coverage that is larger than the critical coverage to prevent coalescence at pH around the isoelectric point and at high ionic strength. This results in a higher number of microbubbles. Avivi & Gedanken<sup>12</sup> found that microspheres covered with streptavidin or poly-glutamic acid could only be made when the carboxylic groups of the polypeptides were protonated: for streptavidin and poly-glutamic acid no microspheres could be made at pH above 6 and 4.5, respectively. For these proteins the most compact conformation was found at pH below the mentioned values, which supports the relationship between protein conformation, surface coverage and microbubble yield. As mentioned in the section '*Effect of storage temperature on the stability of microbubbles*', assuming that the shell around microbubbles is a result of thermal aggregation, the proteins should be partially unfolded to create the microbubble shell. This means that during the second stage

of the sonication the proteins are not in their most compact conformation. The interplay between maximization of the surface coverage and sufficiently unfolding of the proteins to form a sufficiently elastic gel is not well understood.

In Fig. 2.8 the effect of pH and ionic strength on both the yield and stability is shown.

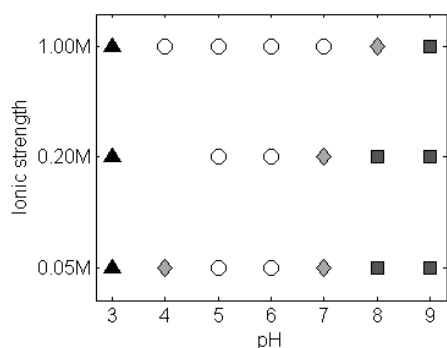


Fig. 2.8. Yield (number of microbubbles at day 0): no microbubbles (black), less than  $2 \cdot 10^9$  microbubbles per ml (dark grey), between  $2 \cdot 10^9$  and  $5 \cdot 10^9$  microbubbles per ml (light grey), more than  $5 \cdot 10^9$  microbubbles per ml (white).

Stability (number of microbubbles at day 22): less than  $1 \cdot 10^6$  microbubbles per ml (dark grey), between  $1 \cdot 10^6$  and  $1.8 \cdot 10^9$  microbubbles per ml (light grey), more than  $1.8 \cdot 10^9$  microbubbles per ml (white).

At pH 3 no microbubbles could be made. This is in accordance to Tchuenbou-Magaia et al. <sup>3</sup>, but in contradiction to Benjamins et al. <sup>13</sup>. In our study flocculation occurred at pH 3. According to Yahya Khan & Salahuddin <sup>24</sup>, most of the BSA molecules present in a solution at pH 3 are denatured. Benjamins et al. <sup>13</sup> used slightly different preparation parameters (lowering pH with citric acid, preheating at  $50^\circ\text{C}$ , sonication time 1.5 minutes, power level 10 and duty cycle 50%). Also using these parameter settings, we could not obtain microbubbles at pH 3. The only difference between our experiments and those of Benjamins et al. <sup>13</sup> is the supplier of the BSA. As described above, a different protein batch may lead to a different ability to form microbubbles. We hypothesize that for other batches the interplay between maximizing of the surface coverage and sufficient unfolding of

the proteins is different than for the batch described in this study. For the batches mentioned in section '*Production and characterization of microbubbles*', more protein unfolding was needed, as at a duty cycle of 90% (so more energy and thereby probably more heat), microbubbles could be made. For the batch used by Benjamins et al. <sup>13</sup>, that BSA could probably still cover an air-water interface at pH 3, where our BSA could not. The molecular properties leading to these differences are outside the scope of this study.

At pH 4 and ionic strength 0.2 M the number of microbubbles could not be analysed with image analysis (Fig. 2.8), since the microbubbles were surrounded by an abundance of protein aggregates. From the microscopic pictures it can be seen that the number of microbubbles in this sample was lower than for the sample at pH 4 with ionic strength 0.05 M (Fig. 2.9).

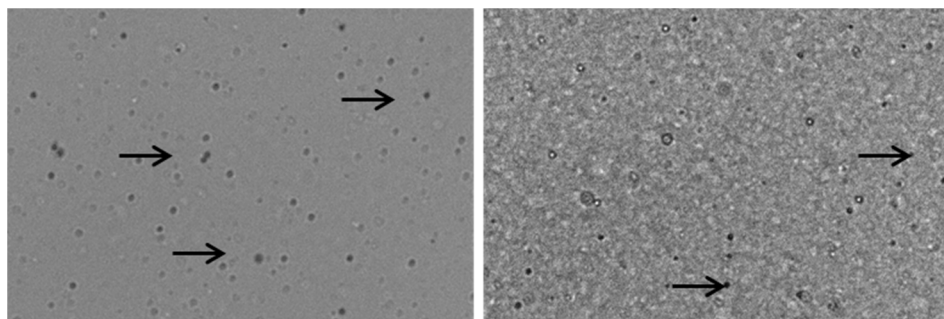


Fig 2.9. Micrographs of microbubble dispersions made at pH 4 with an ionic strength of 0.05 M (left) and 0.2 M (right). In the right picture protein aggregates are visible on the background. Microbubbles correspond to the dark spots. Some of the microbubbles are indicated by arrows for clarity.

The effect of pH and ionic strength on the average size of the microbubbles immediately after production is shown in Fig. 2.10.

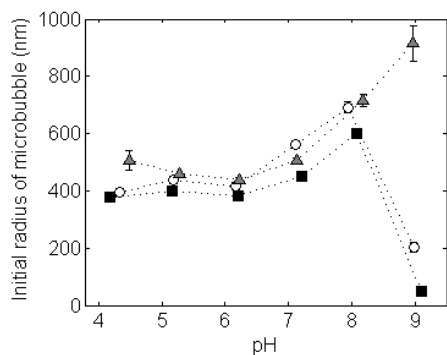


Fig. 2.10. Size of microbubbles immediately after preparation as a function of pH of the BSA solution for different ionic strengths: 0.05M (squares), 0.2M (circles) and 1M (triangles).

Above pH 6 an increase in size with increasing pH was observed. Tchenbou-Magaia et al. <sup>3</sup> also reported that the size of the microbubbles increased when moving away from the isoelectric point ( $\sim 4.8$ ). The smaller size observed at pH close to the isoelectric point can be explained by a higher surface coverage in the first stage of sonication. As mentioned the interplay between surface coverage and unfolding of the protein is not well understood, especially when the conformation of the BSA is not compact, as is the case at high pH. Therefore it is hard to explain the results shown in Fig. 2.10.

At pH close to the isoelectric point and at high ionic strength the average radius of the microbubbles hardly changed during storage (data not shown), which is a confirmation of the high microbubble stability at those conditions.

### Effect of preheating temperature on formation and stability of microbubbles

Since the temperature of the solution to be sonicated is considered an important parameter, we investigated the effect of preheating temperature on the formation and stability of microbubbles (Fig. 2.11).

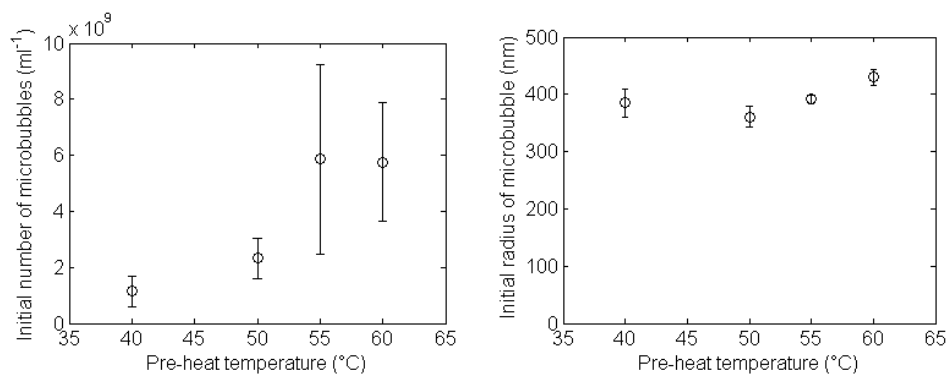
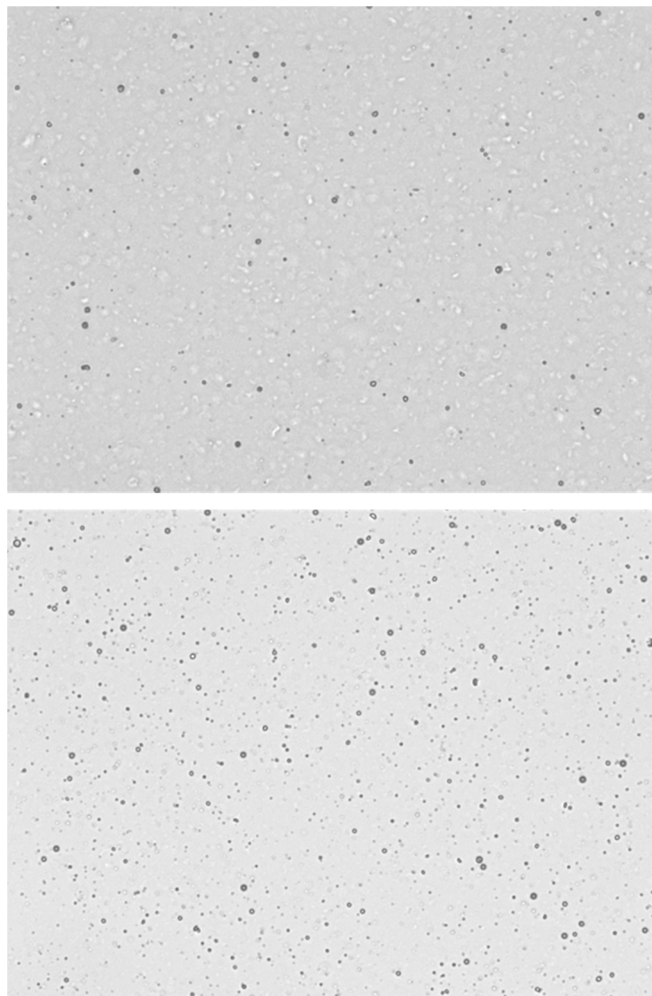


Fig. 2.11. Number (left) and size (right) of microbubbles immediately after preparation as a function of the preheating temperature.

An increase in preheating temperature from 40°C to 55°C led to an increase in the initial number of microbubbles. A further increase to 60°C did not have a notable effect.

Samples that were preheated at 70°C showed after sonication, besides microbubbles, also a lot of protein aggregates (Fig. 2.12).





*Fig. 2.12. Micrograph of a sonicated BSA solution that was preheated at 70°C (top) and 60°C (bottom). Dark spots correspond to air filled microbubbles, lighter spots to protein aggregates.*

The presence of the protein aggregates hindered the determination of the number of microbubbles by image analysis. It can be seen in Fig. 2.12 that the number of microbubbles in a solution preheated at 70°C was significantly lower than that in a solution preheated at 60°C.

As mentioned, the microbubble shell can be considered as a multi-layered network of BSA molecules bound by thermally induced protein-protein interactions. As far as we know, thermal aggregation of BSA was studied only at liquid-solid interfaces

<sup>25</sup>, whereas for air-water interfaces thermal aggregation of  $\beta$ -lactoglobulin and lysozyme has been described <sup>26</sup>. The findings of these papers suggest that in bulk BSA starts to unfold at 50°C and can aggregate and form intermolecular bonds at 70°C. At the air-water interface unfolding and intermolecular association occur simultaneously over a wide range of temperatures from 40°C to 70°C.

Regardless of the preheating temperature or any other measured preparation parameter, we observed that sonication for 3 minutes always induced a temperature increase of circa 5°C. The highest number of microbubbles was obtained in solutions with final temperatures in a range between 60°C and 65°C. This is average temperature too low for the formation of protein aggregates in the bulk. After sonication, the temperature of solutions preheated at 70°C was around 75°C, which was sufficiently high for the formation of protein aggregates in the bulk. So, in order to obtain the highest yield of microbubbles, it is important that the temperature after sonication is lower than the temperature for intermolecular association in bulk, which is slightly above 70°C.

In summary, microbubbles are stabilized by a protein network in the shell. In order to have this network formed, protein aggregation needs to occur, preferably in the later stages of the sonication process. If aggregation takes place too early in the process or when the temperature is already close to the aggregation temperature, aggregation will also take place in the bulk. We assume that these bulk protein aggregates cannot adsorb at the air-water interface, and thus hinder the adsorption of BSA molecules at the air-water interface. This diminishes the amount of proteins for bubble stabilization dramatically and results in much lower yields. A pre-heating temperature of 5°C below the aggregation temperature is recommended as the sonication process (with our settings) increase the temperature by 5°C.

The number of microbubbles made at different preheating temperatures was followed in time (results not shown). The findings were comparable with those presented for samples made at different protein concentrations: the number of microbubbles was rather stable in the first seven weeks, but for most of the samples less than half of the microbubbles remained intact after ten weeks. After

ten weeks only the sample preheated at 60°C had more than half of the original number of microbubbles.

The effect of preheating temperature on the average size in time is shown in Fig. 2.13.

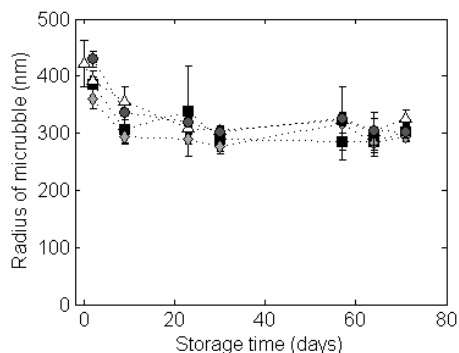


Fig. 2.13. Average radius of microbubbles as a function of storage time for different preheating temperatures: 40°C (squares), 50°C (diamonds), 55°C (triangles), 60°C (circles).

As observed for the samples made at different protein concentrations, the size of the microbubbles made at different preheating temperatures decreased up to a certain level, after which it became stable. We assume that this shrinking can be explained by the same mechanism given for the samples with different protein concentrations.

## Conclusion

For the preparation of microbubbles with BSA, a higher protein coverage of the air-water interface leads to a higher number of microbubbles in the first stage of sonication, and to more stable microbubbles. A high coverage is favoured by a compact conformation of the protein molecules and limited repulsions between them. In the second stage of sonication, the temperature of the system increases, leading to a network of protein molecules at the air-water interface linked by thermally induced interactions. A higher number of microbubbles is obtained when the temperature after sonication is just slightly lower than the temperature required for intermolecular association in the bulk.

Microbubbles stored at 4°C are more stable than those stored at room temperature. This is explained by the fact the microbubble shell is less rigid at high temperatures.

During the first three weeks of storage microbubbles tend to shrink to a radius between 300 nm and 350 nm and subsequently stay constant in size. The shrinking is probably due to the fact that the modulus of the shell reaches a value able to withstand the pressure difference at the end of shrinkage.

## References

1. M. A. Borden and M. L. Longo, *Langmuir*, 2002, **18**, 9225-9233.
2. K. S. Suslick, M. W. Grinstaff, K. J. Kolbeck and M. Wong, *Ultrasonics Sonochemistry*, 1994, **1**, S65-S68.
3. F. L. Tchuembou-Magaia, N. Al-Rifai, N. E. M. Ishak, I. T. Norton and P. W. Cox, *Journal of Cellular Plastics*, 2011, **47**, 217-232.
4. F. L. Tchuembou-Magaia and P. W. Cox, *Journal of Texture Studies*, 2011, **42**, 185-196.
5. F. L. Tchuembou-Magaia, I. T. Norton and P. W. Cox, *Microbubbles with protein coats for healthy food air filled emulsions*, Royal Soc Chemistry, Cambridge, 2010.
6. E. Stride and M. Edirisinghe, *Medical & Biological Engineering & Computing*, 2009, **47**, 883-892.
7. E. Stride and M. Edirisinghe, *Soft Matter*, 2008, **4**, 2350-2359.
8. M. J. Borrelli, W. D. O'Brien, L. J. Bernock, H. R. Williams, E. Hamilton, J. N. Wu, M. L. Oelze and W. C. Culp, *Ultrasonics Sonochemistry*, 2012, **19**, 198-208.
9. F. Cavaliere, M. Ashokkumar, F. Grieser and F. Caruso, *Langmuir*, 2008, **24**, 10078-10083.
10. M. F. Zhou, F. Cavaliere and M. Ashokkumar, *Soft Matter*, 2011, **7**, 623-630.
11. M. Ashokkumar, *Ultrasonics Sonochemistry*, 2011, **18**, 864-872.
12. S. Avivi and A. Gedanken, *Biochemical Journal*, 2002, **366**, 705-707.
13. J. Benjamins, A. Sein, and C. van Vliet *United States of America Pat.*, 2002, patent nr US2002/0155208.
14. D. G. Shchukin and H. Mohwald, *Physical Chemistry Chemical Physics*, 2006, **8**, 3496-3506.
15. K. Katsuta, D. Rector and J. E. Kinsella, *Journal of Food Science*, 1990, **55**, 516-521.
16. T. Van Vliet, H. J. M. Van Dijk, P. Zoon and P. Walstra, *Colloid and Polymer Science*, 1991, **269**, 620-627.
17. S. Tcholakova, N. D. Denkov, I. B. Ivanov and B. Campbell, *Advances in Colloid and Interface Science*, 2006, **123**, 259-293.
18. E. Talu, K. Hettiarachchi, R. L. Powell, A. P. Lee, P. A. Dayton and M. L. Longo, *Langmuir*, 2008, **24**, 1745-1749.
19. M. B. J. Meinders and T. van Vliet, *Advances in Colloid and Interface Science*, 2004, **108**, 119-126.
20. T. Hagiwara, H. Kumagai and T. Matsunaga, *Journal of Agricultural and Food Chemistry*, 1997, **45**, 3807-3812.
21. E. M. Dibbern, F. J. J. Toublan and K. S. Suslick, *Journal of the American Chemical Society*, 2006, **128**, 6540-6541.
22. L. G. C. Pereira, O. Theodoly, H. W. Blanch and C. J. Radke, *Langmuir*, 2003, **19**, 2349-2356.
23. B. A. Noskov, A. A. Mikhailovskaya, S. Y. Lin, G. Loglio and R. Miller, *Langmuir*, 2010, **26**, 17225-17231.
24. M. Yahiya Khan and A. Salahuddin, 1990, **15**, 361-376.
25. R. J. Green, I. Hopkinson and R. A. L. Jones, *Langmuir*, 1999, **15**, 5102-5110.

26. S. A. Holt, M. J. Henderson and J. W. White, *Australian Journal of Chemistry*, 2002, **55**, 449-459.

## Chapter 3:

### Disintegration of protein microbubbles in presence of acid and surfactants: a multi-step process

---

The stability of protein microbubbles against addition of acid or surfactants was investigated. When these compounds were added, the microbubbles first released the encapsulated air. Subsequently, the protein shell completely disintegrated into nanometer-sized particles. The decrease in the number of intact microbubbles could be well described with the Weibull distribution. This distribution is based on two parameters, which suggests that two phenomena are responsible for the fracture of the microbubble shell. The microbubble shell is first weakened. Subsequently, the weakened protein shell fractures randomly. The probability of fracture turned out to be exponentially proportional to the concentration of acid and surfactant. A higher decay rate and a lower average breaking time were observed at higher acid or surfactant concentrations. For different surfactants, different decay rates were observed. The fact that the microbubble shell was ultimately disintegrated into nanometer-sized particles upon addition of acid or surfactants indicates that the interactions in the shell are non-covalent and most probably hydrophobic. After acid addition the time at which the complete disintegration of the shell was observed coincided with the time of complete microbubble decay (release of air), while in the case of surfactant addition, there was a significant time gap between complete microbubble decay and complete shell disintegration.

This chapter is published as:

T.A.M. Rovers, G. Sala, E. van der Linden and M. B.J. Meinders (2015) Disintegration of protein microbubbles in presence of acid and surfactants: a multi-step process, *Soft Matter*, 11, 6403-6411

## Introduction

Protein stabilized microbubbles are micron-sized air bubbles with a relatively thick interfacial layer that makes them stable with respect to disproportionation <sup>1-3</sup>. Conventional ways of making microbubbles include sonication, high shear mixing, template-layer-by-layer deposition and membrane emulsification. Recently, new technologies to produce microbubbles, like microfluidic devices, electrohydrodynamic atomization and pressurized gyration, have been developed <sup>2, 4-9</sup>. Microbubbles are considered as a food ingredient with high potential as fat replacer or for the creation of new textures in foods <sup>10, 11</sup>. In *Chapter 2* we showed that preparation conditions determined yield, size and stability of Bovine Serum Albumin (BSA) microbubbles made by sonication. The stability of microbubbles was related to the interactions that are formed between BSA molecules at the microbubble surface during sonication <sup>1</sup>. The interactions in the microbubble shell and their role for the stability of the microbubbles are subject of debate in literature. Suslick et al. <sup>3</sup> claimed that covalent disulfide bonds between the cysteine residues of BSA molecules are the main interactions in the shell of microbubbles prepared with this protein. Protein microbubbles are mostly made using cysteine-rich proteins, which seems to support this claim. However, it was observed that microbubbles can also be obtained with proteins that have no cysteine residues, implying that other interactions are responsible for the formation and stability of protein microbubbles made by sonication <sup>12</sup>. For polyglutamate microspheres, it was shown that interactions in the shell are non-covalent <sup>13</sup> and according to Cavalieri et al. <sup>1</sup> the interactions in a protein microbubble shell are a combination of covalent bonds and hydrophobic interactions. With this study we aim to get more insight on the nature of the interactions responsible for formation and stability of protein microbubbles. Furthermore, for practical applications, it is very important to get insights on the behaviour of microbubbles in different environments. Some studies on the stability of protein microbubbles under changing environment have already been reported. When subjected to a temperature of 121°C for 15 minutes, BSA microbubbles stayed intact and formed a gel of microbubbles <sup>14</sup>. Microbubbles prepared with BSA and dextrose were stable



against ultrasound of 1 MHz and 3 MHz when their size was 1  $\mu\text{m}$  or smaller, while bigger microbubbles were destructed at this high frequency ultrasound <sup>15</sup>. For food applications, insights on the stability of microbubbles in presence of food components are needed. It has been described that microbubbles were stable for 2 months in the presence of oil droplets <sup>11</sup>. In the current study we investigated the stability of microbubbles made by sonication upon addition of surfactants, more specifically Sodium dodecyl sulphate (SDS), or acid. We aim to relate the stability of the microbubbles to physical phenomena.

## **Materials and methods**

### **Materials**

Bovine serum albumin (BSA, fraction V, lot nrs: 100m1900V, SLBF0550V and SLBC8307V), sodium dodecyl sulphate (SDS) polysorbate 20 (Tween 20), sucrose monolaurate and hydrochloric acid (HCl) were purchased from Sigma-Aldrich (St. Louis, MO, USA). For all experiments demineralized water was used.

### **Preparation and washing of microbubble dispersions**

Microbubbles were prepared as described in *Chapter 2*. In short, 5% (w/w) BSA was dissolved in demineralized water, and the BSA solution was stirred for at least 2 hours. The pH of the solution was adjusted to 6.0 by addition of 2.0 M HCl and 0.2 M HCl. The solution was subdivided in portions of 25 ml, which were transferred to 50 ml beakers. The samples were heated for 10 minutes in a 55°C water bath and subsequently sonicated for 3 minutes at power level 8 and duty 30% cycle (when protein lot nr 100M1900V was used) or 90% duty cycle (when protein lot nr SLBF0550V or SLBC8307V were used), using a Branson 450 sonicator (Branson Ultrasonics Corporation, Danbury, CT) with a 20kHz, 12.7 mm probe. The probe was placed at the air-water interface of the solution.

The microbubble dispersions made with the protein from lot nr SLBF0550V or SLBC8307V contained, besides microbubbles, also protein aggregates. For further experiments, the microbubble dispersions were washed. They were centrifuged for

45 minutes at 400 g. The top layer, mainly consisting of microbubbles, was collected. The remaining dispersion was centrifuged for 45 minutes at 800 g. Also from this dispersion the top layer was collected. The collected top layers were diluted with demineralized water in order to obtain a concentration of microbubbles (number per volume) that was comparable to that of the microbubble dispersion before washing.

### **Visualization of microbubble disappearance**

The effect of the studied parameters on microbubbles was visualized by taking pictures of microbubble dispersions to which HCl or a solution of SDS was added. One drop of microbubble dispersion was placed on an object glass, which was covered with a cover glass. Subsequently, one drop of 1 M HCl or one drop of a 1% SDS solution was placed just next to the cover glass, allowing the HCl or SDS to diffuse into the microbubble dispersion. The object glass was placed under a phase contrast microscope (Leica Reichert Polyvar, Leica Microsystems, Wetzlar, Germany) or a light microscope (Axioskop, Carl Zeiss AG, Oberkochen, Germany) at a 40x magnification. A camera (MC120 HD, Leica Microsystems, Wetzlar, Germany or AxioCam HRC, Carl Zeiss AG, Oberkochen, Germany) connected to the microscope took pictures with a time interval of 1 second.

### **Determination of microbubbles number and size after acid or surfactant addition**

#### **Preparation of the samples**

Predetermined volumes of 2 M HCl were added under continuous stirring to the microbubbles dispersions. The exact pH values reached as a result of these additions were noted after the determination of the number or size of the microbubbles.

A stock solution of 2% (w/v) SDS was made and stirred for more than 2 hours. From this stock solution dilutions were made to concentrations that were twice the concentration desired in the final solution. These SDS solutions were mixed 1:1

with the microbubble dispersions and subsequently vortexed for 15 seconds. The final BSA concentration in these microbubble-SDS mixtures was 2.5% (0.376 mM). The final SDS concentrations in the different samples were 0.011% (0.376 mM), 0.044% (1.50 mM), 0.075% (2.60 mM), 0.10% (3.47 mM) and 0.125% (4.33 mM). Therefore, the [SDS]:[BSA] ratios were 1.0, 4.0, 6.9, 9.2 and 11.5. SDS was added to the washed microbubble dispersions, containing 0.89% BSA (0.134 mM) to obtain final concentrations of 0.011% (0.376 mM), 0.022% (0.75 mM), 0.044% (1.50 mM), giving [SDS]:[BSA] ratios of 2.8, 5.6, and 11.2. To compare the effect of SDS to that of other surfactants, also Tween 20 and sucrose laurate were added to unwashed microbubble dispersions at a [surfactant]:[BSA] ratio of 6.9.

### **Determination of the number of microbubbles**

Immediately after stirring or vortexing, one drop (20  $\mu$ l) of acidified microbubble dispersion or one drop of the microbubble-surfactant mixture was put on the object glass. This was covered by a cover glass. To prevent evaporation, all sides of the cover glass were sealed with Sellotape. Microscope (Axioskop, Carl Zeiss AG, Oberkochen, Germany) images (40x magnification) of one specific spot of the acidified microbubble dispersion or the microbubble-surfactant mixture were taken at standard time intervals with a camera (Axiocam HRc, Carl Zeiss AG, Oberkochen, Germany). From the microscope pictures, the number of microbubbles was estimated by image analysis using ImageJ (1.44n, National Institutes of Health, Bethesda, MD). All experiments were done at least in duplicate.

### **Determination of the size of microbubbles**

The size of microbubbles and microbubbles shell remainders after SDS or HCl addition was measured with dynamic light scattering, using a Zetasizer Nano ZS (Malvern Instruments Ltd, Malvern, United Kingdom).

### **Data processing**

Data were analysed using Matlab (R2013a, Mathworks Natick, MA, United States) and built-in functions for non-linear fitting. Average breaking times,  $t_b$ , were calculated with

$t_b = \frac{\sum_1^n (\Delta N_n \cdot t_n)}{\sum_1^n \Delta N_n}$ , in which  $\Delta N_n = N_n - N_{n-1}$ , with  $N_n$  and  $N_{n-1}$  the number microbubbles on time  $t_n$  and  $t_{n-1}$ , respectively.

## **Results and discussion**

### **Stability against acid**

#### **Visualization of microbubble disintegration after acid addition**

The addition of a drop of 1 M HCl to a microbubble dispersion induced the disappearance of the microbubbles, as can be seen in Fig. 3.1.

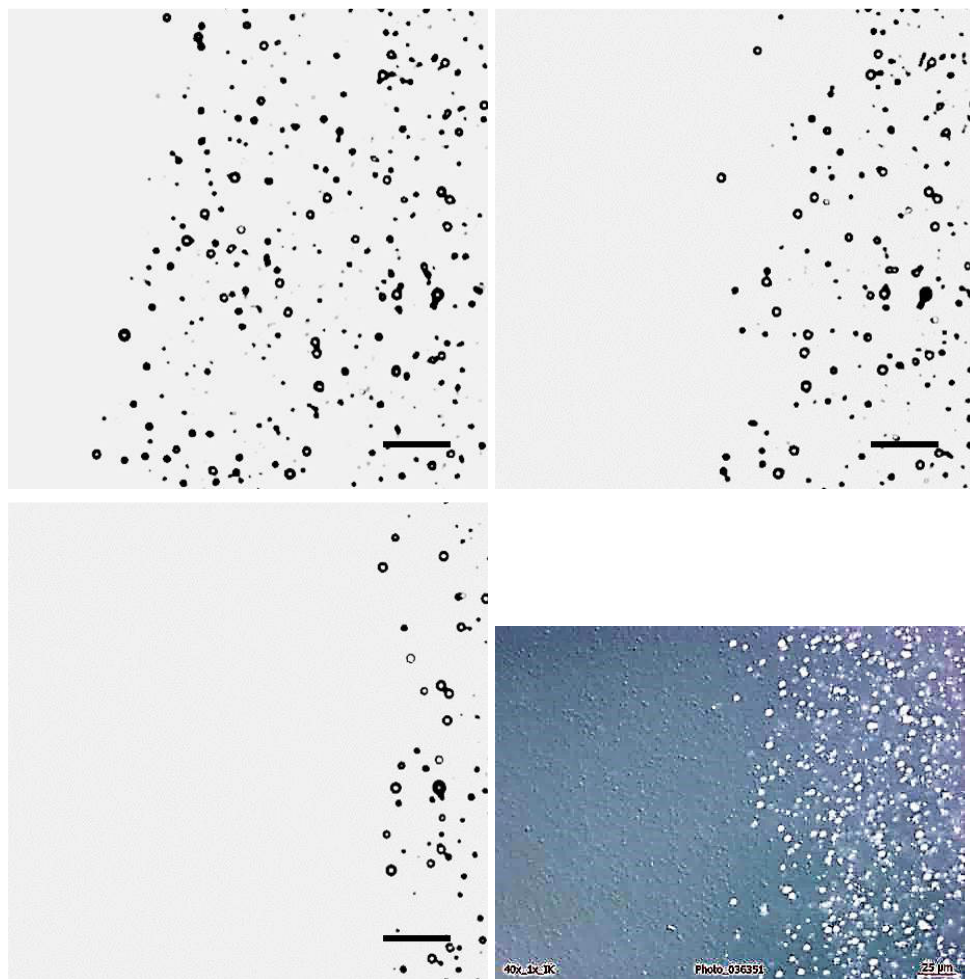


Fig. 3.1. Micrograph of microbubble dispersion to which at the left side a 1 M HCl solution is added. Micrographs taken with a normal light microscope at different time points:  $t=0$  s (top left),  $t=5$  s (top right),  $t=10$  s (bottom left) with a scale bar of  $10\ \mu\text{m}$ . Micrograph taken with a phase contrast microscope, in which the white spots correspond to the intact microbubbles and the grey irregular shaped objects correspond to the remaining broken shell (bottom right) with a scale bar of  $25\ \mu\text{m}$ .

The drop of HCl was placed at the left side of the sample. HCl diffused into the dispersion from the left to the right side. The microbubbles disappeared within seconds. The micrographs on the top left, top right, and bottom left of Fig. 3.1 show pictures made with a normal light microscope at 0, 5, and 10 seconds after addition

of the acid. The micrograph at the bottom right of Fig. 3.1 shows a picture made with a phase contrast microscope. It seems that at the moment the microbubbles came in contact with the concentrated acid solution they disappeared almost immediately. Also, in the micrographs taken with a phase contrast microscope, a front of disappearing white spots was visible that moved from left to right. These white spots corresponded to the air in the intact microbubbles. This means that the microbubbles released their air quickly after the acid reached them. After the release of air, some remainders of the microbubbles were visible (Fig. 3.1, bottom right). These corresponded to the shells or parts of the shells, which remained after the microbubbles lost their enclosed air. After some time, also the grey spots disappeared (not shown), indicating a complete breakdown of the microbubble shell. The two stages of microbubble disappearance, the release of air and the complete disintegration of the microbubble shell, are described in more detail in the two following paragraphs.

### **Escape of air from microbubble after acid addition**

In this section we will focus on the first part of the microbubble disintegration, i.e. the release of air from the microbubbles. Using a normal bright field microscope the air-filled microbubbles are visible, while water filled microbubbles are not. This allows the determination of the number of microbubbles after addition of acid or surfactant. Fig. 3.2 shows the relative number of microbubbles measured as a function of time for different changes in pH value,  $\Delta\text{pH} = \text{pH}_{\text{add}} - \text{pH}_0$ , in which  $\text{pH}_{\text{add}}$  is the pH after acid addition and  $\text{pH}_0$  is the pH before acid addition, i.e. pH 6.

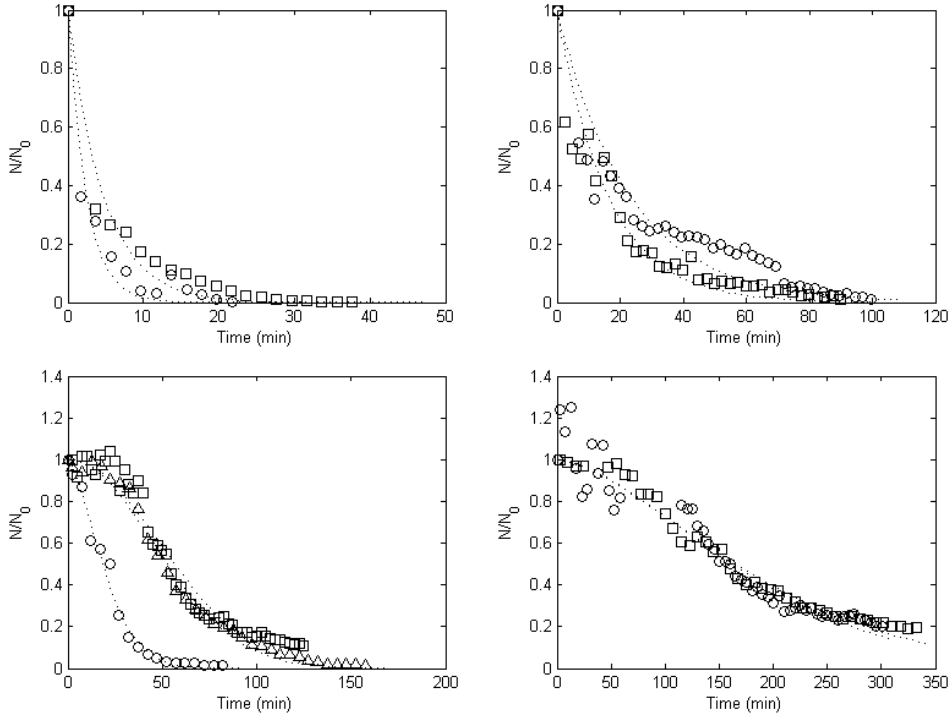


Fig. 3.2.  $N/N_0$ , with  $N$  and  $N_0$  being the number of microbubbles at time  $t$  and time  $t=0$ , as function of the time after addition of HCl for different  $\Delta pH$ : top left: 2.68 (circles) and 2.66 (squares), top right: 2.46 (circles and squares), bottom left: 2.37 (circles), 2.33 (squares) and 2.29 (triangles), bottom right: 2.05 (circles) and 1.91 (squares). The data are fitted with the Weibull distribution, depicted with the dotted lines.

The time until the number of microbubbles decreased by 50% of the original number ( $t_{1/2}$ ) was above 150 minutes at  $\Delta pH$  around 2.0. For  $\Delta pH$  around 2.7,  $t_{1/2}$  turned out to be almost zero. In samples with a lower  $\Delta pH$  there was a lag time before the microbubbles released the air. This behaviour might be due to the superposition of two phenomena, each with a characteristic time, the first corresponding to a weakening of the protein shell caused by a change in pH, and the second corresponding to the fracture of the weakened shell that could not withstand the Laplace pressure anymore. Therefore, we fitted our data to the univariate Weibull distribution,  $e^{-(\alpha t)^\beta}$  <sup>16</sup>. The fitted Weibull functions are depicted by the dotted lines in Fig. 3.2. The parameter  $\beta$  is often called the shape factor and

describes the wearing rate of a process. The parameter  $\alpha$  represents the Poisson killing rate, the decay rate of the distribution, and corresponds to the average failure time of a stochastic failure process<sup>16-18</sup>. In our case the aforementioned weakening of the shell is described by the wearing rate  $\beta$ . When the shape parameter  $\beta$  is larger than one, a certain lag in the fracture process is observed. In our study the parameter  $\alpha$  corresponds to the decay rate of the microbubbles, which describes how fast the shell ruptured upon release of air. The parameters  $\alpha$  (on a log-linear scale) and  $\beta$  (on a linear-linear scale) are plotted as function of  $\Delta\text{pH}$  (top graphs of Fig. 3.3).

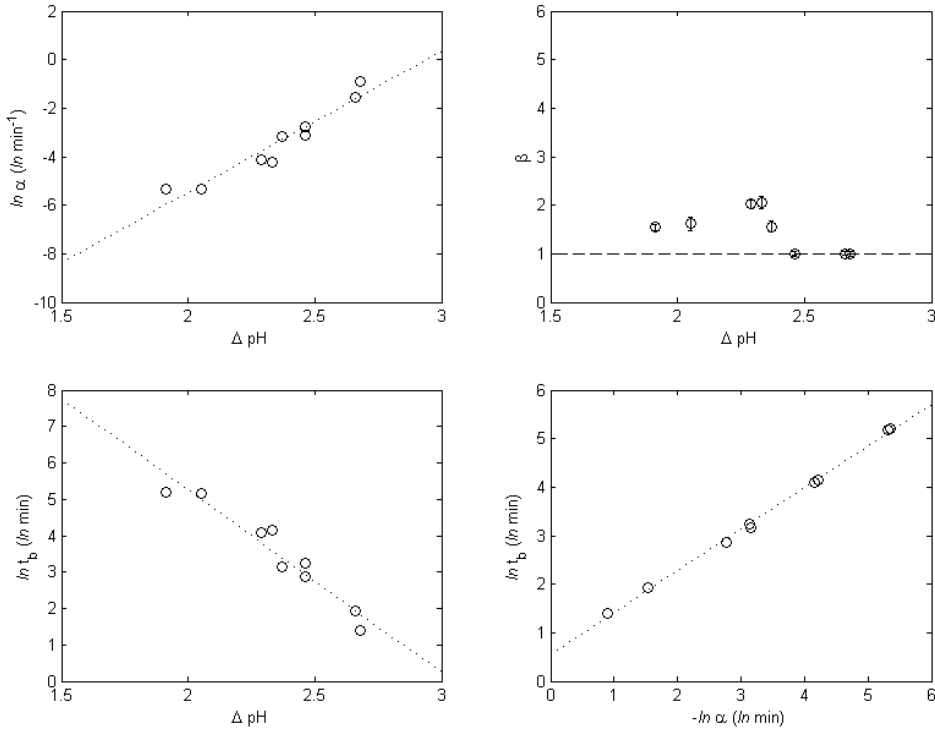


Fig. 3.3. Natural logarithm of parameter  $\alpha$  as function of  $\Delta\text{pH}$  (top left), and parameter  $\beta$  as function of the  $\Delta\text{pH}$  (top right). Natural logarithm of the average breaking time,  $t_b$ , as function of  $\Delta\text{pH}$  (bottom left) and as function of the negative natural logarithm of parameter  $\alpha$  (bottom right).

For samples with a  $\Delta\text{pH}$  smaller than 2.4,  $\beta$  was slightly larger than 1. This means that at low acid concentrations there is a time lag in the release of air from the microbubble. We hypothesize that the parameter  $\beta$  can be defined by the result of



several phenomena that weaken the microbubble shell. One phenomenon that controlled the weakening rate of the shell was the diffusion of acid to and through the microbubble shell, which at lower acid concentration was lower than at high acid concentrations. Subsequently, the addition of acid protonated the BSA molecules in the microbubble shell, making them more positively charged. Higher concentrations of acid resulted in a higher degree of protonation and BSA molecules that were more positively charged, resulting in a larger inter- and intra-molecular repulsion. Furthermore, at pH further away from the isoelectric point (4.7) BSA molecules are in a more stretched conformation, resulting in a higher excluded volume for every BSA molecule <sup>19</sup>. All these phenomena (diffusion, protonation and resulting repulsion and BSA conformation change) resulted in a weaker shell at higher acid concentrations.

The decay rate  $\alpha$  increased exponentially with  $\Delta\text{pH}$ . The decay of the microbubble might be described as a random fracture phenomenon of a hollow sphere with a thin protein shell under constant (Laplace) pressure. In literature random fracture has been described for gels <sup>20</sup>. According to Bonn et al. <sup>20</sup> the random fracture model is only applicable when the fracture has a random nature, which means that the decay can be described as a univariate distribution. Since the parameter  $\alpha$  describes an exponential, univariate distribution, the decay of the microbubble shells is assumed to fulfil those criteria. The shell fractured randomly with a higher probability of breaking and a lower average breaking time,  $t_b$ , at higher  $\Delta\text{pH}$  (Fig. 3.3, bottom left). The probability of breaking, and consequently the average breaking time, could be well described by the decay rate  $\alpha$ , as shown on the bottom right graph of Fig. 3.3.

### **Disintegration of microbubble shell after acid addition**

After air release, the remaining shell of the microbubbles (shown in right bottom micrograph of Fig. 3.1) disappeared, as well. In order to further investigate this, we added acid to the microbubble dispersion and measured the size of microbubbles and remainders in time. In Fig. 3.4 an example of the measured size distributions is

given for an acidified microbubble dispersion at  $\Delta\text{pH}$  2.19 at different times after acid addition.

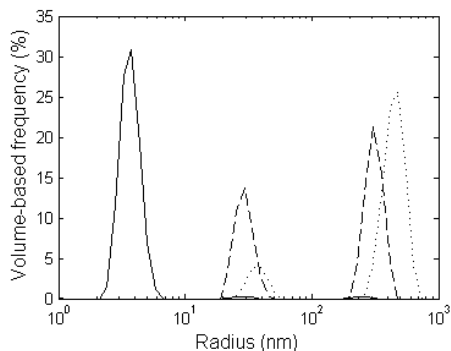


Fig. 3.4. Volume-based size distribution of an acidified microbubble dispersion with  $\Delta\text{pH}$  2.19, after 0 minutes (dotted line), 18 minutes (dashed line) and 62 minutes (solid line) on linear-log scale.

The volume-based mean radius of the microbubbles decreased in time to a size of several nanometers. The size of the final particles coincide with that of BSA monomers or dimers. This means that weak acid concentrations can break the intermolecular bonds in the microbubble shell, indicating that the interactions in the microbubble shell are non-covalent. In Fig. 3.4 a gradual decrease in size of microbubble and microbubble remainders is observed for dispersions with  $\Delta\text{pH}$  2.19. The time span in which the microbubbles were broken down to nanometers particles was of the same order of magnitude as the time required to break the microbubble shell and release the air in dispersions with  $\Delta\text{pH}$  around 2.3. This can be seen in the bottom left graph of Fig.3.2. It suggests that the time between first fracture (leading to the release of air) and subsequent disintegration, leading to breakdown to nanometer particles, was very short. This was also observed at higher values of  $\Delta\text{pH}$ , where the decrease in size was not gradual. In those dispersion the size directly dropped from sizes typical of microbubble to nanometers, suggesting a very short time between first fracture and subsequent disintegration. The parameter  $\beta$  for the decay of the microbubbles upon acid addition was low. This means that the shell weakened relatively quickly, resulting in a short lag phase and in a shell that quickly disintegrated.

## Stability against surfactants

### Visualization of microbubble disintegration after SDS addition

Similar as observed for the experiments with acid, addition of a drop of 1% SDS solution resulted in the disappearance of microbubbles, as can be seen in Fig. 3.5. The drop of SDS solution was placed at the right side of the sample and SDS was allowed to diffuse from the right to the left side. The micrographs shown in Fig. 3.5 were made with a phase contrast microscope at three different times after the addition of the SDS solution.

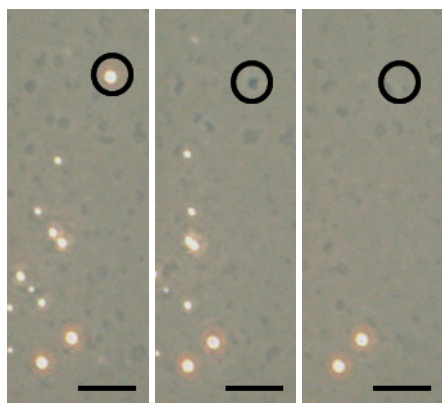


Fig. 3.5. Micrographs of a microbubble dispersion to which at the right side a 1% SDS solution was added. Micrographs from the phase contrast microscope taken at different time points:  $t=0$  s (left),  $t=2$  s (middle),  $t=10$  s (right). The encircled part shows a typical example of the breakdown process with from left to right: a white spot (corresponding to a microbubble), a dark grey spot (corresponding to the remaining shell) and no spot. Scale bar is  $10\ \mu\text{m}$ .

The disintegration of microbubbles by SDS was similar to that observed after acid addition. First the white spots disappeared from the micrographs, which means that the air escaped from the microbubble. Dark spots remained visible, as can be seen in the second micrograph. These dark spots corresponded to the protein shell and/or parts of the shell. After some time the darker spots also disappeared, as can be seen in the third micrograph. This implies a complete disintegration of the microbubble shell.

### Escape of air from microbubble after SDS addition

As described for the experiments with acid, we followed the number of microbubbles in time, also after SDS addition. At higher SDS concentrations the number of microbubbles decreased more quickly and it took less time before all microbubbles had disappeared. The decrease in the number of microbubbles due to SDS addition was fitted with a Weibull distribution as well. For all ratios, except for  $[\text{SDS}]:[\text{BSA}]=1.0$ , it was observed that directly after addition of SDS a large fraction of the microbubbles disappeared. The result is that the microbubble cannot be fitted well with the Weibull function. In dispersions to which acid was added such disappearance of a large fraction of microbubbles directly after acid addition was not observed. A difference in preparation was that the latter samples were washed before the addition of acid. Although the reason for washing was to remove the existing protein aggregates from the dispersion, it is very likely that during the centrifugation also the weakest microbubbles were removed. In order to check if this could be a reason for the disappearance directly after addition, we also washed the microbubble used for experiments with SDS. When SDS was added to these washed microbubble dispersions it was observed that the decay of the microbubbles followed the Weibull distribution quite well. Therefore, it seems that a fraction of the microbubbles in the unwashed microbubble dispersion had weaker shells that were more vulnerable to SDS and disappeared quickly after addition of this surfactant. This fraction could be removed by centrifugation. In the top graphs of Fig. 3.6 we plotted the parameter  $\alpha$  and  $\beta$  as function of the ratio  $[\text{SDS}]:[\text{BSA}]$ .

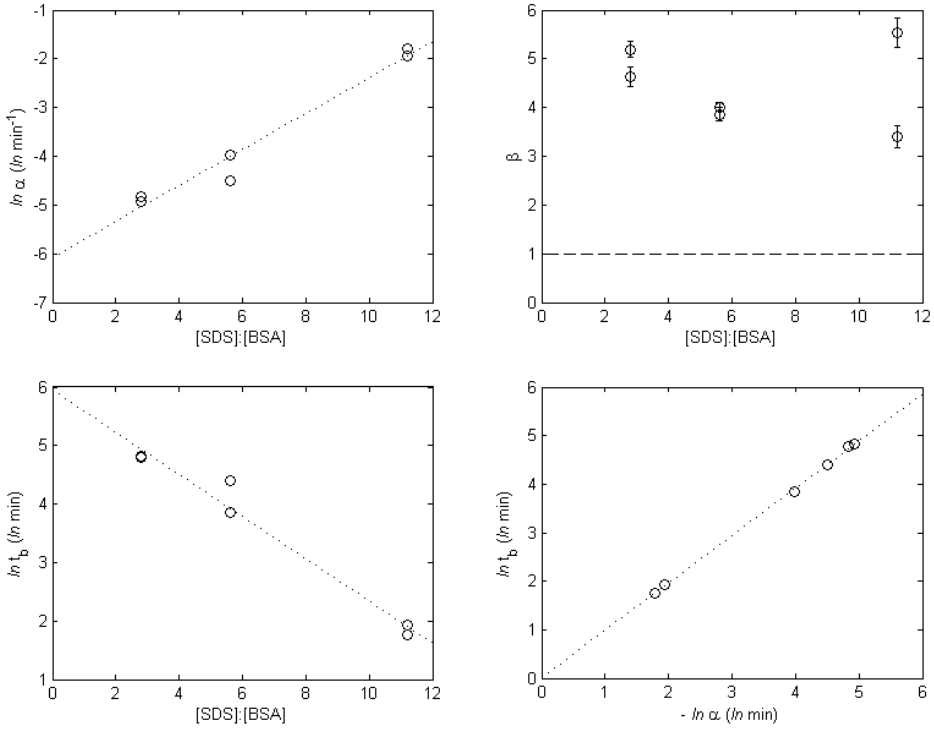


Fig. 3.6. Natural logarithm of parameter  $a$  as function of the ratio  $[\text{SDS}]:[\text{BSA}]$  (top left), and parameter  $\beta$  as function of the ratio  $[\text{SDS}]:[\text{BSA}]$  (top right). Natural logarithm of the average breaking time,  $t_b$ , as function of the ratio  $[\text{SDS}]:[\text{BSA}]$  (bottom left) and as function of the negative natural logarithm of  $a$  (bottom right).

Higher SDS concentrations resulted in larger decay rates. Furthermore, at all concentrations a lag phase was observed before the microbubbles started to fracture, resulting in values of  $\beta$  larger than 1. We propose to describe the fracture of the microbubbles shell and the subsequent release of air due to SDS addition by the two aforementioned steps. First, SDS weakened the microbubble shell. Phenomena that controlled the weakening of the shell upon SDS addition include diffusion of SDS to and through the microbubble shell and interactions of SDS with the hydrophobic patches of the proteins, thereby weakening the hydrophobic protein-protein interactions in the shell. Secondly, the weakened shell was not able to withstand the Laplace pressure anymore and therefore fractured, a phenomenon that could be described as a random process. Probability of fracture increased with

increasing SDS concentrations. With a high probability of fracture, the average breaking time,  $t_b$ , is lower and the decay  $\alpha$  rate is higher. This can be seen in the bottom graphs of Fig. 3.6 in which the natural logarithm of  $t_b$  is plotted against the ratio  $[\text{SDS}]:[\text{BSA}]$  and against the negative natural logarithm of  $\alpha$ .

### Comparison between surfactants

We compared the microbubble instability caused by the addition of SDS to the instability caused by other surfactants. The breakdown followed the same pattern; release of air followed by a complete disintegration of the shell (results not shown). For the first phase (release of air) the relative number of microbubbles was plotted as function of time. These microbubbles were not washed. No large decrease in the number of microbubbles was observed directly addition of 2.6 mM surfactant. Also for these samples, the decay pattern could be well described by the Weibull distribution.

We studied microbubble decay by surfactants with the same hydrophobic tail (laurate), but differing in the hydrophilic head group. We assume that the disintegration caused by the other surfactants followed the same pattern as the disintegration caused by SDS: after the surfactants had diffused to and through the shell and adhered to the BSA molecules, the shell was weakened and subsequently fractured randomly. Parameter  $\beta$  was around 1 for all surfactants (results not shown) indicating that at the used concentration the fracture started immediately after the addition of surfactant without any lag phase. The decay rate  $\alpha$  was for sucrose laurate, Tween 20 and SDS, 0.49, 0.10, and 0.029, respectively. No clear relation between surfactant properties, such as critical micelle concentration (CMC), molecular weight (M), hydrophilic-lipophilic balance (HLB), and fracture properties could be identified. The reason for difference in fracture behaviour due to different surfactants should be topic of further research.

### **Disintegration of microbubble shell after SDS addition**

After release of air from the microbubbles (second micrograph of Fig. 3.5), the remaining shell seemed to disappear as well (third micrograph of Fig. 3.5). In order to further investigate this, we added SDS to the microbubble dispersion, and measured the size of microbubbles and remainders by dynamic light scattering.

As observed for the disintegration of the microbubble shell by acid, the size of the final particles was comparable to that of BSA monomers or dimers. This means that SDS was able to break down (most of) the bonds in the microbubble shell. This confirms that the interactions in the microbubble shell are non-covalent, since SDS is not able to break covalent bonds. Both ionic as non-ionic surfactants could disintegrate microbubbles. Therefore, the interactions between proteins in the microbubble shell are believed to be of hydrophobic nature. SDS, Tween 20 and sucrose laurate can bind to the hydrophobic patches of the BSA, with binding energies of around 30 kJ/mol in all cases <sup>21-24</sup>.

Fig. 3.7 shows the average sizes of microbubbles and their remainders function of time after SDS was added for different [SDS]:[BSA] ratios.

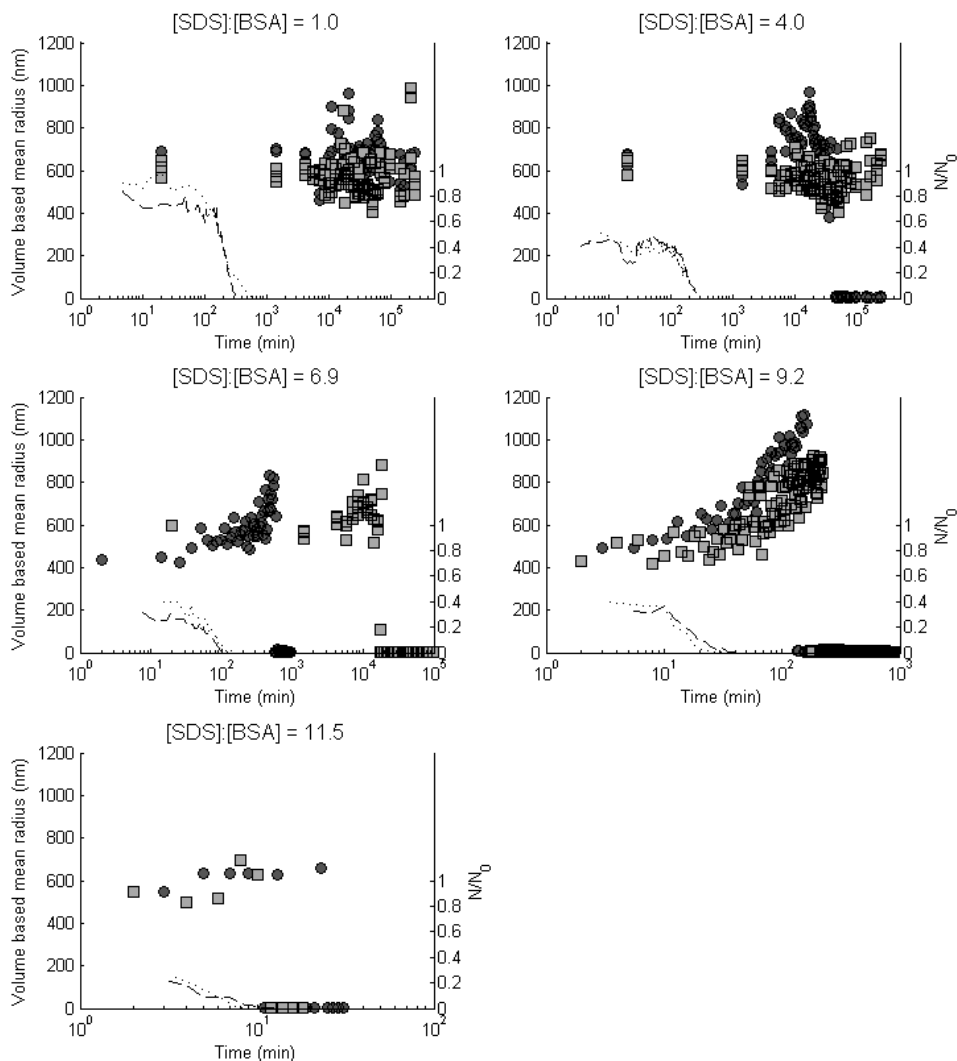


Fig. 3.7. Volume-based mean radius of microbubbles and microbubbles remainders as function of the time after addition of SDS for different [SDS]:[BSA] ratios: 1.0 (top left), 4.0 (top right), 6.9 (middle left), 9.2 (middle right) and 11.5 (bottom left) on linear-log scale. Sizes are measured for samples at 4°C (squares) and room temperature (circles). The dashed and dotted lines represent the decay in the number of microbubbles.

At higher surfactant-protein ratios and higher temperature the complete disintegration of the shell occurred faster. After the microbubbles had lost their air, the size of the remainders kept increasing for quite some time, after which the



microbubble shells completely disintegrated. This pattern is different from the disintegration of the shells after the addition of acid. In those samples the disintegration of the shell happened shortly after the microbubbles lost their air. The parameter  $\beta$  for the decay of the microbubbles with surfactant was relatively high, implying a relatively slow weakening of the shell and long lag phase. This also resulted in a long time between the first fracture (with subsequent release of air) and the complete shell disintegration. After the microbubble had lost its air, the shell was still present and this water-filled shell appeared to be larger than the air-filled shell, as also can be seen in a microscopy picture of a sample to which SDS was added (Fig. 3.8).

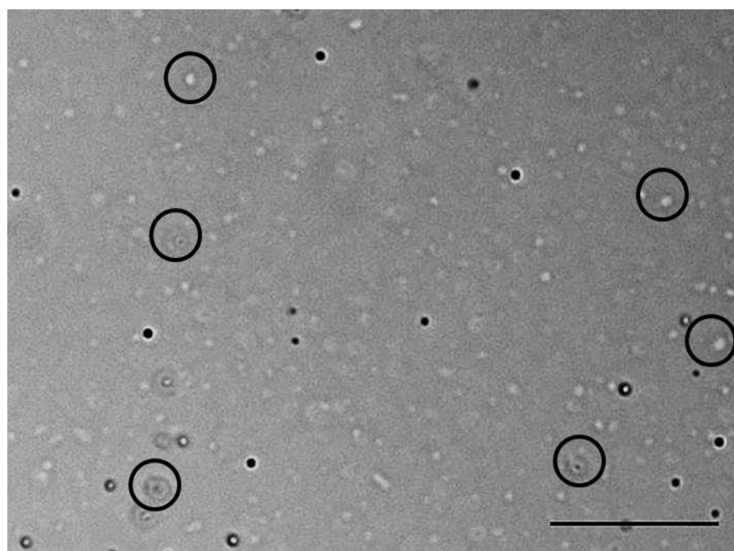


Fig. 3.8. Micrograph of a microbubbles dispersion to which SDS was added at [SDS]:[BSA] ratio of 9.2 after 38 min (i.e. just before the microbubble size dropped to nanometers). The black dots correspond to the microbubbles. The encircled particles correspond to the remainders of the microbubbles after air release. Scale bar is 25  $\mu\text{m}$ .

## Conclusion

The disintegration pattern of microbubbles upon surfactant or acid addition appears to be similar. Three different steps can be identified. The disintegration of the microbubble, where air dissolves quickly, can be well described with the two-parameter Weibull process. This suggests two processes: 1) a shell-weakening process and 2) a random fracture of the weakened shell. Subsequently, 3) the shell disintegrates completely into monomeric proteins. . For low changes in acid concentrations and all surfactant concentrations, a lag phase is observed in the microbubble decay, indicating that the weakening time is comparable to the breaking time. This is also implied by the Weibull shape factor  $\beta$  being larger than 1. Decay rates ( $\alpha$ ) increase exponentially and average breaking times ( $t_b$ ) decrease exponentially with increasing concentrations of acid or surfactant. This means that the probability of a random fracture is larger at a large change in acid or surfactant concentration. During the second step of the microbubble disintegration, the microbubble disintegrates into nanometer-sized protein particles. This means that the bonds between BSA molecules in the microbubble shell can be broken by acid and by ionic as well as non-ionic surfactants. This implies that the interactions in the shell are non-covalent, and most probably hydrophobic. Bonds between the proteins can be broken because surfactants occupy the hydrophobic patches of the BSA molecules in the shell, or because acid changes the conformation and charge of the BSA molecule.

## References

1. F. Cavalieri, M. Ashokkumar, F. Grieser and F. Caruso, *Langmuir*, 2008, **24**, 10078-10083.
2. E. Stride and M. Edirisinghe, *Soft Matter*, 2008, **4**, 2350-2359.
3. K. S. Suslick, M. W. Grinstaff, K. J. Kolbeck and M. Wong, *Ultrasonics Sonochemistry*, 1994, **1**, S65-S68.
4. Z. Ekemen, H. Chang, Z. Ahmad, C. Bayram, Z. Rong, E. B. Denkbaz, E. Stride, P. Vadgama and M. Edirisinghe, *Biomacromolecules*, 2011, **12**, 4291-4300.
5. M. Elsayed, J. Huang and M. Edirisinghe, *Materials Science and Engineering: C*, 2015, **46**, 132-139.
6. M. Lee, E. Y. Lee, D. Lee and B. J. Park, *Soft matter*, 2015, **11**, 2067-2079.
7. S. Mahalingam, M. B. J. Meinders and M. Edirisinghe, *Langmuir*, 2014, **30**, 6694-6703.
8. S. Mahalingam, B. T. Raimi-Abraham, D. Q. M. Craig and M. Edirisinghe, *Langmuir*, 2015, **31**, 659-666.
9. G. Mohamedi, M. Azmin, I. Pastoriza-Santos, V. Huang, J. Pérez-Juste, L. M. Liz-Marzán, M. Edirisinghe and E. Stride, *Langmuir*, 2012, **28**, 13808-13815.
10. F. L. Tchuenbou-Magaia, N. Al-Rifai, N. E. M. Ishak, I. T. Norton and P. W. Cox, *Journal of Cellular Plastics*, 2011, **47**, 217-232.
11. F. L. Tchuenbou-Magaia and P. W. Cox, *Journal of Texture Studies*, 2011, **42**, 185-196.
12. S. Avivi and A. Gedanken, *Biochemical Journal*, 2002, **366**, 705-707.
13. E. M. Dibbern, F. J. J. Toublan and K. S. Suslick, *Journal of the American Chemical Society*, 2006, **128**, 6540-6541.
14. F. L. Tchuenbou-Magaia, I. T. Norton and P. W. Cox, *Microbubbles with protein coats for healthy food air filled emulsions*, Royal Soc Chemistry, Cambridge, 2010.
15. M. J. Borrelli, W. D. O'Brien, L. J. Bernock, H. R. Williams, E. Hamilton, J. N. Wu, M. L. Oelze and W. C. Culp, *Ultrasonics Sonochemistry*, 2012, **19**, 198-208.
16. W. Weibull, *Journal of Applied Mechanics-Transactions of the Asme*, 1951, **18**, 293-297.
17. C. Lu, R. Danzer and F. D. Fischer, *Phys. Rev. E*, 2002, **65**, 067102.
18. H. Rinne, *The Weibull Distribution: A handbook*, Chapman and Hall/CRC, 2008.
19. B. A. Noskov, A. A. Mikhailovskaya, S. Y. Lin, G. Loglio and R. Miller, *Langmuir*, 2010, **26**, 17225-17231.
20. D. Bonn, H. Kellay, M. Prochnow, K. Ben-Djemaa and J. Meunier, *Science*, 1998, **280**, 265-267.
21. T. Chakraborty, I. Chakraborty, S. P. Moulik and S. Ghosh, *Langmuir*, 2009, **25**, 3062-3074.
22. C. Hoffmann, A. Blume, I. Miller and P. Garidel, *European Biophysics Journal with Biophysics Letters*, 2009, **38**, 557-568.
23. S. Makino, S. Ogimoto and S. Koga, *Agricultural and Biological Chemistry*, 1983, **47**, 319-326.
24. A. D. Nielsen, K. Borch and P. Westh, *Biochimica Et Biophysica Acta-Protein Structure and Molecular Enzymology*, 2000, **1479**, 321-331.



## Chapter 4:

### Effect of temperature and pressure on the stability of protein microbubbles

---

For the application of microbubbles in the food industry, it is important to gain insights in their stability under food processing conditions. In this study we tested the stability of protein microbubbles against heating and pressurizing. Microbubbles could be heated up to 50°C for 2 minutes or pressurized up to 1 bar overpressure for 15 seconds without significantly affecting their stability. At higher pressures and temperatures the microbubbles became unstable and buckled. Addition of crosslinkers like glutaraldehyde and tannic acid resulted in microbubbles that were stable against all tested temperatures and overpressures, more specifically up to 120°C and 4.7 bar, respectively. Buckling was observed above a critical pressure, and was influenced by the shell modulus. We found a relation between the storage temperatures of microbubble dispersions (4°C, 10°C, 15°C and 21°C) and the decrease in the number of microbubbles, with the highest decrease at the highest storage temperature. The average rupture time of microbubbles stored at different storage temperatures followed an Arrhenius relation, with an activation energy for rupture of the shell of about 27 kJ.

This chapter is going to be submitted as:

T.A.M. Rovers, G. Sala, E. van der Linden and M. B.J. Meinders (2015) Effect of temperature and pressure on the stability of protein microbubbles

## Introduction

Protein microbubbles have been used in a range of different areas, like medical diagnostics as contrast agent, clinical research and waste-water purification <sup>1-4</sup>. It has been proposed that microbubbles could be used as ingredients in food systems <sup>5-9</sup>. For applications in the food industry, it is important to gain insights in the stability of microbubbles at different environments and conditions. In *Chapter 3* we investigated the effects of addition of acid and small molecular weight surfactants on the stability of bovine serum albumin (BSA) covered microbubbles. Besides the addition of food ingredients, the microbubble stability might also be influenced by processes typical of the food industry like heating and pressurizing, but also by variations of storage conditions like storage temperature. The literature regarding heat treatment on microbubble dispersions is limited. It has been reported that BSA covered microbubbles stayed intact and formed a gel of microbubbles when subjected to a temperature of 121°C for 15 minutes <sup>6</sup>. To our knowledge, no other results on heat treatments of microbubbles have been published. Experiments applying static pressure showed that human serum albumin covered microbubbles lost their activity as contrast agent after 15 seconds at 0.25 bar <sup>10</sup> and lost 40% of their gas volume after 10 seconds at 1.37 bar <sup>11</sup>. When increasing the overpressure from 0.02 to 1.8 bar for more than an hour, polyester covered microbubbles with a diameter of 1  $\mu\text{m}$  ruptured at pressures around 1 bar for microbubbles <sup>12</sup>. The onset of instability as a result of pressure variations turned out to be mainly determined by the ratio between the shell thickness and the bubble radius ( $\frac{d}{R}$ ) and the Young's elastic modulus (E) of the microbubble shell <sup>12</sup>. The microbubble elastic modulus, measured with Atomic Force Microscopy (AFM), resulted to be dependent on the material used for the shell. The reported values are around 0.6 MPa for lysozyme shells of air-filled microbubbles <sup>13</sup> and about 8 to 40 MPa for phospholipid shells of fluorocarbon gas filled microbubbles <sup>14</sup>. With regard to storage temperature, we showed in *Chapter 2* that after about 36 days all microbubbles stored at 21°C disappeared, while microbubbles stored at 4°C remained intact even after 43 days. When stored at 8°C, the number of BSA microbubble after 14 days of storage diminished in comparison with 2 days of storage <sup>6</sup>, while microbubbles composed

of BSA and dextrose were reported to be stable for more than a year when stored at 5°C <sup>5</sup>.

In this study we investigated the underlying mechanism of microbubble instability as function of changing environments. We analysed the stability of protein covered microbubbles as function of heating temperatures (in the range of 30°C to 120°C), overpressure (ranging from 0 to 4.7 bar) and storage temperature (ranging from 4°C to 21°C).

## **Materials and methods**

### **Materials**

Bovine serum albumin (BSA, fraction V, lot nrs: 100m1900V and SLBC8307V), glutaraldehyde (GA), tannic acid (TA), sodium azide, rhodamine-B and hydrochloric acid (HCl) were purchased from Sigma-Aldrich (St. Louis, MO, USA). For all experiments demineralized water was used.

### **Production of microbubble dispersions**

Microbubbles were produced as previously described in *Chapter 2*. In short, BSA was dissolved in demineralized water at a concentration of 5% (w/w) and the solution was stirred for at least 2 hours. The pH of the solution was adjusted to 6.0 by addition of 2.0 M HCl and 0.2 M HCl. The solution was divided in portions of 25 ml, which were transferred to 50 ml beakers. These specimens were heated for 10 minutes in a 55°C water bath and subsequently sonicated for 3 minutes at power level 8, using a Branson 450 sonicator (Branson Ultrasonics Corporation, Danbury, CT) with a 20kHz, 12.7 mm probe. The probe was placed at the air-water interface of the solution. When protein lot nr 100M1900V was used, samples were sonicated applying a duty cycle of 30%, but when protein lot nr SLBC8307V was used a 60% duty cycle was applied. We reported earlier (*Chapter 2*) that sonicating BSA samples with a 30% duty cycle only resulted in microbubbles when protein lot nr 100M1900V was used, while for other batches a higher duty cycle was required to obtain microbubbles.

### **Chemically crosslinking the proteins in the microbubble shell**

We chemically crosslinked the protein in the microbubble in order to change the microbubble shell properties. Before adding the crosslinking agents, the microbubble dispersion was washed in order to diminish the excess of protein. After preparation, the microbubble dispersions were cooled down to room temperature and were diluted with demineralized water (volume top layer: volume water =1:1). Subsequently, the dispersions were centrifuged for 30 minutes at 300 g. The top layer, mainly consisting of microbubbles, was collected and diluted with demineralized water (volume top layer: volume water =1:4) and subsequently centrifuged for 30 minutes at 300 g. Again, the top layer was collected and kept at 4°C until crosslinking agents were added.

Glutaraldehyde or tannic acid were added to the washed microbubble dispersion to a final crosslinker concentration of 1 mg/ml. After addition of the crosslinker, the microbubble dispersions were stirred for 1 hour before being further used. We tested the samples in such a sequence that a possible effect of the crosslinking time before measurement was eliminated.

### **Stability against buckling at different pressures**

#### **Turbidity of microbubble samples after pressure treatment**

Microbubble dispersion made with BSA batch 100M1900V contained only microbubbles and no protein aggregates. As a consequence, microbubble instability caused by induced pressure could be observed by the transparency of the dispersion. Samples of 1 ml microbubble dispersion (unwashed, washed and washed after crosslinking treatment) were transferred to 2 ml vials. These vials placed in a pressure vessel without screw caps. In the vessel, gas overpressures of 0, 1, 2, 3, 4 and 4.7 bar were applied for 15 seconds. Subsequently, the vessel was decompressed and photographs of the vials were taken. The transparency of the samples was quantified as the light transmission at a height of 120, measured with a dispersion analyser (LUMiFuge, LUM GmbH, Berlin, Germany) at a speed of 200 rpm ( $\approx 4.7$  g).



### **Quantification of the effect of pressure on the disappearance of microbubbles**

Microscope (Axioskop, Carl Zeiss AG, Oberkochen, Germany) images (40x magnification) of  $3.52 \cdot 10^{-7}$  ml of the microbubble dispersions after the pressure treatment were taken with a camera (Axiocam HRc, Carl Zeiss AG, Oberkochen, Germany). From the microscopic picture the number of microbubbles per volume was estimated by image analysis using ImageJ (1.44n, National Institutes of Health, Bethesda, MD).

### **Stability against buckling at different temperatures during heating**

#### **Quantification of the effect of heating on the disappearance of microbubbles**

Samples of 1 ml microbubble dispersion (unwashed, washed and washed after crosslinking treatment) were transferred to 8 ml glass tubes. The glass tubes were placed in an oil bath. After a pre-heating phase of 3 minutes (time required to reach the desire temperature), the samples were kept in the oil bath for 1 or 2 minutes at the following temperatures: 30°C, 50°C, 75°C, 100°C and 120°C. The microbubble dispersions were then taken out of the oil bath and cooled to room temperature. Subsequently, microscope (Axioskop, Carl Zeiss AG, Oberkochen, Germany) images (40x magnification) of  $3.52 \cdot 10^{-7}$  ml of the heated microbubble dispersions were taken with a camera (Axiocam HRc, Carl Zeiss AG, Oberkochen, Germany). From the microscopic picture the number of microbubbles per volume was estimated by image analysis using ImageJ (1.44n, National Institutes of Health, Bethesda, MD).

#### **Heating of samples visualised with light microscope**

Washed microbubble dispersions were placed on an object glass, covered with cover glass and it was sealed using 125 µl Gene Frame adhesive system (Thermo Fisher Scientific, Waltham, MA, USA). The object glasses were placed in an hot-stage (LTS120, Linkam Scientific Instruments, Surrey, United Kingdom) that was placed under a microscope (Axioskop 2 Plus, Carl Zeiss AG, Oberkochen,

Germany). The temperature of the hot-stage increased from 20°C to 90°C with a heating rate of 1°C/minute. Every 5 minutes a picture was made using a camera (Axiocam ERc 5s, Carl Zeiss AG, Oberkochen, Germany) connected to the microscope.

### **Fluorescence microscopy after pressure and heat treatment**

After preparing microbubbles as described in section above, rhodamine-B was added to the microbubble dispersion to a final concentration in the solution of 0.003%. Subsequently, the microbubble dispersions were washed. To part of the washed dispersions glutaraldehyde was added (final concentration 0.1%) and to another part no crosslinking agent was added. Both type of samples were stirred for one hour. Subsequently, they were placed in an pressure vessel, to which 2 bar and 4.7 bar overpressure was applied for 15 seconds. After decompressing the pressure vessel, the microbubble dispersions were stored at 4°C. Micrographs of these dispersions were made with a camera (Axiocam ICc 3, Carl Zeiss AG, Oberkochen, Germany) attached to fluorescence light microscope (Axioskop, Carl Zeiss AG, Oberkochen, Germany), illuminated with a 100W halogen lamp. Similarly, micrographs of the dispersions, heated to 75°C and 120°C, were made using fluorescence light microscopy.

### **Stability against rupture at different storage temperatures**

After preparation, a microbubble dispersion from BSA sample 100M1900V was cooled to room temperature and subsequently transferred to 20 ml vials and stored in climate chambers at 10°C and 15°C, in the refrigerator (4°C), and a thermostated lab (21°C). At predetermined time intervals, microscope (Axioskop, Carl Zeiss AG, Oberkochen, Germany) images (40x magnification) of  $3.52 \cdot 10^{-7}$  ml of the microbubble dispersion were taken with a camera (Axiocam HRc, Carl Zeiss AG, Oberkochen, Germany). From the microscope pictures, the number of microbubbles per volume was estimated by image analysis using ImageJ (1.44n, National Institutes of Health, Bethesda, MD). The portion of intact microbubbles per volume was plotted as function of the storage time for the different storage temperatures.

### **Scanning electron microscopy**

The microbubbles from a washed microbubble dispersion without crosslinker were allowed to adhere on a surface of poly-lysine coated glass and were subsequently submerged in glutaraldehyde to increase fixation to the glass. Thereafter, the samples were put in acetone and air-dried. The air-dried samples were sputtered with platinum or iridium to form a layer of approximately 10 nm. The samples were examined with a FEI Magellan 400 (Hillsboro, OR, USA) electron microscope at room temperature, operating at 2 kHz

## **Results and discussion**

### **Stability against buckling at different pressures**

With increasing applied pressure, the microbubble dispersions became more transparent, as can be seen in Fig. 4.1.

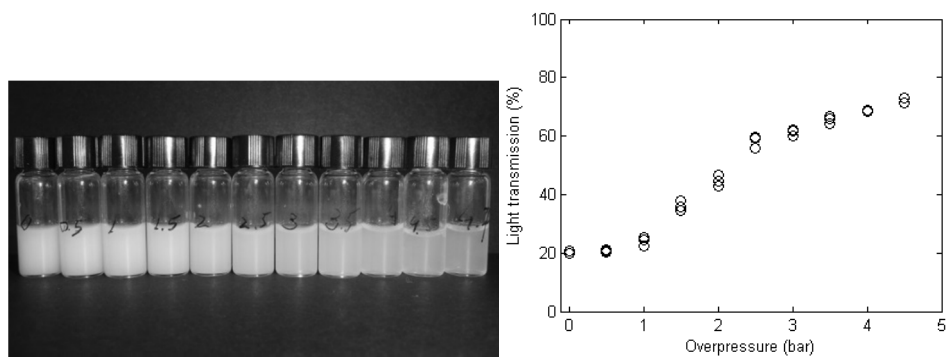


Fig. 4.1. Left: Samples containing microbubbles dispersions pressurized in the pressure vessel: from left to right, increasing order of applied overpressure from 0 bar to 4.7 bar. Right: Light transmission of the microbubble dispersion as function of the applied over pressure.

This decrease in turbidity was caused by the disappearance of the microbubbles upon pressure increase. In order to quantify this disappearance, the number of microbubbles was determined after pressurizing the washed microbubble for 15 seconds. Fig 4.2. shows the relative number of microbubbles after pressure treatment as function of the applied overpressure.

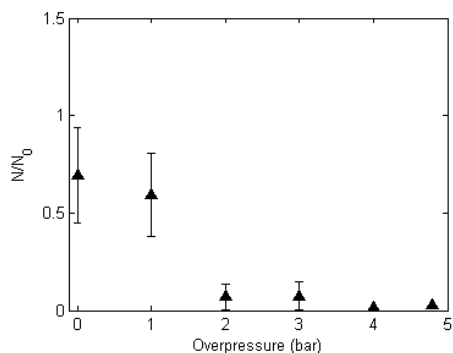


Fig. 4.2.  $N/N_0$  as function of the applied overpressure ( $N$  and  $N_0$ : number of microbubbles per volume after and before the pressure treatment, respectively).

It can be seen that the number of microbubbles decreased with increasing pressure. Dispersions to which a 2 bar overpressure was applied contained hardly any microbubbles. We checked whether the stability could be increased by addition of

crosslinkers. The preparation of BSA gels in which the BSA molecules were crosslinked with glutaraldehyde has been reported (Hopwood, 1998). Also, upon addition of the food-grade crosslinker tannic acid, protein films were shown to strengthen, resulting in higher tensile strength and elongation at break (Nuthong, Benjakul, & Prodpran, 2009). We added glutaraldehyde and tannic acid to our sample before pressure treatment. Fig. 4.3 shows the relative number of microbubbles after the pressure treatment as function of the applied overpressure.

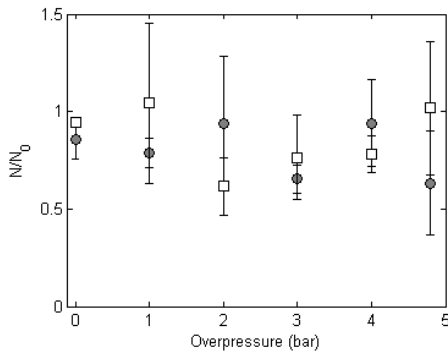


Fig. 4.3.  $N/N_0$  as function of the applied overpressure for microbubble dispersions with added glutaraldehyde (circles) and tannic acid (squares) ( $N$  and  $N_0$ : number of microbubbles per volume after and before the pressure treatment, respectively).

Samples to which a crosslinker was added did not show a decrease in the number of microbubbles upon increasing pressure. Apparently, the shell was reinforced by the crosslinkers, thereby making the microbubbles more stable during the pressure treatment as compared to microbubbles to which no crosslinking agent was added. Fig. 4.4 shows the fluorescence micrograph of a reference sample and of dispersions containing crosslinked microbubbles that were pressurized for 15 seconds at 2 bar and 4.7 bar overpressure.

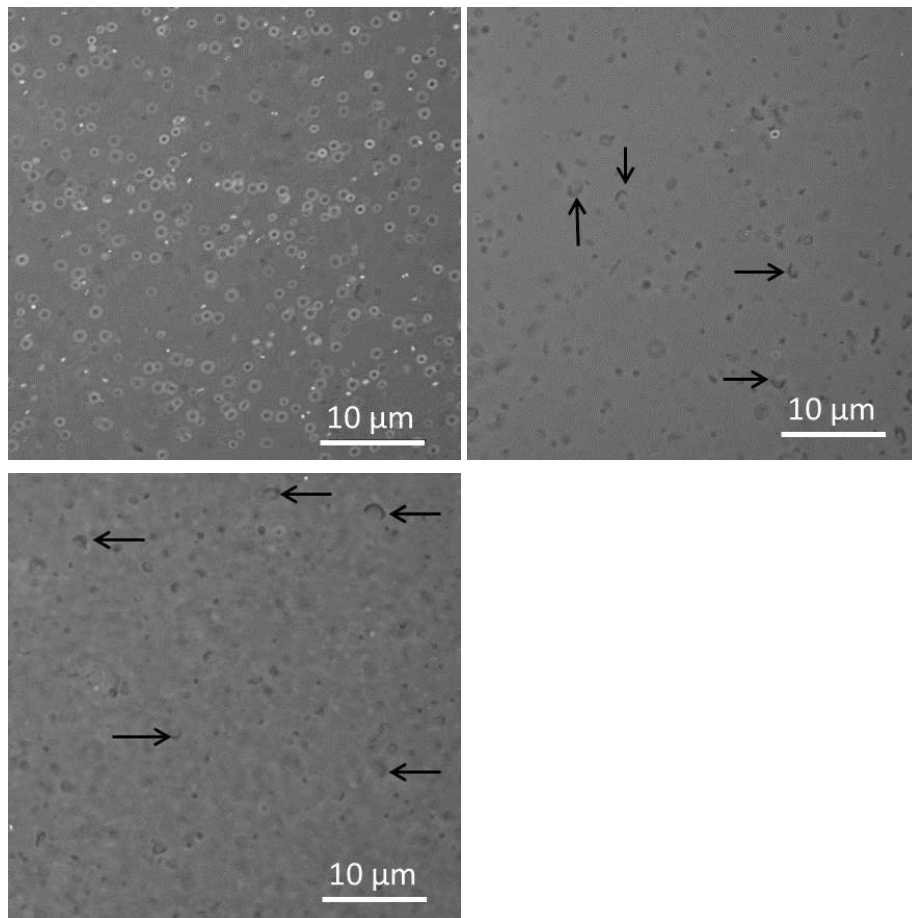


Fig. 4.4. Fluorescence micrographs of a reference washed microbubble dispersion (top left) and of dispersions that were pressurized for 15 seconds at 2 bar overpressure (top right) and for 15 seconds at 4.7 bar overpressure (bottom left). The light circles in the top panel represent the microbubbles; the dark irregular shapes in the middle and bottom panel represent the remainders of the shell after air releasing. The arrows indicate moon-shaped particles.

After the disappearance of the microbubbles, remainders of the microbubbles were visible. The remainders appeared like collapsed microbubbles. These were seen as moon-shaped particles, some of which are indicated with an arrow in Fig. 4.4. Since the shell remained intact and showed a collapsed morphology, we propose that as a result of pressure the microbubbles buckled. After buckling, the air of the microbubble dissolved into the surrounding solution. Fig. 4.5 shows a typical

example of buckled microbubble observed in a former experiment using scanning electron microscopy.

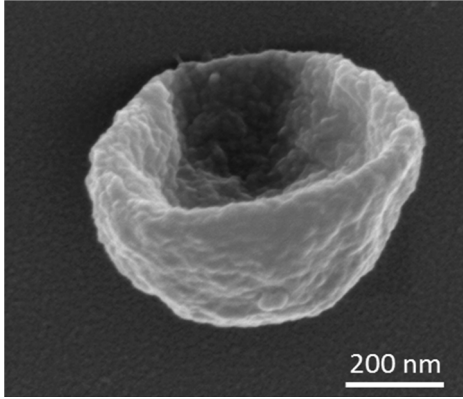


Fig. 4.5. Scanning electron microscopy picture of a buckled microbubble.

Pressure increase results in an increase of air solubility. Therefore, the air from the microbubbles will have a tendency to dissolve and leave the bubble. This will result in an external pressure on the bubble shell. This pressure can be estimated by the sum of the Laplace pressure and the applied overpressure. It has been reported that when this pressure exceeds a critical pressure,  $P_{crit}$ , the shell will buckle<sup>15, 16</sup>:

$$P_{crit} = \frac{2E_B d^2}{R^2 \sqrt{3(1 - \nu^2)}}$$

with  $d$  being the shell thickness ( $\sim 50$  nm),  $\nu$  the Poisson ratio (assumed to be 0.5),  $R$  the bubble radius ( $\sim 500$  nm), and  $E_B$  the bulk Young's modulus of the protein shell.

Based on the parameters typical of our microbubbles, we obtained  $\frac{P_{crit}}{E_b} \approx 0.013$ .

The Laplace pressure was estimated to be 2 bar, assuming a surface tension of 50 mNm<sup>-1</sup>. In Fig. 4.2 it can be seen that the number of microbubbles disappeared between 1 and 2 bar overpressure, implying the critical pressure has a value between 3 and 4 bar. This means that the Young's modulus of the shell was between 23 MPa and 31 MPa. With the addition of crosslinkers (both tannic acid and glutaraldehyde), the microbubbles were stable up to the highest overpressure applied of 4.7 bar. This implies that the elastic modulus of the shell was at least 52

MPa, which represents at least a 2-fold increase compared to the shell modulus without crosslinkers.

High internal phase emulsions (HIPE) in which the emulsion droplets were covered with BSA nanoparticles were reported to show solid like behaviour<sup>17</sup>. A common feature of HIPEs is that the elastic modulus of the HIPE is determined by the elastic modulus of the emulsion droplets, which in turn is determined by that of the interface shell. Upon addition of glutaraldehyde (12.5% as weight percentage of the protein weight), the storage ( $G'$ ) and loss modulus ( $G''$ ) of HIPE showed a 5-fold increase<sup>17</sup>. In our study the amount glutaraldehyde was 20% of the weight of the protein content. A 5-fold increase of the modulus (assumed to be at least 23 MPa) of our microbubbles would lead to a modulus to withstand an overpressure of around 13 bar. We investigated whether the microbubbles with added glutaraldehyde were also stable when pressurized for a longer time (1, 5 and 30 minutes). It was found that after 30 minutes at 2 bar overpressure all the microbubbles remained intact and that more than 50% of the microbubbles could withstand 30 minutes at 4.7 bar.

When we applied pressure on a microbubbles dispersion by screwing a cap on a vial with an excess volume of microbubble dispersion, the dispersion turned from turbid to almost transparent (Fig. 4.6). No difference in turbidity was observed when the dispersion was depressurized by unscrewing the cap. This implies that the microbubbles disappeared during compression and not during decompression.



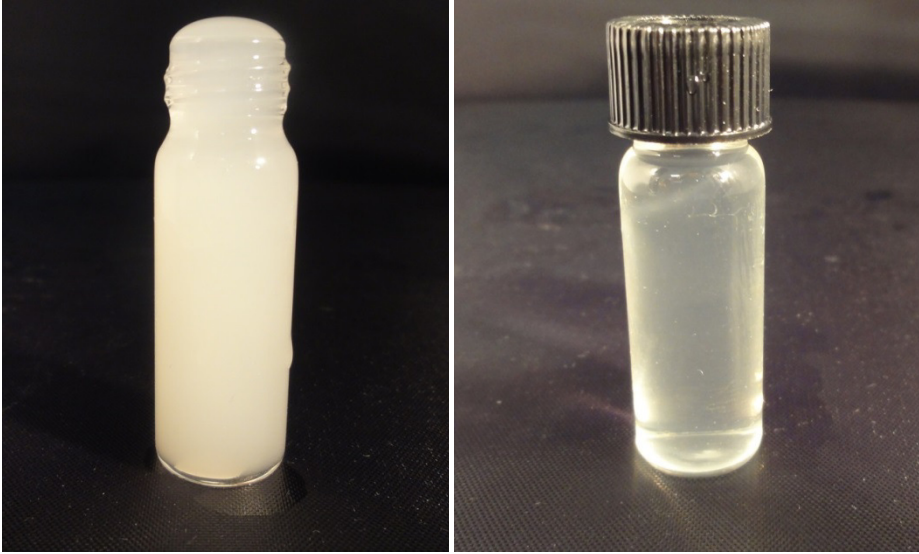


Fig. 4.6. Bottle with an excess volume of microbubble dispersion (left) and the same bottle after it had been closed with a cap (right).

### Stability against buckling upon temperature increase

Washed microbubbles samples to which no crosslinkers were added were heated for 4 and 5 minutes at temperatures ranging from 30°C to 120°C. Fig. 4.7 shows the relative number of microbubbles as function of the temperature during the heat treatment.

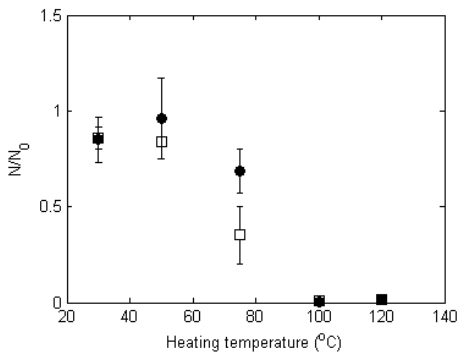


Fig. 4.7.  $N/N_0$  as function of the heating temperature ( $N$  and  $N_0$ : number of microbubbles per volume after and before the heat treatment, respectively; closed symbols: 4 minutes heating; open symbols: 5 minutes heating).

It can be seen that the number of microbubbles did not significantly change when the microbubble dispersion was heated at 30°C and 50°C. However, when heated at 100°C and 120°C, all microbubbles disappeared. At 70°C the sample heated for 5 minutes lost more than half of the microbubbles, while the same sample heated for 4 minutes retained more than half of the microbubbles. After the air dissolved from the microbubbles, the protein shells remained in the suspension. This can clearly be seen in Fig. 4.8, where we show fluorescence micrographs of washed microbubble dispersions heated for 4 minutes at 75°C and 120°C.

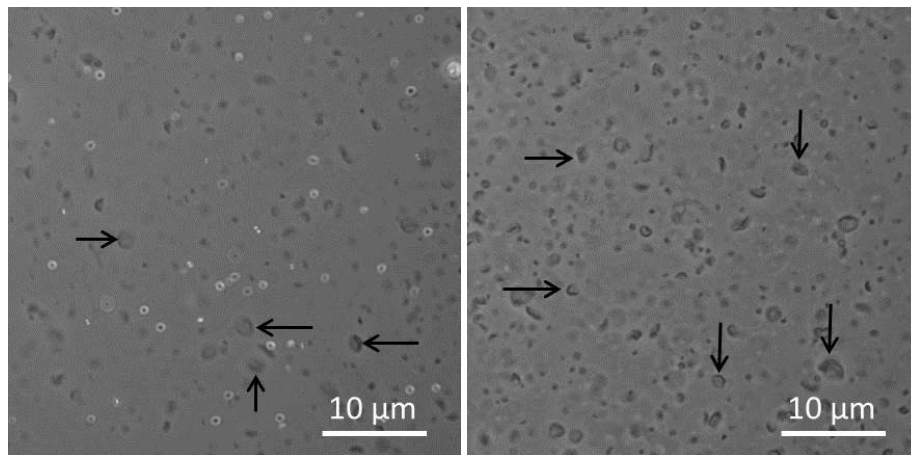


Fig. 4.8. Fluorescence micrographs of washed microbubble dispersions heated for 4 minutes at 75°C (left) or 120°C (right). The light circles in the top panel represent the microbubbles, the dark irregular shapes in both panels represent the remainder of the shell after air releasing. The arrows indicate moon-shaped particles.

In order to better understand how the microbubbles behave at elevated temperatures, a microbubble dispersion was heated under the microscope from 20°C to 90°C, using a hot-stage. Micrographs were made after temperature increase steps of 5°C and the number of microbubbles was estimated using image analysis (results not shown). The error in the measurements was large due to the inaccuracy of sampling and analysis, inherent to the used method. However, the applied method was still much more accurate than others that are commonly used to measure the number of microbubbles in a microbubble suspension, like turbidity measurements that cannot discriminate microbubbles from aggregate (see also

*Chapter 2*). However, despite the large error, we could still conclude that for temperatures up to 55°C the number of microbubbles was comparable to the number microbubbles at 20°C. At temperatures above 55°C, the number of microbubbles decreased by more than 50% (compared to the number at 20°C). The temperatures at which the number of microbubbles decreased coincided with the temperature at which the microbubble volume increased. In Fig. 4.8 we can also see that a large part of the remainders were bigger in size than the (air-filled) microbubbles. This suggests that the air disappeared after the microbubble expanded due to heating the sample. We regard the microbubble as an air bubble for which the Laplace pressure is opposed by the stress in the microbubble shell. Three factors that influence the microbubble volume upon heating were considered: 1) thermal expansion following the ideal gas law, 2) increase in the number of air molecules in the microbubble caused by a decrease of air solubility in water at elevated temperatures (air solubility decreases from 0.020 ml air/ml at 20°C water to 0.015 ml air/ml at 75°C) and 3) elastic stress in the microbubble shell limiting microbubble expansion. Assuming that i) the microbubble will not disproportionate, ii) the elastic modulus of the shell will not change during heating and iii) the difference in total amount of dissolved air between an equilibrated dispersion at 20°C and at elevated temperature of 75°C will go to the microbubble, the contributions of the three above mentioned factors on the microbubble increase in volume could be estimated, using the ideal gas law and rheological properties of a sphere under a homogenous (under)pressure <sup>16</sup>. We found that the volume increase caused by thermal expansion was around 6%, the increase due to the difference in solubility of air was about 11% and the volume decrease owing to the stresses in the microbubble shell was about 5%. This results in a total volume increase of 12%. In *Chapter 2*, we proposed that the shell of BSA stabilised microbubbles might be considered as a thermally induced gel. It was reported in literature that completely hardened BSA gels showed a decrease in  $G'$  of about 30% to 40% when the temperature increased from 20°C to 70°C <sup>18</sup>. This suggests that the shell modulus probably decreases upon heating. Assuming a 40% decrease in the shell modulus results in a volume increase upon heating of 20% instead of 12%.

From the pictures in Fig. 4.8 it can be seen that after the heating treatment and subsequent cooling down, air had disappeared from the microbubble, leaving moon-shaped particles behind. Upon cooling, the volume of gas in the microbubble decreased again, mainly as a result of the increase in air solubility. The temperature of the microbubble decreased from 75°C to 20°C within about 2 seconds. It seems that the elastic modulus of the shell was too low to withstand the stresses due to the fast volume decrease of air, resulting in buckling of the shell quickly after cooling.

The samples to which glutaraldehyde or tannic acid were added were also placed in an oil bath for 4 or 5 minutes at temperatures ranging from 30°C and 120°C. Fig. 4.9 shows the relative number of microbubbles after heat treatment as function of the treatment temperature for these samples.

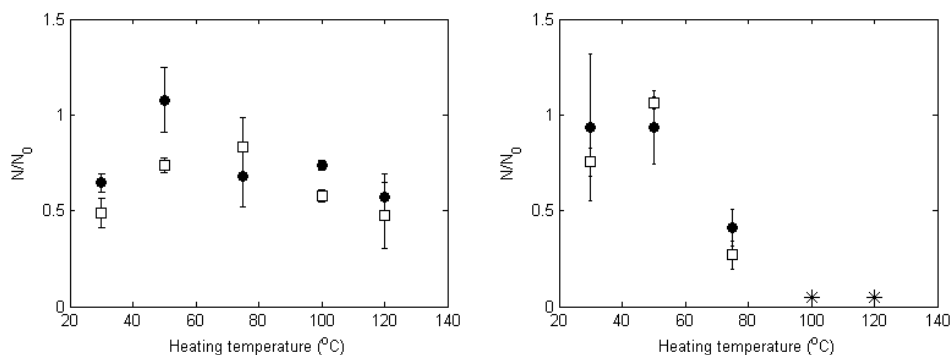


Fig.4.9.  $N/N_0$  as function of the heating temperature for samples with added glutaraldehyde (left) and added tannic acid (right). ( $N$  and  $N_0$ : number of microbubbles per volume after and before the heat treatment, respectively; closed symbols: 4 minutes heating; open symbols: 5 minutes heating) The asterisks correspond to precipitation.

In contrast to the samples without crosslinkers, the samples with glutaraldehyde could be heated up to 120°C without a significant decrease in number of microbubbles compared to the sample at 30°C. As mentioned above, upon addition of glutaraldehyde the modulus of the shell is expected to increase about 5 times. A shell with increased elastic modulus is able to withstand higher pressures before it starts to buckle. Furthermore, an increased modulus restricts the microbubble extension and expansion. Not only the increased modulus, but also the nature of

the bonds between protein molecules make the microbubble less sensitive to temperature change. The interactions in the shell before crosslinking are of a hydrophobic nature (as shown in *Chapter 3*). Addition of glutaraldehyde results in covalent bonds, which are less sensitive to temperature. Assuming that i) the elastic modulus increased by a factor of 5 and ii) the temperature was not affecting the modulus, the volume of the microbubbles was expected to increase by about 2% instead of 12%. The results for the sample with tannic acid were comparable to those of the sample without crosslinkers. The samples with tannic acid heated to 100°C and 120°C formed large aggregates. It has been reported that at high temperatures, when the degree of attachment of tannic acid to protein is high, complexes are formed and precipitate<sup>19</sup>.

### Stability against rupture at different storage temperatures

Microbubble dispersions were stored at different temperatures. In time, the number of microbubbles was measured. The results are shown in Fig. 4.10.

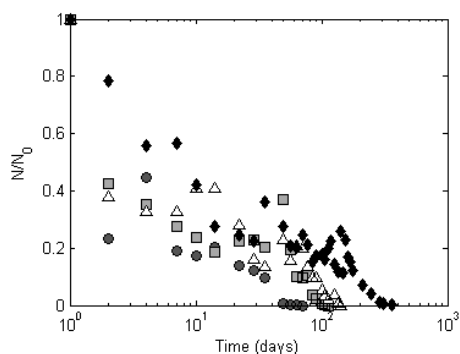


Fig. 4.10.  $N/N_0$  as function of the storage time (on log-linear scale), ( $N$  and  $N_0$ : number of microbubbles per volume after and before the storage, respectively) for different storage temperatures: 4°C (diamonds), 10°C (triangles), 15°C (squares) and 21°C (circles).

As reported in *Chapter 2*, at higher storage temperatures the number of microbubbles decreased faster. In Fig. 4.10 we see that the stability of samples stored at 10°C and 15°C was higher than that of samples stored at 21°C and lower than that of samples stored at 4°C. The difference between the samples stored at 10°C and 15°C was small. We plotted the natural logarithm of the average rupture

time (defined as  $t_b = \frac{\sum_1^n (\Delta N_n \cdot t_n)}{\sum_1^n \Delta N_n}$ , in which  $\Delta N_n = N_n - N_{n-1}$ , with  $N_n$  and  $N_{n-1}$  the number microbubbles per volume on time  $t_n$  and  $t_{n-1}$ ) as function of the inverse storage temperature (Fig. 4.11).

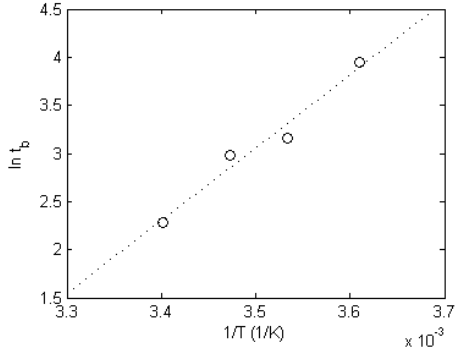


Fig. 4.11. Natural logarithm of the average breaking time,  $t_b$ , as function of the inverse temperature ( $1/T$ ).

Assuming  $t_b \sim e^{E_{act}/kT}$ , with  $E_{act}$  the activation energy to break a molecular bond in the shell, we found from the slope of Fig. 4.11  $E_{act} = 27 \text{ kT}$ . Transferring this value into an energy per characteristic molecular volume ( $4 \cdot 10^{-27} \text{ m}^3$ ) leads to a value of 25 MPa. This compares reasonably well with the Young's modulus of 23 to 30 MPa estimated on the basis of the expression of the critical pressure for buckling.

## **Conclusion**

The stability of protein microbubbles upon heat or pressure treatments depends on the elastic modulus of the microbubble shell and of course on the applied pressure and temperature. When the pressure on a microbubble shell exceeds a certain critical value, the microbubble shell buckles. From this pressure a shell modulus can be estimated. When crosslinkers are added to a microbubble dispersion, the microbubbles stability against pressure and temperature increases. This can be ascribed to an increase in the shell modulus and consequently an increase in the critical buckling pressure. An activation energy to break intermolecular protein bonds can be deduced from the average breaking time for rupture at different storage temperatures. This leads to an estimation of a typical shell modulus which, corresponds well to the estimated value obtained from the critical buckling pressure.

## References

1. F. Cavalieri, M. Ashokkumar, F. Grieser and F. Caruso, *Langmuir*, 2008, **24**, 10078-10083.
2. S. Khuntia, S. K. Majumder and P. Ghosh, *Reviews in Chemical Engineering*, 2012, **28**, 191-221.
3. M. Lee, E. Y. Lee, D. Lee and B. J. Park, *Soft matter*, 2015, **11**, 2067-2079.
4. E. Stride and M. Edirisinghe, *Soft Matter*, 2008, **4**, 2350-2359.
5. M. J. Borrelli, W. D. O'Brien, L. J. Bernock, H. R. Williams, E. Hamilton, J. N. Wu, M. L. Oelze and W. C. Culp, *Ultrasonics Sonochemistry*, 2012, **19**, 198-208.
6. F. L. Tchuénbou-Magaia, N. Al-Rifai, N. E. M. Ishak, I. T. Norton and P. W. Cox, *Journal of Cellular Plastics*, 2011, **47**, 217-232.
7. F. L. Tchuénbou-Magaia and P. W. Cox, *Journal of Texture Studies*, 2011, **42**, 185-196.
8. F. L. Tchuénbou-Magaia, I. T. Norton and P. W. Cox, *Microbubbles with protein coats for healthy food air filled emulsions*, Royal Soc Chemistry, Cambridge, 2010.
9. R. N. Zuniga, U. Kulozik and J. M. Aguilera, *Food Hydrocolloids*, 2011, **25**, 958-967.
10. C. Vuille, M. Nidorf, R. L. Morrissey, J. B. Newell, A. E. Weyman and M. H. Picard, *Journal of the American Society of Echocardiography : official publication of the American Society of Echocardiography*, 1994, **7**, 347-354.
11. S. Podell, C. Burrascano, M. Gaal, B. Golec, J. Maniquis and P. Mehlhaff, *Biotechnology and Applied Biochemistry*, 1999, **30**, 213-223.
12. P. V. Chitnis, P. Lee, J. Mamou, J. S. Allen, M. Böhmer and J. A. Ketterling, *Journal of applied physics*, 2011, **109**, 084906.
13. F. Cavalieri, J. P. Best, C. Perez, J. Tu, F. Caruso, T. J. Matula and M. Ashokkumar, *Acs Applied Materials & Interfaces*, 2013, **5**, 10920-10925.
14. E. Buchner Santos, J. K. Morris, E. Glynos, V. Sboros and V. Koutsos, *Langmuir : the ACS journal of surfaces and colloids*, 2012, **28**, 5753-5760.
15. M. B. J. Meinders and T. van Vliet, *Advances in Colloid and Interface Science*, 2004, **108**, 119-126.
16. W. C. Young, *Roark's formulas for stress & strain*, McGraw-Hill Book Company, 1989.
17. Z. Li, M. Xiao, J. Wang and T. Ngai, *Macromol. Rapid Commun.*, 2013, **34**, 169-174.
18. A. Tobitani and S. B. Ross-Murphy, *Macromolecules*, 1997, **30**, 4845-4854.
19. N. Cao, Y. H. Fu and J. H. He, *Food Hydrocolloids*, 2007, **21**, 575-584.



## Chapter 5:

### Effect of microbubbles on rheological, tribological and sensorial properties of model food systems

---

The rheological and tribological properties of microbubble containing food model systems were compared to the same system without microbubbles and to a system where the microbubbles have been partially or totally replaced by emulsion droplets. The model food systems considered were fluids with and without added thickener and mixed gelatine-agar gels. A sensory test was performed in which we investigated whether panellists could discriminate between samples containing microbubbles, emulsion droplets, or samples containing neither microbubbles or emulsion droplets. It was found that the friction force of emulsions was lower than that of microbubble dispersions and of protein solutions. The emulsions could be well discriminated sensorially from the microbubble dispersions and protein solutions. Samples containing a mixture of emulsion droplets and microbubbles showed friction coefficients comparable to those of samples containing only emulsion droplets. Also microbubble dispersions with and without protein aggregates (induced by sonication during the preparation of the microbubbles) were investigated. The samples with protein aggregates had a much higher viscosity (for fluids with and without thickener) and higher Young's modulus and fracture stress (for the gelled samples). The perceived difference between gelled samples could be mainly explained by the difference in fracture behaviour. We conclude that samples having a volume fraction of 5% microbubbles with sizes around 2  $\mu\text{m}$  sensorially were not comparable to oil-in-water emulsions, and that the same microbubble dispersions were sensorially comparable to protein solutions, implying that microbubbles do not contribute to the mouthfeel at volume fractions of 5% or less.

This chapter is going to be submitted as:

T.A.M. Rovers, G. Sala, E. van der Linden and M. B.J. Meinders (2015) Effect of microbubbles on rheological, tribological and sensorial properties of model food systems

## Introduction

Protein microbubbles have been used in a range of different areas, like diagnostics and clinical research <sup>1-3</sup>. It has been proposed that microbubbles could be used as ingredients in food systems <sup>4-9</sup>. An important reason for this interest to incorporate microbubbles in food systems is the fact that aerated foods are often perceived as creamy<sup>10-12</sup>, and that therefore microbubbles might be used as fat replacers.

The mouthfeel attribute creamy is a multimodal attribute. This means that it is perceived by several different sets of stimulus receptors, resulting in different taste modalities, like thick, soft, and slippery <sup>13</sup>. Several authors linked the creaminess perception of oil-containing products to parameters obtained from instrumental measurements, like viscosity and friction. According to Dresselhuis et al. <sup>14</sup>, friction between the oral surfaces decreases the most when the emulsion droplets are sensitive to surface-induced coalescence. This decrease in friction is positively correlated to sensorially perceived creaminess. For creaminess perception, also viscosity plays an important role. Liquids were described to be perceived as creamy when the viscosity was at the crossover from low viscous fluids (1-1000 mPas) to high viscous fluid (0.1-100 Pas) at shear rates in the range between 10 Hz and 100 Hz <sup>15</sup>.

A few recent studies report about the use of microbubbles in food systems. Microbubbles were investigated as fat replacer, in oil and water emulsions <sup>7, 8</sup>. In these systems, microbubbles covered with bovine serum albumin (BSA), egg white protein (EWP) and hydrophobins were used. Dispersions of microbubbles with a size in the range 1-10  $\mu\text{m}$  and made with EWP had similar friction coefficients as EWP solutions, whereas BSA microbubbles dispersion showed much lower friction coefficients than BSA solutions. Friction was also tested for emulsions in which part of the fat droplets was replaced by microbubbles prepared with EWP or BSA. the mixed samples had friction coefficients comparable to those of the emulsions <sup>7</sup>. The incorporation of emulsion droplets in a gel results in a decrease of the friction coefficient of the sheared gel <sup>16</sup>. Liu et al. <sup>17</sup> and Sala et al. <sup>18</sup> found that gels with unbound droplets exhibit stronger fat-related sensory perception than gels with

bound droplets. Liu et al.<sup>17</sup> related this increased fat-related perception to an increase in coalescence and a decrease in friction.

Gelled systems with microbubbles have not been described so far, but studies on gels and semi-solids in which air bubbles were enclosed have been published<sup>9, 11</sup>. The bubbles in these systems were at least one order of magnitude larger than microbubbles and did not have a rigid shell. Therefore, a direct comparison is difficult.

In this study we compared the effect of microbubbles with the effect of oil droplets on the rheological, tribological and sensorial properties of liquids with and without thickener and of gels. The aim of this comparison was to investigate whether microbubbles might be suitable as fat replacers. Although results of rheological and tribological measurements of model systems containing microbubbles have been published, to our knowledge no sensorial studies have yet been conducted for these systems.

## **Materials and methods**

### **Materials**

Egg white protein (EWP) was kindly donated by Bouwhuis Enthoven (Raalte, the Netherlands). Titanium dioxide (E171) was kindly donated by Pomona Aroma (Hedel, the Netherlands). Rhodamine-B and hydrochloric acid (HCl) were purchased from Sigma-Aldrich (St. Louis, MO, USA). Kappa-carrageenan (GENU texturizer type 101F) and xanthan gum (Keltrol advanced performance) were purchased from CPKelco (Atlanta, GA, USA). Agar (Ferwo Agar 700) was purchased from Caldic Ingredients (Oudewater, The Netherlands) and edible pig skin gelatine (bloom 240-260) was kindly donated by Rousselot (Gent, Belgium). Sugar, vanilla sugar and sunflower oil were purchased at a local supermarket. For all experiments, demineralized water was used.

## **Preparation and storage of the microbubbles**

EWP was dissolved in demi water at a concentration of 7% (w/w), and the EWP solution was stirred for at least 2 hours. The pH of the EWP solution was adjusted to 4.0 by addition of 1.0 M HCl. The acidified protein solution was centrifuged at 4500 rpm for 30 minutes and subsequently filtered. The filtered solution was subdivided in portions of 25 ml, which were transferred to 50 ml beakers. The solutions were heated for 5 minutes in a 50°C water bath and subsequently sonicated for 2 minutes at power level 8 and duty cycle 30% using a Branson 450 sonicator (Branson Ultrasonics Corporation, Danbury, CT) with a 20kHz, 12.7 mm probe. The probe was placed at the air-water interface of the solution. After preparation the microbubble dispersions were cooled down to room temperature and centrifuged for 30 minutes at 400 g. The top layer, mainly consisting of microbubbles, was collected and diluted with demineralized water (volume top layer : volume water = 1:1). The diluted top layer and the remaining dispersions were centrifuged for 30 minutes at 400 g. The top layers of all dispersions were collected and diluted with demineralized water (volume top layer : volume water = 1:9). These diluted dispersions were centrifuged for 30 minutes at 400 g. The top layers of all diluted samples were collected in a 250 or 500 ml plastic container, which was covered with a paper tissue. Samples were quickly frozen by immersing the container in a box with liquid nitrogen. The frozen samples were freeze-dried using the Christ 1-4 LD Plus freeze-drier (Martin Christ Gefriertrocknungsanlagen GmbH, Osterode am Harz, Germany). After freeze-drying, the microbubble powder was stored at 4°C. The microbubble powder was prepared in two batches. For most experiments, the 1<sup>st</sup> batch was used. A specific mention will be made in the text for experiments in which the 2<sup>nd</sup> batch was used. The difference between the preparation and properties of both batches is described in in section '*Preparation of the microbubble dispersions*'.

## **Preparation of the samples**

In this study microbubble dispersions were compared with oil-in-water emulsions and EWP solutions. Samples without thickening agent, with thickening agent and with gelling agent were prepared.

### **Preparation of the microbubble dispersions**

A 50 mg/ml dispersion of the 1<sup>st</sup> batch of freeze-dried microbubbles was made and, after stirring, the sample was centrifuged for 5 minutes at 400g to remove protein aggregates. The microbubbles in this centrifuged sample had an average diameter of 1.8  $\mu\text{m}$  (as obtained by static light scattering, Mastersizer 2000, Malvern Instruments Ltd, Malvern, United Kingdom). The average number of microbubbles was determined as described before in *Chapter 2*. In short, we made microscopic pictures of the samples and using image analysis the number of microbubbles was determined. For the 1<sup>st</sup> batch, the number of microbubbles was  $4.5 \cdot 10^9$  per ml. Based on the size and number of microbubbles, we estimated the volume fraction of microbubbles in this dispersion to be 1.25% (v/v). In order to obtain a volume fraction of 5.0% (v/v), it was determined that a 200 mg/ml dispersion of freeze-dried microbubbles had to be made. The dry matter content of the 200 mg/ml dispersion of freeze-dried microbubbles, consisting of microbubbles, protein and protein aggregates (which were still present, despite the centrifugation step) was determined by weighing the sample before and after overnight drying in an oven at 105°C and was found to be 13.5%. The sensory properties of microbubbles dispersions made with the 1<sup>st</sup> batch of freeze-dried microbubbles were compared to those of an oil-in-water emulsion and an EWP solution. Also these samples were prepared with an EWP concentration of 13.5%. The 2<sup>nd</sup> batch of freeze dried microbubbles was dissolved at a concentration of 15 mg/ml. The microbubbles in the dispersion had an average diameter of 2  $\mu\text{m}$ . The number of microbubbles was  $1.15 \cdot 10^{10}$  per ml. This corresponded to 5% (v/v) of microbubbles. The dry matter content of this sample was 1.08%.

### **Preparation of the oil-in-water emulsions**

A 40% oil-in-water stock emulsion was made by homogenising (by means of a Ariete, NS1001L-Panda homogenizer, Niro Soavi, Parma, Italy) a 1% EWP solution with sunflower oil. This stock emulsion was diluted with an EWP solution to obtain an emulsion with a 5% oil volume fraction and the same protein content as the microbubble dispersion (13.5%).

### **Preparation of the EWP solutions**

EWP solutions were made with the same protein contents as the microbubble dispersions (13.5% and 1.08%). These EWP solutions were diluted, pH-adjusted and centrifuged as described above.

### **Addition of thickening agent and gelling agent**

Concentrated xanthan solutions (2% w/w) were made and heated at 80°C for 30 minutes and subsequently cooled to 40°C. These concentrated solutions were added to the samples (microbubble dispersion, oil-in-water emulsion, EWP solution and water) in order to obtain a xanthan concentration of 0.2% in the water phase of the system.

Concentrated solutions (10% w/w) of a mixture of gelatine and agar (8.13% gelatine and 1.88% agar) were made and heated to 80°C for 30 minutes and subsequently cooled to 40°C. These concentrated solutions were added to the samples (microbubble dispersion, oil-in-water emulsion, EWP solution and water) in order to obtain a gelling agent concentration, expressed on the water phase, of 4.0%, (3.25% gelatine and 0.75% agar).

### Addition of other components

To all samples also 10% (w/w) sugar and 0.2% (w/w) vanilla sugar were added in order to mask the smell and taste of the EWP. Furthermore,  $\kappa$ -carrageenan (0.1%, w/w) was added to partly screen the positive charges of the proteins. As a colorant, 0.2% (w/w) titanium dioxide was added so that also samples without emulsion droplets would acquire a milky white appearance. In Tab. 5.1, the composition of all samples is summarized. In this table the amount of sugar, vanilla sugar, titanium dioxide and  $\kappa$ -carrageenan is reported as '10.5% additives'.

Tab. 5.1. Composition of the samples.

	Blank	EWP solution	O/W emulsion	MB dispersion
<b>Liquid</b>	10.5%	13.5% EWP	5.0 % oil	13.5% EWP
<b>without</b>	additives	10.5% additives	13.5% EWP	10.5% additives
<b>thickener</b>	89.5% water	76.0% water	10.5% additives 71.0% water	76.0% water
<b>Liquid</b>		1.08% EWP		<i>2<sup>nd</sup> batch</i>
<b>without</b>		10.5% additives		1.08% EWP
<b>thickener</b>		88.4% water		10.5% additives
<b>(2nd batch)</b>				88.4% water
<b>Liquid with</b>	10.5%	13.5% EWP	5.0 % oil	13.5% EWP
<b>thickener</b>	additives	10.5% additives	13.5% EWP	10.5% additives
	0.18% xanthan	0.15% xanthan	10.5% additives	0.15% xanthan
	89.3% water	75.8% water	0.14% xanthan 70.6% water	75.8% water
<b>Gels</b>	10.5%	13.5% EWP	5.0 % oil	13.5% EWP
	additives	10.5% additives	13.5% EWP	10.5% additives
	3.58% gelling	3.04% gelling	10.5% additives	3.04% gelling
	agent	agent	2.84% gelling	agent
	85.9% water	73.0% water	agent 68.2% water	73.0% water

### **Mixtures of samples**

For one specific experiment, mixtures of the microbubble dispersions (*'Preparation of the microbubble dispersions'*) and the oil-in-water emulsions (*'Preparation of the oil-in-water emulsions'*) were made. The samples were prepared with the following ratios (v/v) of oil-in-water emulsion: 0%, 25%, 50%, 75% and 100%, corresponding to oil volume fractions of respectively 0%, 1.25%, 2.50%, 3.75% and 5.0%.

### **Rheological measurements of the samples**

#### **Small deformation measurements of the liquid samples**

The viscosity of the liquid samples was measured with a rheometer (Anton Paar MC502 rheometer Graz, Austria), using a double gap geometry (DG 26.7/Ti). Viscosities were measured at shear rates from 1 Hz to 1000 Hz at a constant temperature of 21°C. Every sample was measured in duplicate.

#### **Large deformation measurements of the gels**

After adding the gelling agents, the samples were transferred to paraffin-lubricated tubes and stored at 4°C overnight. Gels were cut into cylindrical pieces (2 cm × 2 cm) using a steel wire. From each sample, 4 cylindrical pieces were measured. A compression test was performed using a Texture Analyzer (TA-Xt plus, Stable Micro Systems Ltd., Godalming, U.K.). Paraffin oil was applied to the top and bottom surface of the cylinder, allowing sufficient lubrication. Samples were compressed in a single compression test to 90% of their initial height at a compression speed of 1 mm/s. The Young's modulus and the fracture stress and strain were determined.

#### **Tribological measurement of the samples**

The tribological properties of the samples were determined with a self-built Optical Tribological Configuration (OTC), using the same method as described by Liu et al<sup>17</sup>. In short, the samples were sheared in the OTC between two surfaces. The upper surface was a flat-bottom rough rubber (PDMS) probe and the lower



surface was glass. 150 µl of the liquids and gels (squeezed through a syringe in which it was gelled) were placed on the bottom surface of the OTC. The load between the upper surface and sample was 0.5 N. During each measurement the lower glass plate was oscillating 10 cycles over a distance of 16 mm at an increasing oscillating speed from 10 mm/s to 80 mm/s, with incremental steps of 10 mm/s. During the movement of the glass plate, the friction force was determined. Each measurement was performed at room temperature and for each measurement a new probe was used. The surfaces of the probe and glass were cleaned with ethanol and water before each measurement. All measurements were conducted in triplicate.

## **Sensory test**

### **Panellists**

In total 7 panellists were selected among students and staff of the Wageningen University. They were selected on their ability to rank oil-in-water emulsion with different volume fractions of oil (1%, 5% and 10%).

### **Tetrad testing**

Due to limitations in the preparation of large amounts of microbubbles, a sensory tests was chosen for which relatively small amounts of samples were required. Therefore, we decided to perform as a first screening a discrimination test, the tetrad test. The selected panellists performed a tetrad test in which 4 samples were presented in random order; 2 samples of one set and 2 samples of another set. The panellists were asked to group the 4 samples in 2 groups of 2 samples, based on similarity. The number of panellists that were able to correctly distinguish one set from another was determined. In total 7 tetrad combinations were presented to the panellists (Tab. 5.2). After assessing each sample the panellists were asked to rinse their mouth with water.

Tab. 5.2. Overview of presented tetrad combinations.

<b>Tetrad number</b>	<b>Set 1 (two samples)</b>	<b>Set 2 (two samples)</b>
1	MB dispersion without thickener	O/W emulsion without thickener
2	O/W emulsion without thickener	EWP solution without thickener
3	MB dispersion (2 <sup>nd</sup> batch) without thickener	EWP solution (2 <sup>nd</sup> batch) without thickener
4	MB dispersion with thickener	O/W emulsion with thickener
5	O/W emulsion with thickener	EWP solution with thickener
6	Gelled MB dispersion	Gelled O/W emulsion
7	Gelled O/W emulsion	Gelled EWP solution

### Samples used in the sensory tests

The samples were prepared as described above. 5 ml of every sample was transferred to 20 ml cups, which were closed with a lid and stored overnight at 4°C. Every sample was coded with a randomized 3-digit number.

### Microstructure

The microstructure of liquid samples was visualized before and after rheological measurements in order to unveil possible changes as a result of shearing in the rheometer. Microscopy (Axioskop, Carl Zeiss AG, Oberkochen, Germany) images (40x) were taken with a camera (Axiocam HRc, Carl Zeiss AG, Oberkochen, Germany). The microstructure of the mixed samples was visualized before and after shearing with the OTC. Microscopy (Reichert Polyvar, Leica Microsystems, Wetzlar, Germany) images (40x) were taken with a camera (Leica MC120 HD, Leica Microsystems, Wetzlar, Germany).

Rhodamine-B was added to the gels to reach a final concentration of 0.003%. The samples were placed in cuvettes (especially designed for CLSM) and allowed to gel overnight at 4°C. Confocal Laser Scanning Microscopy (CSLM) images were recorded on a Leica TCS SP5 Confocal Laser Scanning microscope (Leica Microsystems CMS GmbH, Mannheim, Germany) equipped with an inverted microscope (Leica DM IRBE), using an Ar/Kr visible light laser.

## Results and discussion

### Rheological properties of the studied samples

The viscosity of all liquid samples was determined at shear rates ranging from 1 Hz to 1000 Hz. Fig. 5.1 shows the values of the viscosity at a shear rate around 50 Hz. We choose to present the values of the viscosity obtained at this shear rate because it was reported that the viscosity at shear rates in the range between 10 Hz and 100 Hz can be related to the creamy perception<sup>15</sup>.

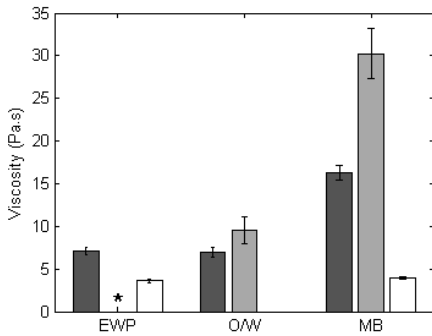


Fig. 5.1. Viscosity of liquids without thickener (dark grey), liquids with thickener (light grey) and liquids without thickener prepared with the 2<sup>nd</sup> microbubble powder batch (white) at a shear rate of 49.1 Hz.

The viscosity of the microbubble dispersion without thickener prepared with the 1<sup>st</sup> freeze-dried microbubbles batch was clearly higher than that of the protein solution and the oil-in-water emulsion. Most probably the higher viscosity was caused by the presence of small amounts of protein aggregates in the 1<sup>st</sup> microbubbles batch (Fig. 5.2)

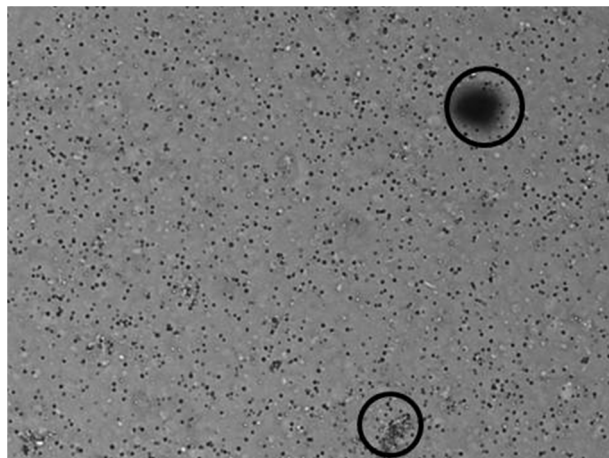


Fig. 5.2. Micrograph of a microbubbles dispersion without thickener. The encircled spots indicate protein aggregates.

Since we assumed that these protein aggregates would affect the rheological, tribological and sensorial properties of the samples, an additional batch of freeze-dried microbubbles was made in order to perform measurements with microbubbles dispersions with a much lower protein aggregate content. As mentioned above, a lower amount of the 2<sup>nd</sup> batch powder was needed to get a microbubble volume fraction of 5%. As a consequence of the lower amount of aggregates in the 2<sup>nd</sup> batch, the microbubble dispersion made with this batch had a significantly lower viscosity than that prepared with the 1<sup>st</sup> batch. This 2<sup>nd</sup> batch was only used to prepare fluid samples without thickener and was only analysed in one of the tetrad combinations. The samples for tribology and large deformations rheology experiments and for the majority of the sensory tests were made from the 1<sup>st</sup> batch. For the samples prepared with the 2<sup>nd</sup> batch, only the viscosity was determined.

As expected, also the viscosity of the protein solution with a protein concentration of 13.5% (w/w) was higher than that with a protein concentration of 1.08% (w/w). The viscosities of the emulsions and microbubble dispersion with thickener were obviously higher than those of these samples without thickener. The viscosity of the thickened protein solution could not be determined properly, since it contained large aggregates (not shown).

For the gels, the effect of microbubbles on Young's modulus, fracture stress and fracture strain was compared to that of emulsion droplets (Fig. 5.3)

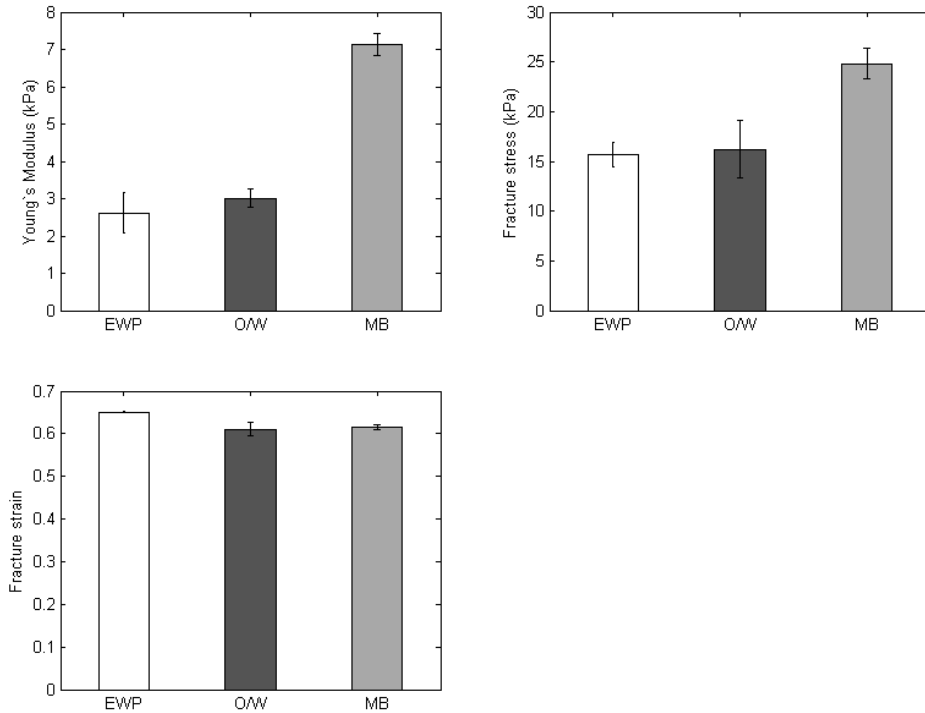


Fig. 5.3. Young's modulus (top left), fracture stress (top right) and fracture strain (bottom left) of gels without fillers (white), with emulsion droplets (dark grey) and with microbubbles (light grey).

The Young's modulus and fracture stress of gels without fillers were similar to those of gels with emulsion droplets, while for gels with microbubbles the values of these parameters were significantly higher. The fracture strain of the sample without filler was slightly higher than that of the samples with filler, which implies that the fillers made the gels slightly more brittle. As mentioned before, the microbubble dispersion contained, besides microbubbles, also protein aggregates. This was also observed for the gels with microbubbles (not shown). Sala et al.<sup>19</sup> showed that with increasing volume fraction of bound fillers the Young's modulus increases. In our case the concentration of fillers was higher in the gels with microbubbles (since besides the microbubbles, also the protein aggregates might

act as filler) than in the gels with emulsion droplets or in the gels without fillers. This resulted in a higher Young's modulus for the gels with microbubbles. Contrary to Sala et al.<sup>19</sup>, we observed that an increase in the concentration in bound fillers resulted in an increase in fracture stress. We cannot explain the underlying reason for this difference. We note that Sala et al.<sup>19</sup> studied emulsion-filled gels in which the gel matrix consisted only of gelatine, while in our study the gel matrix consisted of gelatine and agar.

### Tribological properties of studied samples

In Fig 5.4. the friction force of the liquid samples with and without thickener is shown.

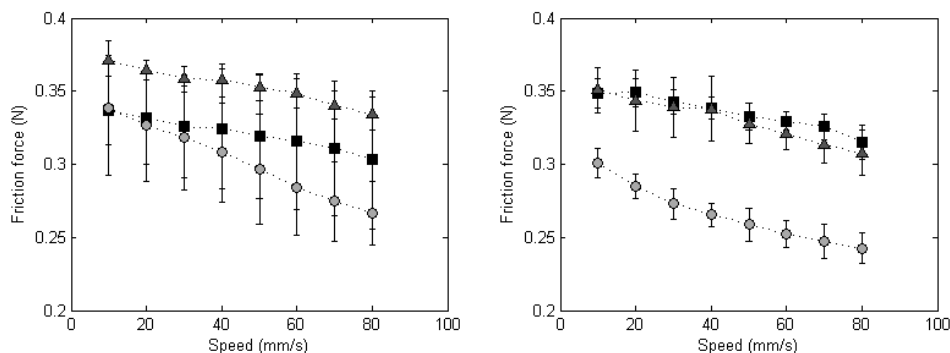


Fig. 5.4. Friction force as function of the speed for liquids without (left) and with (right) thickener. EWP (triangle), oil-in-water-emulsion (circle) and microbubble dispersion (square).

For the liquids without thickener, it can be seen that the friction force of the microbubble dispersion was higher than that of the oil-in-water emulsion, but lower than that of protein solution. For the thickened samples, the friction force of the microbubble dispersion was comparable to that of the protein solution, while the friction force of the oil-in-water emulsion was much lower. The friction force was also determined for mixtures of microbubble dispersions and oil-in-water emulsions without thickener (Fig. 5.5).

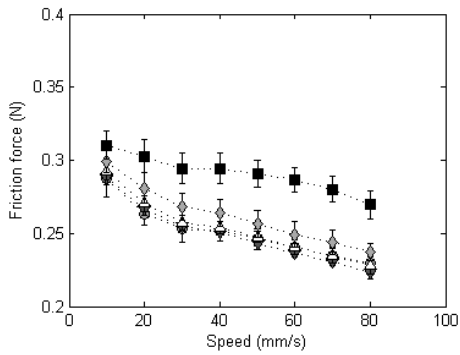


Fig. 5.5. Friction force as function of the speed for mixtures of oil-in-water-emulsion and microbubble dispersion at the different oil volume fractions: 0% (square), 1.25% (diamond), 2.50% (upward triangle), 3.75% (downward triangle) and 5.0% (circle).

Upon addition of 1.25% emulsion droplets, the friction force of the microbubble dispersion approached that of the 5% oil-in water emulsion. The mixtures with 2.50% and 3.75% oil had comparable friction curves as the emulsion with 5% oil. Micrographs of the mixed samples were made before and after shearing with the OTC (Fig. 5.6).

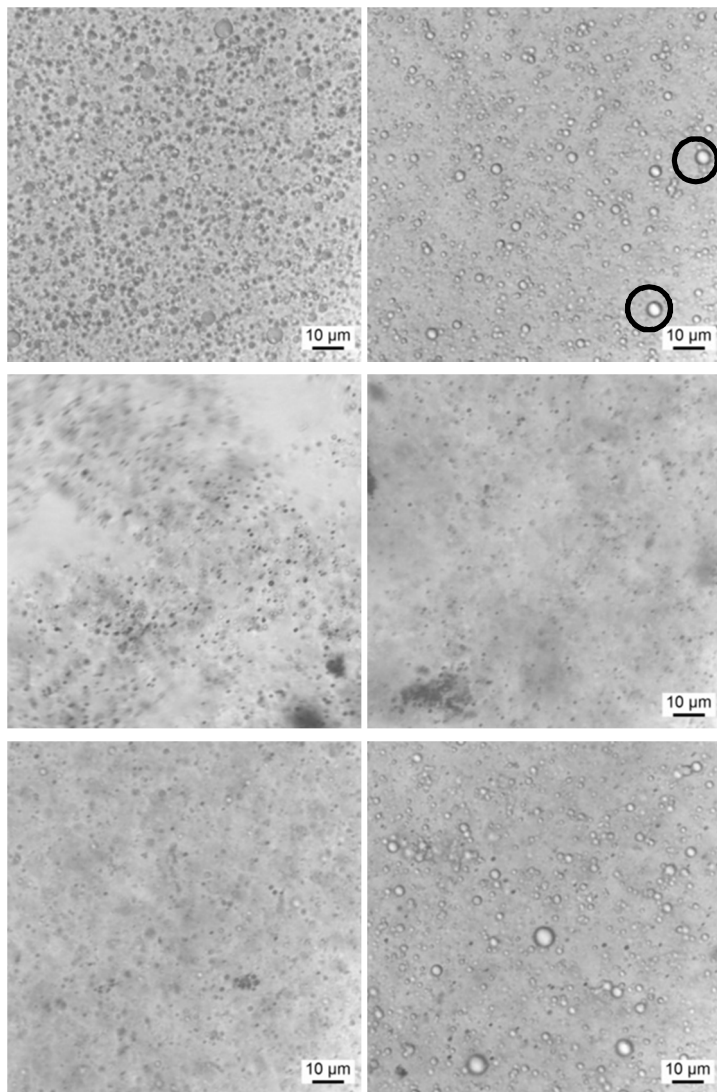


Fig. 5.6. Micrographs of emulsions (top) and microbubble dispersions (middle) before (left) and after (right) shearing, and of mixed samples after shearing (bottom) containing 1.25% oil (left) and 2.50% oil (right).

The encircled parts of the top right picture of Fig. 5.6 show emulsion droplets that are larger than those before shearing (top left of Fig. 5.6), which indicates that the emulsion droplets coalesced during measurement in the OTC. The microbubbles stayed intact during the shearing. The lower friction of the emulsion as compared



to the microbubbles dispersion could be ascribed to the coalescence of the emulsion droplets. As previously reported, friction can be lowered by the formation of an oil film on a surface as a result of coalescence of emulsion droplets<sup>14</sup>. The formation of an oil film can explain the lower friction of emulsion compared to the other two samples (MB dispersion and EWP solution). The friction can also be lowered by a ball-bearing mechanism<sup>20</sup>. It has been reported that the modulus of a particles in a dispersion influences its friction: particles with a higher elastic modulus will give a lower friction compared to particles with lower modulus<sup>21</sup>. We reported in *Chapter 4* that the modulus of the microbubble is in the order of magnitude of megaPascals, while the modulus of the emulsion droplets is in the order of kilopascals. This implies that based on the ball bearing mechanism it was expected that the microbubble dispersion would have a lower friction than the emulsion. Since we found a lower friction for the emulsion we can conclude that in our systems the formation of an oil film had a more pronounced effect on the friction than the bear-ball mechanism.

Our finding that already a low oil concentration (1.25%) was sufficient to decrease friction to values typical of emulsions with higher oil volume fractions is in agreement with another study that showed that the friction of a 1% (v/v) oil-in-water emulsion was comparable to that of a 40% (v/v) emulsion<sup>14</sup>. This indicates that the microbubbles did not contribute significantly to the friction in the mixed samples. A previous study on mixtures of microbubbles dispersions and emulsions also showed comparable friction forces for the mixed sample and the oil-in-water emulsion<sup>7</sup>. However, in that study oil concentrations between 18% and 36% were used, which were much higher than the 1.25% used in our study. . A simple comparison between our data and those of Tchenbou-Magaia and Cox<sup>14</sup> is not possible also because in the latter study friction was measured using a ball-disc set-up, while in our study we used a parallel plate geometry. The main difference between the two geometries is that the contact area between two parallel plates is larger than that between the ball and the disc. Consequently, the friction forces are slightly higher when using the parallel plate geometry.

The friction force was also determined for the gelled samples (Fig. 5.7).

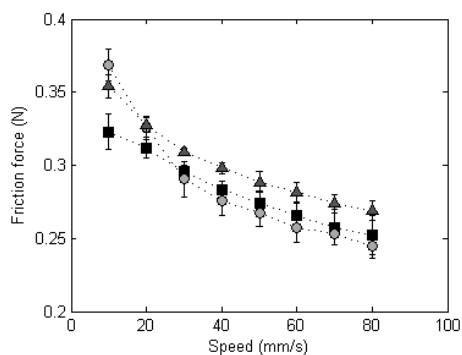


Fig. 5.7. Friction force as function of the speed for gelled EWP solution (triangle), oil-in-water-emulsion (circle) and microbubble dispersion (square).

The friction values of the different gelled samples showed only minor differences. The values measured at the higher speed followed the same order as the liquid samples (from high to low: protein solution, microbubble dispersion and oil-in-water emulsion). We assume that the two mechanisms described above for liquids can explain the differences in friction also for gelled samples.

### Sensory evaluation

We determined the number of panellists that could correctly group together two samples of two sets when four samples were offered. The results of this test are shown in Tab. 5.3.

Tab. 5.3. Discrimination ability of the panel members between two sets of samples.

Set 1 (two samples)	Set 2 (two samples)	Percentage of panellists that correctly distinguished between the two sets
<b>MB dispersion without thickener</b>	O/W emulsion without thickener	85.7%
<b>MB dispersion with thickener</b>	O/W emulsion with thickener	100%
<b>Gelled MB dispersion</b>	Gelled O/W emulsion	85.7%
<b>MB dispersion (2<sup>nd</sup> batch) without thickener</b>	EWP solution (2 <sup>nd</sup> batch) without thickener	42.9%
<b>O/W emulsion without thickener</b>	EWP solution without thickener	100%
<b>O/W emulsion with thickener</b>	EWP solution with thickener	100%
<b>Gelled O/W emulsion</b>	Gelled EWP solution	100%

For all studied food systems, all panellists were able to discriminate the samples of oil-in-water emulsion from those consisting of a protein solution. For the tetrad with microbubbles dispersions and oil-in-water emulsions without thickener and the tetrad with gelled microbubbles dispersions and gelled oil-in-water emulsions, the majority of the panellists could well distinguish between samples from the two sets. Only one combination was offered with microbubble dispersions and protein solutions. This was a tetrad with microbubbles from the 2<sup>nd</sup> batch. We can conclude that panellists could not discriminate between protein solution and microbubble dispersion, since more than half of the panellist did not correctly distinguish between the two sets of samples in this tetrad combination.

Since the viscosity of emulsions and protein solutions were comparable, we suggest that these samples could be distinguished because of the difference in friction which was lower for the oil-in-water emulsion.

All the samples of this study had a viscosity significantly higher than 1000 mPa·s at 50 Hz, which means that they can be considered as highly viscous fluids <sup>15</sup>. Since

liquids are considered as most creamy at the cross-over viscosity between high viscous and low viscous fluids, we expect that our sample could not be perceived as creamy <sup>15</sup>.

The majority of the panellists could distinguish between emulsion and microbubble dispersion. The samples differed in viscosity, probably because of the presence of the protein aggregates in the microbubble dispersion. Also the friction was different, with a lower friction for the emulsion, probably caused by the formation of an oil film. We saw above that perceived differences between the emulsions and the protein solutions could be attributed to friction alone. The large difference in viscosities even further facilitated the panellist to distinguish between emulsions and microbubble dispersions.

The gel with emulsion droplets could be easily discriminated from both the other gels. The perceived difference from the gelled microbubble dispersion can be ascribed to the difference in fracture stress and Young's modulus: the gel with microbubbles was stiffer and stronger. The discrimination of the gel with emulsion droplets from the gelled protein solution can be ascribed to the slightly higher fracture strain and friction force of the latter.

The reason for the incorrect discrimination between microbubble dispersions and protein solution from the 2<sup>nd</sup> batch might be found in the fact that these samples had a comparable viscosity. Other factors that could facilitate the panellists to make the distinction between samples, like the presence of protein aggregates or the possible formation of an oil layer, lacked in these samples.

For samples with larger air bubbles (20 to 200  $\mu\text{m}$ ) in a semi-solid food system, it was reported that at air volume fractions of 5% air bubbles could not mimic emulsion droplets, while it was claimed that at volume fractions of 80% small air bubbles are perceived as more 'creamy', thereby somewhat mimicking emulsion droplets <sup>11</sup>. However, it was also noted that these samples were far less creamy than oil containing samples <sup>11</sup>.

Knowing that microbubbles decrease friction less than emulsion droplets and expecting that microbubbles are perceived as less creamy than emulsion droplets, it is not likely that microbubbles can substitute emulsion droplets as fat replacer.

This consideration is further supported by the fact that in our study the friction of mixed samples was comparable to that of an emulsion with 5% oil, which indicates that only the oil had an influence on friction.

## **Conclusion**

The lubrication properties of oil-in-water emulsions were better than those of microbubble dispersions and protein solutions. This difference in friction might be the main reason of the fact that most panellists could distinguish between oil-in-water emulsion and samples without oil. In mixtures of emulsion and microbubble dispersion the friction was largely determined by the oil, while the contribution of the microbubble was limited. For gels, the differences in fracture behaviour could explain why the different samples could be well discriminated. In general, we can conclude that the sensory properties of microbubbles dispersions with microbubbles up to a volume fraction of 5% and having size of about 2  $\mu\text{m}$  are not comparable to those of emulsions with similar oil-droplet volume fractions and sizes. The feasibility of using microbubbles as fat replacers should be further studied at higher volume fractions or with microbubbles with different physicochemical properties.

## **Acknowledgements**

We would like to acknowledge Franklin Zoet, Jaap Hulstein and Nick van Lanen for their assistance in the preparation of the freeze-dried microbubbles and the sensory samples. We gratefully thank Bouwhuis Enthoven and Pomona Aroma for their donation of, respectively, egg white protein, and titanium dioxide.

## References

1. F. Cavalieri, M. Ashokkumar, F. Grieser and F. Caruso, *Langmuir*, 2008, **24**, 10078-10083.
2. M. Lee, E. Y. Lee, D. Lee and B. J. Park, *Soft matter*, 2015, **11**, 2067-2079.
3. E. Stride and M. Edirisinghe, *Soft Matter*, 2008, **4**, 2350-2359.
4. J. Benjamins, A. Sein, and C. van Vliet *United States of America Pat.*, 2002, patent nr US2002/0155208.
5. M. J. Borrelli, W. D. O'Brien, L. J. Bernock, H. R. Williams, E. Hamilton, J. N. Wu, M. L. Oelze and W. C. Culp, *Ultrasonics Sonochemistry*, 2012, **19**, 198-208.
6. F. L. Tchuénbou-Magaia, N. Al-Rifai, N. E. M. Ishak, I. T. Norton and P. W. Cox, *Journal of Cellular Plastics*, 2011, **47**, 217-232.
7. F. L. Tchuénbou-Magaia and P. W. Cox, *Journal of Texture Studies*, 2011, **42**, 185-196.
8. F. L. Tchuénbou-Magaia, I. T. Norton and P. W. Cox, *Microbubbles with protein coats for healthy food air filled emulsions*, Royal Soc Chemistry, Cambridge, 2010.
9. R. N. Zuniga, U. Kulozik and J. M. Aguilera, *Food Hydrocolloids*, 2011, **25**, 958-967.
10. D. Kilcast and S. Clegg, *Food Quality and Preference*, 2002, **13**, 609-623.
11. M. Minor, M. H. Vingerhoeds, F. D. Zoet, R. de Wijk and G. A. van Aken, *International Journal of Food Science and Technology*, 2009, **44**, 735-747.
12. H. Wildmoser, J. Scheiwiller and E. J. Windhab, *LWT - Food Science and Technology*, 2004, **37**, 881-891.
13. J. L. Kokini and E. L. Cussler, *Journal of Food Science*, 1983, **48**, 1221-1225.
14. D. M. Dresselhuys, H. J. Klok, M. A. C. Stuart, R. J. de Vries, G. A. van Aken and E. H. A. de Hoog, *Food Biophysics*, 2007, **2**, 158-171.
15. G. A. Van Aken, in *Understanding and controlling the microstructure of complex foods*, ed. D. J. McClements, 2007, ch. 17, pp. 449-482.
16. A. Chojnicka, G. Sala, C. G. de Kruif and F. van de Velde, *Food Hydrocolloids*, 2009, **23**, 1038-1046.
17. K. Liu, M. Stieger, E. van der Linden and F. V. De Velde, *Food Hydrocolloids*, 2015, **44**, 244-259.
18. G. Sala, F. van de Velde, M. A. C. Stuart and G. A. van Aken, *Food Hydrocolloids*, 2007, **21**, 977-985.
19. G. Sala, T. van Vliet, M. A. C. Stuart, G. A. van Aken and F. van de Velde, *Food Hydrocolloids*, 2009, **23**, 1381-1393.
20. B. J. Hamrock and D. Dowson, 1981.
21. D. A. Garrec and I. T. Norton, *Food Hydrocolloids*, 2013, **33**, 160-167.

# Chapter 6:

## General Discussion

---

## Introduction

Microbubbles are a subject of research in many areas, like medical imaging, waste water purification, and therapeutics. Lately, microbubbles have received the attention of food researchers who proposed that microbubbles can be made from food ingredients and might be used in food systems <sup>1-5</sup>. In order to be able to evaluate the feasibility of the incorporation of microbubbles in food systems, it is important to know the effect of preparation parameters on the yield and stability of the microbubbles. Also it requires understanding of the stability of the microbubbles in the presence of ingredients present in real food systems, and as a function of temperature and pressure. Finally, the behaviour and effects of food systems, in which microbubbles are incorporated, should be understood (e.g. breakdown behaviour, texture, and creaminess). In particular, the effect of microbubbles on tribological, rheological and sensorial characteristics of food systems should be investigated. This thesis addresses the above mentioned topics and aims to investigate the key parameters for application of microbubbles in food systems. In Fig 6.1 a schematic overview of the thesis is given.



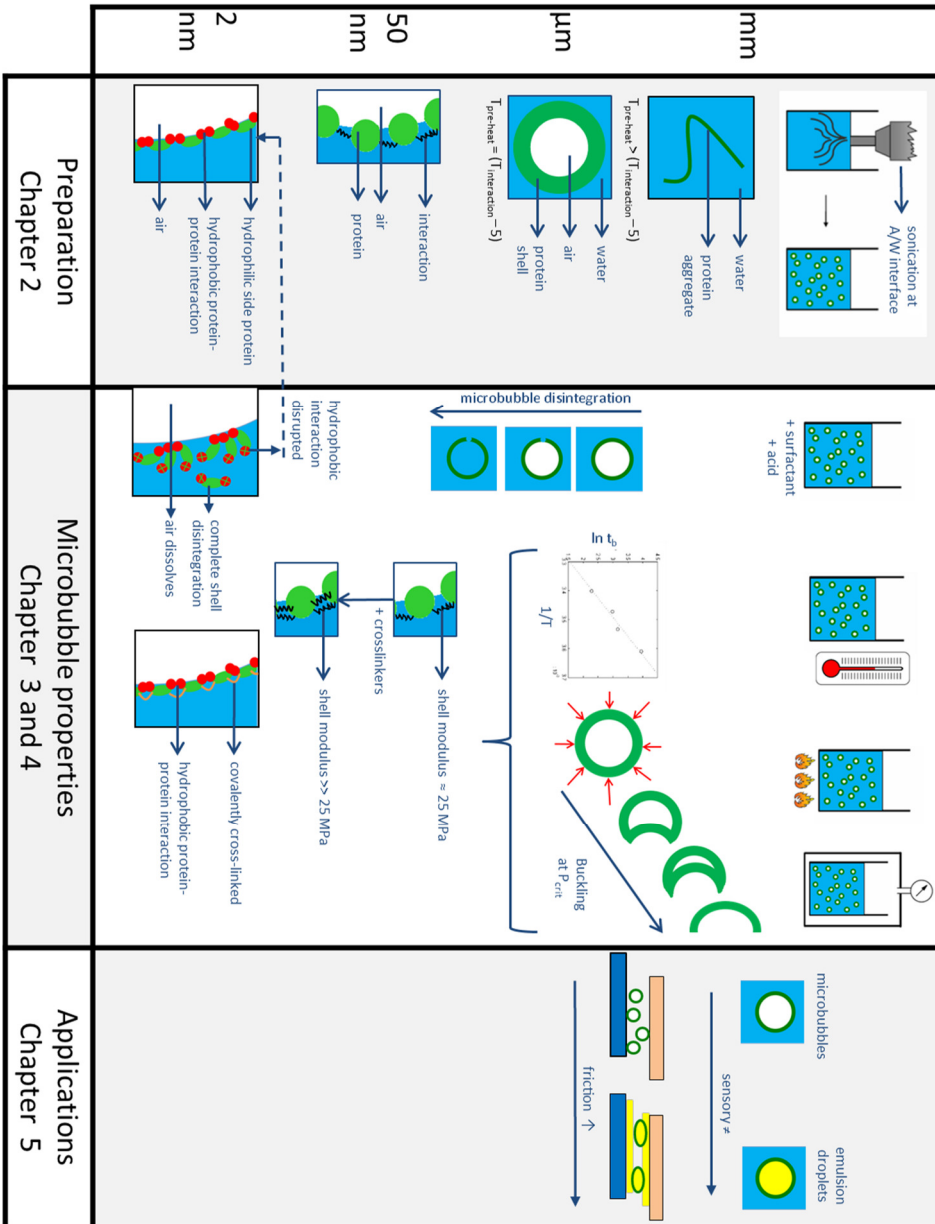


Fig 6.1 Overview of the research topics and main findings of the thesis

## Mechanism of microbubbles formation

The properties of protein stabilized microbubbles depend on the preparation parameters <sup>2-4, 6, 7</sup>. Whereas other groups investigated the influence of the sonication parameters, like the frequency, sonication power and sonication time <sup>3, 6, 7</sup>, we focussed on the effect of protein concentration pH, ionic strength and temperature on the yield and stability of BSA microbubbles. In the first part of sonication, air bubbles are introduced in the liquid and broken down into smaller particles <sup>8</sup> (see also Fig. 1.1). During this phase of sonication, the air bubbles become covered with protein. In *Chapter 2* we show that the pH and ionic strength influence the coverage of the interface and, consequently, the yield of microbubbles. The effect of pH <sup>1, 4</sup> and salt <sup>1</sup> on microbubble yield and stability have already been described by other authors. In our study we investigated the combined effect of pH and ionic strength, also in relation to the coverage of the air bubble at the beginning of sonication. We showed that the highest coverage is obtained when the pH is close to the iso-electric point of the BSA.

During the second phase of sonication, air bubbles violently collapse and a temperature transition zone emerges at the air-water interface with slightly higher temperatures than in the liquid <sup>9, 10</sup>. It is believed that the microbubble shell is formed in this temperature transition zone at the bubble interface <sup>10</sup> as a result of heat-induced protein-protein interactions. Furthermore, sonication results in heating of the solution, which causes formation of protein aggregates. As mentioned in *Chapter 2*, during 3 minutes sonication the bulk temperature of the protein solution increases by about 5°C above the pretreatment temperature of 55°C. For the protein batch 100M1900V, which was mostly used in *Chapter 2*, we found that at a final temperature of 60°C the highest number of microbubbles was obtained, without aggregates formation. For solution temperatures closer to and above the denaturation temperature (63°C <sup>11, 12</sup>), protein aggregate formation is enhanced and efficiency of microbubble formation is thereby decreased. This is in agreement with the earlier reported findings that only in a narrow range of sonication powers and sonication times microbubbles were obtained <sup>7</sup>. The temperature increases with both the power and the sonication time. When the

power or the sonication time are too low, no microbubbles are formed, while at too high power or sonication time, only protein aggregates are formed <sup>7</sup>. Using a pretreatment temperature of 55°C, we found that the obtained microbubble had a shell thickness of about 50 nm, comparable to reported values of shell thicknesses of BSA stabilized microbubbles <sup>10</sup>. We assume that this thick layer is formed according to the mechanism described in the General Introduction and in literature <sup>13</sup>. The importance of the layer thickness is further described in the section *Shell properties*.

Another important finding of *Chapter 2* is that the ability to make microbubbles at certain conditions is dependent on the protein batch. Using the same sonication settings as used for the production of microbubble with batch 100M1900V, no microbubbles were obtained with other BSA batches. However, increasing the so called duty cycle from 30% to 90% resulted in microbubble formation. The increase in duty cycle was always accompanied by the formation of aggregates. Thus, an increase in duty cycle will result in both an increase in number of microbubbles and the amount of protein aggregates. A consequence of increasing the duty cycle is an increase in incorporation of air and in temperature of the solution<sup>14</sup>. The introduction of more air will result in more microbubbles, while an increase in temperature of the solution might result in more microbubbles and/or in more protein aggregates (depending on the exact final temperature).

When further studying the effect of temperature on the formation of protein aggregates, a relation was found between the amount of aggregates and the temperature difference between the measured denaturation temperature (obtained with differential scanning calorimetry, DSC) and the end temperature of the solution (cf. Fig. 6.2).

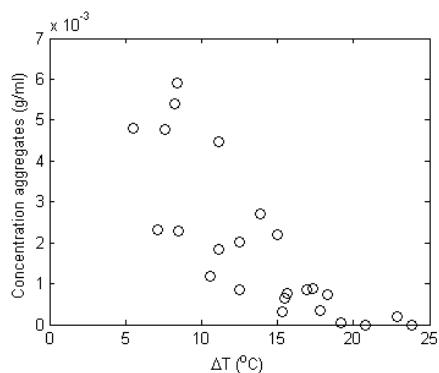


Fig. 6.2. Concentration of protein aggregates as function of the temperature difference ( $\Delta T$ ) between the measured denaturation temperature (obtained with DSC) and the end temperature of the solution.

As can be seen in Fig. 6.2, when the solution temperature was close to the denaturation temperature of the protein (low  $\Delta T$ ) the highest amount of aggregates was formed. The temperatures at which the highest number of microbubbles was obtained for the different protein batches could not be related to any molecular parameter we measured (denaturation time, denaturation enthalpy, zeta-potential, secondary structure, anion composition, anion content, presence of peptides, and hydrophobicity). We therefore hypothesize that the differences in microbubble formation between the protein batches is due to the molecular properties that determine the temperature at which the protein molecules start to interact at the air-water interface, due to (small) changes in conformation.

Sonication is reported to be the method that results in the highest yield. However, although the studied process parameters were optimised to obtain the highest yield, the volume fraction of incorporated air is still very low, as well as the fraction of the protein that ends up in the microbubble shell. Both are in the order of 1% and depend on the protein batch. Microbubbles can be concentrated by centrifugation and collecting the resulting top layer, consisting of microbubbles. After skimming of the microbubbles, the remaining solution still contained a high concentration of BSA. This protein solution could be reused to obtain microbubbles at comparable yields and with comparable characteristics as those made from 'fresh' protein solution. The microbubbles also can be freeze-dried, and subsequently redispersed in aqueous solutions without changing the microbubble

properties. We conclude that by applying a post-sonication treatment, higher volume fractions can be obtained and more proteins end up in the microbubble shell.

## Interactions in the microbubble shell

The nature of the interactions between proteins in the microbubble shell is subject of debate in literature. Two kinds of interactions are proposed. According to several authors the interactions between the proteins are covalent disulphide bonds<sup>15, 16</sup>. It is claimed that during sonication free radicals, like superoxide, are produced, which oxidize the cysteine groups of the protein, inducing inter-protein disulphide bonds<sup>15, 16</sup>. As mentioned in the Introduction, some researchers specifically use cysteine-rich protein to form microbubbles<sup>4</sup>, while others deliberately made cysteine groups available in order to produce microbubbles<sup>3, 7</sup>. Thus, it seems that the presence of covalent interactions in the shell are generally accepted as the main mechanism in the formation of the microbubble shell. However some researchers claim that non-covalent interactions are formed as a function of the temperature during sonication<sup>17, 18</sup>. One of these studies reported that microbubbles could be made with proteins without cysteine<sup>17</sup>, and another one that robust microspheres can be made from poly-glutamate<sup>18</sup>.

In *Chapter 3* we showed that upon addition of low concentrations of surfactants (sucrose laurate, Tween 20, and SDS) and acid, the microbubbles disappear. Moreover, after disappearance of the microbubble the remaining shell is further disintegrated into particles with size comparable to that of the monomeric BSA molecule. It has been reported that the surfactants sucrose laurate, Tween 20, and SDS bind to the hydrophobic patches of the BSA molecule, with binding energies of around 30 kJ/mol ( $\sim 10$  kT)<sup>19-22</sup>. This indicates that the surfactants added to our microbubbles bind to the hydrophobic patches of the BSA molecules in the shell, which results in the complete shell disintegration. We conclude that the interactions between proteins in the microbubble shell are most probably hydrophobic, and that the complex formation between the surfactants and the BSA molecules disrupts these protein-protein interactions.

We further confirmed the possible presence of hydrophobic interactions by addition of several concentrations of SDS before sonication. We measured the change in hydrophobicity of BSA upon SDS addition before sonication and the number of microbubbles after sonication of BSA solutions containing SDS. Fig. 6.3 shows the hydrophobicity and the number of microbubbles for different molar ratios [SDS]:[BSA].

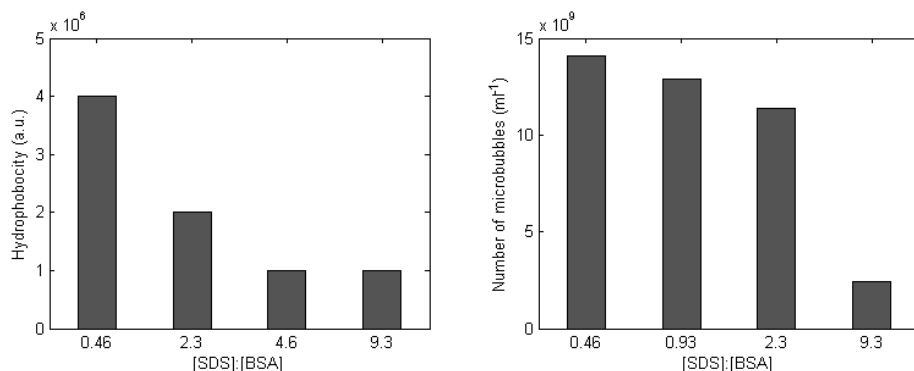


Fig 6.3 Hydrophobicity of BSA solution with several [SDS]:[BSA] ratios (left) and number of microbubbles prepared with the solutions with varying ratios (right.)

BSA molecules to which SDS was added at the highest concentration resulted in lowest hydrophobicity and the lowest number of microbubbles after sonication. It has to be noted that the hydrophobicity of the BSA solution with added SDS is different from the hydrophobicity of the samples during sonication. As noted above, during sonication protein molecules reveal their hydrophobic patch as function of the temperature. We consider three detrimental effects of the addition of SDS on the number of microbubbles. First the occupation of hydrophobic patches of the protein by SDS (changing the protein-protein interactions), secondly, adsorption of SDS to the air-water interface (causing a lower BSA adsorption), and thirdly, interference by SDS with the partially unfolding of the BSA. Currently the relative importance of these factors is not totally clear.

We found that when SDS was added after the production of microbubbles, the average breaking time of microbubbles from the sample with [SDS]:[BSA] ratio of 9.2 (8.98 min) differed from that with a ratio of 1.0 (192 min) by a factor 21. The

difference between the number of microbubble obtained at ratios 9.3 and 0.9 when SDS was added before sonication was a factor 5.

We investigated whether covalent crosslinking between proteins in the shell could prevent the microbubble disintegration by surfactants. The crosslinking was induced by means of glutaraldehyde addition. The crosslinking effect was investigated by comparing samples reinforced with 0.1% of the crosslinker glutaraldehyde and samples without glutaraldehyde. Upon addition of 0.1% SDS to a washed microbubble dispersions ( $[SDS]:[BSA] = 25.9$ ), the microbubble stability was tested (Fig 6.4).



Fig 6.4. Micrographs of microbubble dispersions without glutaraldehyde before (top left) and directly after SDS addition (top right) and of dispersions with 0.1% glutaraldehyde before addition of SDS (bottom left) and 8 hours after SDS addition (bottom right).

As can be seen in the top right picture of Fig 6.4, the microbubbles without crosslinkers disappeared directly after addition of SDS. The microbubbles to which glutaraldehyde was added remained stable, even 8 hours after addition of SDS.

This confirms that the covalent interactions between the protein molecules in the microbubble shell makes the shell stable against SDS.

Interestingly, Tchuénbou-Magaia et al. <sup>4</sup> reported about a microbubble system in which a surfactant was present, that did not destabilize the microbubble. In the described food system microbubbles were added to an oil in water emulsion stabilised by Tween 60. The microbubbles in the mixture were still intact after 2 months. The reason for the difference in stability upon surfactant addition is not known.

Similarly to what we observed for SDS, we also found that when the fluorescent dye FITC was added to BSA before sonication, no microbubbles could be produced. We also found upon addition of different rennets microbubbles disintegrated. Although we know that both FITC and the rennets interact with specific parts of the BSA molecule, the exact underlying mechanism of the disintegration remains unclear.

We verified that the prevention of the disintegration upon the addition of the crosslinker glutaraldehyde is not only limited to the prevention of the disintegration by SDS. We found that also the disintegration of microbubbles by different rennets can be prevented by the addition of glutaraldehyde, as can be seen in Fig 6.5.

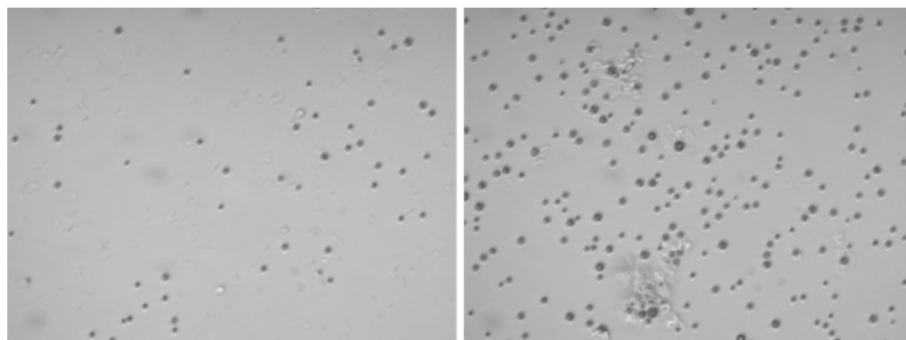


*Fig 6.5 Micrographs of washed microbubble dispersions diluted in milk permeate 300 minutes (45 minutes at 34°C, followed by 255 minutes at 20°C) after addition of 0.02% rennet without glutaraldehyde (left) and with 0.1% glutaraldehyde (right).*



Microbubbles also became unstable and disappeared upon addition of small amounts of acid, lowering the pH from 6.0 to values between 3.3 and 4.1. We expect that the disintegration is caused by the increased repulsion between the proteins within in the shell and by the conformational change of BSA due to the acid addition. In literature it has been described that at pH values lower than 5.0 the BSA molecule changes its configuration from a compact (N) to an extended (F) one <sup>23</sup>. This conformational change leads to higher excluded volume for every BSA molecule, resulting in a lower preferred surface coverage <sup>24</sup>, thereby destabilising the microbubble shell. We note that, in all experiments in which the microbubbles were destabilized by acid, the pH was lower than the isoelectric point of the BSA, resulting in an increased repulsion between the proteins in the shell.

Summarizing the above, the following picture regarding the mechanisms leading to microbubble formation together with the molecular interactions within the shell emerges. First, the protein adsorbs to the air water interface with its hydrophobic parts directed to the air. Due to the temperature increase during sonication, the protein molecules partly unfold and additional hydrophobic patches of the protein are revealed. This leads to hydrophobic protein-protein interactions. Subsequently a multi-layer network of hydrophobic interacting proteins is formed at the microbubble interface. This multi-layer network acts as a shell.

The properties of this shell, such as its modulus and its thickness are important for the microbubble stability. These properties are further discussed in the following section.

## Shell properties

In *Chapter 4* we showed that when a microbubble dispersion is pressurized or cooled after being heated, the microbubbles can buckle. We argued that this buckling is related to the fact that the pressure difference between inner and outer phase of the bubble exceeds a critical value. This argument has also been used to describe buckling of emulsion droplets <sup>25, 26</sup> and lipid covered microbubbles <sup>27</sup>. The critical value of the excess pressure is (1) proportional to the elastic modulus of the

microbubble shell, (2) proportional to the square of the shell thickness and (3) inversely proportional to the square of microbubble radius<sup>28</sup>.

From the experimental values of the excess pressures at which the microbubbles started to buckle during the pressure or heat/cool treatment, it was found that the elastic modulus of the shell had a value about 25 MPa. This value of 25 MPa was also deduced from estimation of the activation energy to break the molecular bonds in the shell. This activation energy was derived from the relationship between the storage temperature of microbubble dispersions and the number of microbubbles. A third way to estimate the elastic modulus stems from experiments on the surface dilatational modulus of an air bubble covered with BSA molecules after it was heated to 74°C, using a drop tensiometer. Fig. 6.6 depicts the surface dilatational modulus as function of time.

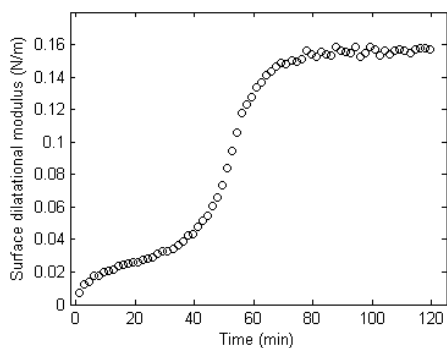


Fig 6.6. Surface dilatational modulus as function of time for a BSA covered air bubble heated at 74°C.

Converting this surface dilatational modulus to an elastic modulus ( $E = \frac{E_d}{d}$ , in which  $E$  is the elastic modulus,  $E_d$  the surface modulus and  $d$  the thickness of the layer), we obtain a value for the elastic modulus of 30 MPa (using  $E_d = 0.15$  N/m and a layer thickness of  $d = 5$  nm). A direct measurement of the modulus of the microbubble shell is possible by using atomic force microscopy<sup>29,30</sup>.

The protein density in the microbubble shell largely determines the modulus of the shell. When we convert the values of shear moduli of heat-induced BSA gels into elastic moduli<sup>31</sup>, we find that macroscopic BSA gels made from a BSA solution of 50 kg/m<sup>3</sup> have an elastic modulus that is more than 1000 times lower than the

modulus we found for the gel-like microbubble shell. This difference might be related to the concentration of protein in the shell, which in the microbubble shell is higher than  $50 \text{ kg/m}^3$ . It is reported that the relation between the protein concentration and the elastic modulus follows a power law <sup>32</sup>. Based on this power law one can estimate (cf. *Chapter 2*) the protein concentration in the gel-like shell to be at least  $300 \text{ kg/m}^3$ . This would imply a protein packing density of at least 22%, an eminently reasonable value.

We found in *Chapter 4* that the elastic modulus can be increased by the addition of crosslinkers. It was shown that upon addition of crosslinkers the microbubbles became stable against all applied pressures and temperatures. We expect that upon addition of the crosslinkers the shell modulus increases 5-fold, making the shell more stable against buckling <sup>33</sup>. Non-food grade (glutaraldehyde) and food grade (tannic acid) crosslinkers were added. For both, it is known that they enhance protein gel strength <sup>33, 34</sup>.

The modulus of the microbubble shell has, besides an elastic component, also a viscous component. This viscous component determines creep within the microbubble shell. Creep occurs when a constant pressure is put on a material. It is known that creep is temperature dependent. Higher temperature will make the creep to occur at a faster rate. In addition, at higher temperature the activation energy will be overcome more effectively, according to the Arrhenius equation. Both effects point to an increased number of bubbles disappearing per unit of time upon increasing temperature.

In *Chapter 2* we report that microbubbles generally tend to decrease in size to a radius of 320 to 350 nm after their original formation. The reason for this change in size could be found in a flux of air to the head space of the solution. The reason why the shrinkage stops at a radius of 350 nm is not exactly known. Due to a reduction in size, a higher critical excess pressure is needed for buckling. We assume that as a consequence of this reduction in size the microbubble shell became thicker, which results in an even larger critical excess pressure. Fig 6.7 schematically depicts this mechanism.

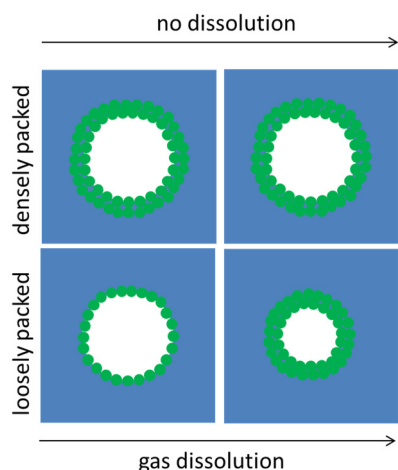


Fig 6.7 Schematic representation of the relation between packing density in the microbubble shell and microbubble shrinkage, modified after Lee et al.<sup>35</sup>

For practical applications it is worthwhile to summarise the conditions at which microbubbles are stable, both with and without crosslinkers. Without crosslinkers microbubbles could be pressurized up to 1 bar overpressure for 15 seconds, and heated up to 50°C for 2 minutes before cooling down, without a significant decrease in the number of microbubbles, while at higher pressures and temperatures, the microbubbles were not stable anymore. After the microbubble shell had been reinforced, by internal crosslinking of the proteins, the microbubbles were stable at all pressures and temperatures up to 4.7 bar overpressure and up to 120°C, respectively. When not crosslinked and kept at room temperature, the microbubbles disappeared all within a few days. In another study microbubbles disappeared at room temperature within a few hours<sup>2</sup>. When stored at 4°C, 25% of the microbubbles remained intact, comparable to other studies<sup>2,3</sup>.

From the current section the following picture regarding shell properties emerges. The hydrophobic protein-protein interactions yield a modulus to the shell. Addition of crosslinkers yield a higher elastic modulus of the shell. This results in much more stable microbubbles. The modulus and thickness define a critical pressure above which the microbubbles buckle.

We have already mentioned that sonication is not an effective method to create microbubbles. It is however being reported as the one method giving the highest yield. Furthermore, the sonication method is reported to yield the most stable microbubbles. Despite these positive annotations, the hydrophobic protein-protein interactions are too weak to have the microbubble withstand normal storage conditions (room temperature and atmospheric pressure) for longer than a few days. This instability can be counteracted by crosslinking the proteins. Overall, the sonication method has its limitations but all of its limitations can be overcome by using the appropriate post-sonication treatment.

## **Applications of microbubbles in food**

Several applications of microbubbles in food systems can be envisaged. We have investigated the suitability of microbubbles to be dispersed in real food systems. For milk, acidified milk and sunflower oil microbubbles could be dispersed. For milk and acidified milk the microbubbles were found to be stable for at least an hour, for the sunflower oil the microbubbles were observed microscopically directly after dispersing, but no storage tests were performed.

Microbubbles can be added to model food systems as fillers, for example in a gel. When this filler is bound to the gel and has a higher modulus than the gel matrix, the elastic modulus of the gel will increase<sup>36, 37</sup>. It has been reported that aerated products are perceived as 'creamy', an attribute mostly related to fat containing foods<sup>38-40</sup>. Since microbubbles have a size in the same order of that of emulsion droplets, the feasibility of their application as fat replacers can be a relevant research topic as well.

In our work we investigated the sensory functionality of microbubbles in model food systems (emulsion systems). To our knowledge, this is the first study on the possible sensorial effects of microbubbles in a food matrix. This part of the work is described in *Chapter 5*. From this study the following conclusions were derived. Firstly, replacing emulsion droplets by microbubbles changes the mouthfeel. Secondly, removing emulsion droplets from the emulsion and leaving behind a protein solution also changes the mouthfeel. Thirdly, addition of microbubbles to a

protein solution does not change the mouthfeel. This indicates that microbubbles, given their size of  $\sim 1\ \mu\text{m}$  and volume fraction of 5%, did not contribute to a specific mouthfeel.

## Concluding remarks and outlook

In this thesis we investigated the production and stability of protein-stabilized microbubbles and investigated application of microbubbles in a model food. In this general discussion, we described the main mechanisms leading to microbubble formation and stability. The following overarching perspective can be outlined.

During sonication, increasing temperatures at the air/water interface make the proteins reveal their hydrophobic patches which causes hydrophobic protein-protein interactions. These interacting proteins form a multilayer network at the air-water interface, i.e. the shell of the microbubble. The hydrophobic interactions within the shell can be weakened by a whole array of components (surfactants, acid, rennets, FITC), all resulting in disintegration of the microbubbles. The stability against pressure and heat could be related to a critical pressure beyond which buckling occurs. To obtain a larger critical pressure against buckling, a larger elastic modulus, smaller radius and/or larger shell thickness are/is needed. Sonication is an ineffective method to obtain large volume fractions of air, to efficiently employ protein, and to control the interactions within the microbubbles shell and thereby its elastic modulus. However, using post sonication treatments all these limitations can be overcome. Microbubbles can be concentrated by centrifugation. The non-used protein in the remaining solution can be re-used and microbubbles can be freeze dried, stored under dry conditions, and re-dispersed into solution. Furthermore, the elastic modulus of the microbubbles can be tuned by the addition of crosslinkers. By the addition of crosslinkers, microbubbles are stabilized against the addition of all components and against all pressures and temperatures.

With regard to the application of microbubbles in food, we found that the microbubbles can be readily dispersed in several food systems. We also found that microbubbles with size of about  $0.8\ \mu\text{m}$  do not contribute to the mouthfeel in

protein solutions and are not suitable as a fat replacer at volume fractions of 5%. Clearly more work is needed to fully establish the suitability for use of microbubbles in foods, including fat replacement.

An important step to bridge the current knowledge gap in the applicability of microbubbles in foods is to be able to make them in different sizes. We have applied some methods which seem promising with regard to increasing the size of the microbubbles. For instance, applying a continuous flow during sonication yields slightly larger microbubbles. Stirring the sample during sonication yielded a high polydispersity, with the largest bubble being significantly larger than the largest microbubble obtained without stirring. Using coaxial electrohydrodynamic atomization (CEHDA), microbubbles could be obtained that are very monodisperse in size. The CEHDA method yields larger droplets than sonication. As such the exploration of this CEHDA method is worthwhile to consider.

A second important aspect for exploring applications of microbubbles in food is the microbubble stability, which is related to the previous aspect. This aspect is important in attaining a wider size range, since large microbubbles will buckle and disproportionate faster.

A third aspect is to explore different proteins for their suitability to form microbubbles and their effect on shell thickness and modulus, and according stability against addition of food ingredients and externally applied temperatures and pressures.

It is envisioned that the results of this thesis will provide a basis for future studies on microbubbles by means of the reported insights in key parameters and their values.

## References

1. J. Benjamins, A. Sein, and C. van Vliet United States of America Pat., 2002, patent nr US2002/0155208.
2. M. J. Borrelli, W. D. O'Brien, L. J. Bernock, H. R. Williams, E. Hamilton, J. N. Wu, M. L. Oelze and W. C. Culp, *Ultrasonics Sonochemistry*, 2012, **19**, 198-208.
3. F. Cavalieri, M. Ashokkumar, F. Grieser and F. Caruso, *Langmuir*, 2008, **24**, 10078-10083.
4. F. L. Tchuembou-Magaia, N. Al-Rifai, N. E. M. Ishak, I. T. Norton and P. W. Cox, *Journal of Cellular Plastics*, 2011, **47**, 217-232.
5. F. L. Tchuembou-Magaia and P. W. Cox, *Journal of Texture Studies*, 2011, **42**, 185-196.
6. A. Brotchie, F. Grieser and M. Ashokkumar, *Physical Review Letters*, 2009, **102**.
7. M. F. Zhou, F. Cavalieri and M. Ashokkumar, *Soft Matter*, 2011, **7**, 623-630.
8. J. A. Feshitan, C. C. Chen, J. J. Kwan and M. A. Borden, *Journal of Colloid and Interface Science*, 2009, **329**, 316-324.
9. M. Ashokkumar, *Ultrasonics Sonochemistry*, 2011, **18**, 864-872.
10. D. G. Shchukin and H. Mohwald, *Physical Chemistry Chemical Physics*, 2006, **8**, 3496-3506.
11. J. I. Boye, I. Alli and A. A. Ismail, *Journal of Agricultural and Food Chemistry*, 1996, **44**, 996-1004.
12. B. Jachimska, M. Wasilewska and Z. Adamczyk, *Langmuir*, 2008, **24**, 6866-6872.
13. T. Leong, M. Ashokkumar and S. Kentish, *Acoustics Australia*, 2011, **39**, 54-63.
14. J. Lee, M. Ashokkumar, S. Kentish and F. Grieser, *Journal of the American Chemical Society*, 2005, **127**, 16810-16811.
15. M. W. Grinstaff and K. S. Suslick, *Proceedings of the National Academy of Sciences of the United States of America*, 1991, **88**, 7708-7710.
16. K. S. Suslick, M. W. Grinstaff, K. J. Kolbeck and M. Wong, *Ultrasonics Sonochemistry*, 1994, **1**, S65-S68.
17. S. Avivi and A. Gedanken, *Biochemical Journal*, 2002, **366**, 705-707.
18. E. M. Dibbern, F. J. J. Toublan and K. S. Suslick, *Journal of the American Chemical Society*, 2006, **128**, 6540-6541.
19. T. Chakraborty, I. Chakraborty, S. P. Moulik and S. Ghosh, *Langmuir*, 2009, **25**, 3062-3074.
20. C. Hoffmann, A. Blume, I. Miller and P. Garidel, *European Biophysics Journal with Biophysics Letters*, 2009, **38**, 557-568.
21. S. Makino, S. Ogimoto and S. Koga, *Agricultural and Biological Chemistry*, 1983, **47**, 319-326.
22. A. D. Nielsen, K. Borch and P. Westh, *Biochimica Et Biophysica Acta-Protein Structure and Molecular Enzymology*, 2000, **1479**, 321-331.
23. J. T. Foster, in *Albumin: Structure, Function and Uses*, eds. V. M. Rosenoer, M. Oratz and M. A. Rothschild, Pergamon Press, Oxford, 1977, pp. 53-84.
24. L. G. C. Pereira, O. Theodoly, H. W. Blanch and C. J. Radke, *Langmuir*, 2003, **19**, 2349-2356.
25. J. Jose, M. Kamp, A. van Blaaderen and A. Imhof, *Langmuir*, 2014, **30**, 2385-2393.



26. M. B. J. Meinders and T. van Vliet, *Advances in Colloid and Interface Science*, 2004, **108**, 119-126.
27. J. J. Kwan and M. A. Borden, *Advances in Colloid and Interface Science*, 2012, **183-184**, 82-99.
28. W. C. Young, *Roark's formulas for stress & strain*, McGraw-Hill Book Company, 1989.
29. E. Buchner Santos, J. K. Morris, E. Glynos, V. Sboros and V. Koutsos, *Langmuir : the ACS journal of surfaces and colloids*, 2012, **28**, 5753-5760.
30. F. Cavalieri, J. P. Best, C. Perez, J. Tu, F. Caruso, T. J. Matula and M. Ashokkumar, *Acs Applied Materials & Interfaces*, 2013, **5**, 10920-10925.
31. A. Tobitani and S. B. Ross-Murphy, *Macromolecules*, 1997, **30**, 4845-4854.
32. T. Hagiwara, H. Kumagai and T. Matsunaga, *Journal of Agricultural and Food Chemistry*, 1997, **45**, 3807-3812.
33. Z. Li, M. Xiao, J. Wang and T. Ngai, *Macromol. Rapid Commun.*, 2013, **34**, 169-174.
34. P. Nuthong, S. Benjakul and T. Prodpran, *Food Hydrocolloids*, 2009, **23**, 736-741.
35. M. Lee, E. Y. Lee, D. Lee and B. J. Park, *Soft matter*, 2015, **11**, 2067-2079.
36. G. Sala, T. van Vliet, M. A. C. Stuart, G. A. van Aken and F. van de Velde, *Food Hydrocolloids*, 2009, **23**, 1381-1393.
37. C. van der Poel, *Rheologica Acta*, 1958, **1**, 198-205.
38. D. Kilcast and S. Clegg, *Food Quality and Preference*, 2002, **13**, 609-623.
39. M. Minor, M. H. Vingerhoeds, F. D. Zoet, R. De Wijk and G. A. Van Aken, *International Journal of Food Science & Technology*, 2009, **44**, 735-747.
40. H. Wildmoser, J. Scheiwiller and E. J. Windhab, *LWT - Food Science and Technology*, 2004, **37**, 881-891.



# Summary

---

Aeration of food is considered to be a good method to create a texture and mouthfeel of food products that is liked by the consumer. However, traditional foams are not stable for a prolonged time. Microbubbles are air bubbles covered with a shell that slows down disproportionation significantly and arrests coalescence. Protein stabilized microbubbles are seen as a promising new food ingredient for encapsulation, to replace fat, to create new textures, and to improve sensorial properties of foods. In order to explore the possible functionalities of microbubbles in food systems, a good understanding is required regarding the formation of protein stabilized microbubbles as well as their stability in environments and at conditions encountered in food products. The aim of this research was to investigate the key parameters for applications of microbubbles in food systems. In *Chapter 1* an introduction to this topic is given.

In *Chapter 2*, the effect of the microbubble preparation parameters on the microbubble characteristics, like the microbubble yield, size and stability, was investigated. The protein bovine serum albumin (BSA) and the method sonication was used to manufacture the microbubbles. The manufactured number and stability of microbubbles was highest when they were prepared at a pH around 5 to 6, just above the isoelectric point, and at an ionic strength of 1.0 M. This can be related to the protein coverage at the air/water interface of air bubbles formed during sonication. At a pH close to the isoelectric point the BSA molecules is in its native configuration. Also the repulsion between the proteins is minimized at these pH values and ionic strength. Both the native configuration and the limited repulsion between the proteins result in an optimal protein coverage during the first part of sonication. Also a high protein concentration contributes to a higher surface coverage. The surface coverage is proportional to the protein concentration up to a concentration of 7.5% after which an increase in protein concentration did not lead to a substantial increase in the number of microbubble . In the second part of sonication the protein layer around the air bubble becomes thicker and stronger by heat induced protein-protein interactions. We found that and at a preheating temperature of 55-60°C, about 5 °C below the BSA denaturation temperature, and a

final solution temperature of 60-65°C most microbubbles were obtained, while at higher temperatures mainly protein aggregates and (almost) no microbubbles are formed. This suggests that at temperature of around 60°C to 65°C protein aggregated mostly at the air-water interface creating a multi-layered shell, while at higher temperature, they also aggregated in bulk. These aggregates cannot form microbubbles. We found that optimal preparation parameters strongly depend on the protein batch. We hypothesize that the differences in microbubble formation between the protein batches is due to (small) differences in the protein molecular and denaturation properties that determine the temperature at which the molecules start to interact at the air-water interface. Microbubbles made with different protein concentration and preheating temperatures shrunk in time to a radius between 300 nm and 350 nm, after which the size remained constant during further storage. We argue that the driving force for the shrinkage was the Laplace pressure, resulting in an air flux from the bubbles to the solution. We argue that the constant final size can be explained by a thickening of the microbubble shell as a result of the microbubble shrinkage, thereby withstanding the Laplace pressure.

In *Chapter 3* and *Chapter 4*, microbubble stability at environments and conditions representative for food products were studied. In *Chapter 3* we investigated the stability upon addition of surfactants and acid. When surfactants or acid were added, the microbubbles disappeared in three subsequent steps. The release of air from the microbubble can be well described with the two-parameter Weibull process. This suggests two processes are responsible for the release of air: 1) a shell-weakening process and 2) a random fracture of the weakened shell. After the air has been released from the microbubble the third process is identified in the microbubble disintegration: 3) the shell disintegrated completely into nanometer-sized particles. The probability of fracture was exponentially proportional to the concentration of acid and surfactant, meaning that a lower average breaking time and a higher decay rate were observed at higher surfactant or acid concentrations. For different surfactants, different decay rates were found. The disintegration of the shell into monomeric proteins upon addition of acid or surfactants shows that

the interactions in the shell are non-covalent and most probably hydrophobic. After surfactant addition, there was a significant time gap between complete microbubble decay (release of air) and complete shell disintegration, while after acid addition the time at which the complete disintegration of the shell was observed coincided with the time of complete microbubble decay.

In *Chapter 4* the stability of the microbubbles upon pressure treatment, upon fast cooling after heating and at different storage temperatures was studied. The microbubble stability significantly decreased when microbubbles were pressurized above 1 bar overpressure for 15 seconds or heated above 50°C for 2 minutes. Above those pressures the microbubbles became unstable by buckling. Buckling occurred above a critical pressure. This critical pressure is determined by the shell elastic modulus, the thickness of the shell, and the size of the microbubble. Addition of crosslinkers like glutaraldehyde and tannic acid increased the shell elastic modulus. It was shown that microbubbles were stable against all tested temperatures (up to 120°C) and overpressures (up to 4.7 bar) after they were reinforced by crosslinkers. From the average breaking time at different storage temperatures, we deduced that the activation energy to rupture molecular bonds in the microbubbles shell is 27 kT.

In *Chapter 5*, we investigated the effect of microbubbles on the rheological, tribological and sensorial properties of model food systems and we compared this effect to the effect on food systems with emulsion droplets and food systems without an added colloid. We investigated the effect in three model food systems, namely fluids with and without added thickener and a mixed gelatine-agar gel. In a sensory test panellists were asked whether they could discriminate between samples containing microbubbles, emulsion droplets or no added colloid. Emulsions could be sensorially well distinguished from the other two samples, while the microbubble dispersion could not be discriminated from the protein solution. Thus, we concluded that at a volume fraction of 5% of these BSA covered microbubbles were not comparable to oil-in-water emulsions. The good

discrimination of emulsion might be ascribed to the fact that emulsions had a lower friction force (measured at shear rates from 10 mm/s to 80 mm/s) than that microbubbles dispersions and protein solutions. Upon mixing emulsions and microbubble dispersions the friction value approximated that of emulsions. This effect was already noticed at only 1.25% (v/v) oil, indicating that microbubbles had not a significant contributions to the friction of these samples. Also microbubble dispersions with and without protein aggregates were compared. The microbubble dispersions with and without thickener containing protein aggregates had a higher viscosity than the those samples without protein aggregates. Protein aggregates in the gelled microbubble sample yielded a higher Young's modulus and fracture stress. The differences between the gelled samples could be well perceived by the panellists. We attribute this mainly to the fracture properties of the gel. In general we concluded that microbubbles, given their size of  $\sim 1 \mu\text{m}$  and volume fraction of 5%, did not contribute to a specific mouthfeel.

Finally in *Chapter 6* the results presented in the previous chapters are discussed and put in perspective of the general knowledge on microbubbles production, stability, and applications in food. We described the main mechanisms leading to microbubble formation and stability. We showed that the production parameters significantly influence the interactions in the microbubble shell, and the those interactions highly determine the stability of the microbubbles under several conditions. We reported about limitations of sonication as a method to produce microbubbles suitable for food applications and we provided some ways to overcome these limitations. The use of microbubbles in food systems has been explored and we clearly see possible applications for microbubbles in food. We reported about directions for possible further research.

In this work we made significant progress in understanding the interactions in the microbubble shell and their relation to microbubble stability. We also advanced in comprehension towards possible applications of microbubbles in food.





# Acknowledgements

---

This thesis is the final step on a path which I have walked for about four years. Some parts of this path I walked with ease, some other parts were much harder, but in the end I am happy with every single step I made. I am feeling blessed that I was surrounded by so many people that contributed to all the steps along the way. Here I would like to take the opportunity to thank some of them personally. Since the list of persons who contributed to this thesis is simply too long, it is inevitable that some names will be omitted, for which I express my apologies.

First and above all, I would like to express my gratitude to my co-promoters, Guido and Marcel, who helped me and taught me so much. Guido, you helped me to critically think, to set-up proper experiments and above all how to write my findings down in a concise way. Although the number of comments were sometimes a bit overwhelming, in the end am very grateful for all the effort you took to make sure the end result was always satisfying. Marcel, I want to thank you for your patience in explaining some physical concepts over and over again and for always looking for what is present in the data rather than what is lacking. Without your help this thesis would not be here. I am also very grateful to my promotor Erik. Your positive attitude and your belief that all data would fit nicely together always motivated me enormously.

I gratefully acknowledge the members of the TIFN Foam Project. First of all, Franklin I really appreciate all your support and help in the lab, which was the basis for this thesis. I want to thank all the other members, Christian, Frederik, Min, Peter, Hans, Ruud and Erik for their fruitfully contributions and lively discussions.

I am really happy that during my research I was surrounded by my great colleagues from the Food Physics group. In the first two years I shared an office with Vaida, Carsten and Claire on the 7th floor of the Biotechnion. It was really nice that we started together and that we followed the path as a PhD together, as well. After two years the group moved to the Axis building, where I shared my office with Anika, Auke, Kun and Maria. I could not have wished for better room-mates. I truly enjoyed our lively chats and the laughs we shared. Pauline and Jacob, the biggest laughs I shared with you, since you have the same kind of humour as I have. Furthermore, we also had a lot of good talks. I feel honoured to have such good colleagues by my side during my defense. I would like to thank the other PhDs and post-docs Alev, Jinfeng, Jissy, Laura, Lenka and Zhili for their nice company. I will cherish the good moments we had together: the PhD-trip to the US and Canada, the chats during the lunch breaks, our labuitjes and our weekends away in Germany and in Maastricht. Furthermore, I also want to thank Ardy, Nam-Phuong, Dilek, Elisabete, Jerome, Silvia, Costas and Diana. Although the time we spent together as colleagues was shorter, I enjoyed your company. Harry, Miranda and Eefjan, I would like to thank you for all your support in the lab. I would like to gratefully acknowledge Leonard, Paul and Elke for our discussions, regarding my research, as well as other topics. Els, I will miss the uncountable times I walked into your office just to have a chat or to having some paper work arranged. Finally, I want thank all the students which contributed to this thesis. Bas, Anne, Linda, Andre, Nick, Michiel, Marjolein, Chenxi, Wilbert, Thomas, Ilona, Anke, Casper, Martin and Dimitris, it was a pleasure supervising you. I learned a lot from you and I hope you also learned a bit from me.

Several persons helped me for specific parts of my research. I want to express my gratitude to Jan for sharing the information regarding protocols to prepare microbubbles. I am grateful to Kees for his technical support in beginning of my project. I want to thank Tiny for getting the nice SEM pictures. I would like to acknowledge Jaap, Nick and Franklin for their help in making the food-grade microbubbles and the samples for the sensory test.

Buiten werktijd was er gelukkig ook tijd om te ontspannen. Deze ontspannende momenten met vrienden en familie zijn ontzettend waardevol voor me.

Ik wil mijn vrienden die ik nog ken uit mijn studententijd bedanken voor het fijne contact dat we nog steeds hebben. Anja, Erwin en Karin, Carla, jullie zijn hele fijne vrienden, met jullie was het altijd gezellig en jullie hadden oprecht interesse in datgene wat ik aan het doen was. Ook de gezellige momenten met de andere ouwe-lullen van Shinto, Mirjam, Elske, Mark, Lennart, Gerdien, Lotte, Loes en Caroline zal ik koesteren. Met mijn jaarclubgenoten, Anja, Bram, Teije, Joris, Fedor, Enna, Irene, Ylvie, Guido en Marcus, heb ik mooie barbecues, spelletjes-avonden en nog ontelbaar meer mooie momenten beleefd en ik hoop dat daar nog ontelbare momenten bijkomen. Als laatste wil ik graag Marianne en Niels bedanken met wie ik (vaak samen met Teije) een heel scala aan leuke activiteiten, gezellige momenten en mooie gesprekken heb beleefd, wat een positief effect op mijn humeur opleverde.

Waar mijn agenda redelijk flexibel was, stond één moment in de week altijd vast. Elke dinsdagavond was gereserveerd voor de pubquiz. Harry, Henny, Elke en Martijn, bedankt voor alle gezellige avonden.

Ik wil mijn familie bedanken voor hun steun en vertrouwen. Pieter, Eefke, Diana, Maarten, Dani en Kyan, jullie waren er altijd voor mij en jullie zorgden ervoor dat het altijd gezellig thuiskomen was. Ten slotte, papa en mama, bedankt voor de onvoorwaardelijke steun en vertrouwen in alles wat ik doe.

Thanks all!

A handwritten signature in black ink, appearing to read 'Tij's'. The letters are stylized and connected, with a long horizontal stroke extending from the bottom of the 'j'.

## List of publications

T.A.M. Rovers, G. Sala, E. van der Linden and M. B.J. Meinders (2016) Temperature is key to yield and stability of BSA stabilized microbubbles, *Food Hydrocolloids*, 52, 106-115

T.A.M. Rovers, G. Sala, E. van der Linden and M. B.J. Meinders (2015) Disintegration of protein microbubbles in presence of acid and surfactants: a multi-step process, *Soft Matter*, 11, 6403-6411

T.A.M. Rovers, G. Sala, E. van der Linden and M. B.J. Meinders (2015) Effect of temperature and pressure on the stability of protein microbubbles, *To be submitted*

T.A.M. Rovers, G. Sala, E. van der Linden and M. B.J. Meinders (2015) Effect of microbubbles on rheological, tribological and sensorial properties of model food systems, *To be submitted*

## **Curriculum vitae**

Tijs Rovers was born on March 26<sup>th</sup> 1983 in Nijmegen, the Netherlands. After attending elementary school in Schaijk and secondary school in Oss, he started his studies in Business and Consumer Studies at Wageningen University, in 2001. After having obtained a bachelor degree in this field, he started in 2004 his master studies in Food Quality Management at same university, which he successfully completed in 2006. In that year, he started a master studies in Food Technology, also at the Wageningen University, of which he received his diploma in 2008. In 2009 and 2010 he held several temporary positions as a research assistant at the Wageningen University and the Ruhr-Universität Bochum in Germany. In 2011 he was appointed as PhD fellow of Top Institute Food and Nutrition (TIFN) to perform his research at the Physics and Physical Chemistry of Foods group of the Wageningen University. The results of this PhD research are covered in this thesis.

## **Overview of completed training activities**

### **Discipline specific activities**

#### *Courses*

1st Course on Food Structure and Rheology 2012 Wageningen, NL

3rd SoMaS school, Polymers on Interfaces, 2013 Mittelwihr, FR

Sustainability Analysis in Food and Biobased Production, 2014 Wageningen, NL

#### *Conferences*

Microbubble symposium, 2011, Leeds, UK

6th International Symposium on Food Rheology and Structure, 2012 Zürich, CH

14th European Student Colloid Conference, 2013, Potsdam, DE

1st Food Structure and Functionality Forum Symposium, 2014, Amsterdam, NL

15th Food Colloids Conference, 2014, Karlsruhe, DE

7th International Symposium on Food Rheology and Structure, 2015 Zürich, CH

### **General courses**

VLAG PhD week, 2011, Baarlo, NL

Course basic intellectual property, 2012 Wageningen, NL

Scientific Writing, 2012, Wageningen, NL

Philosophy and Ethics of Food Science and Technology, 2014, Wageningen, NL

Voice Matters - Voice and Presentation Skills Training, 2014 Wageningen, NL

Career Perspectives, 2014 Wageningen, NL

### **Optional courses and activities**

Organized and participated in PhD trip, 2014, USA and Canada

Food physics group, science meetings, 2011-2015, Wageningen, NL

TIFN Foam project, team meetings, 2011-2015, Wageningen, NL

The research described in this thesis was financially supported by Top Institute Food & Nutrition.

Financial support from Wageningen University and Top Institute Food & Nutrition for printing this thesis is gratefully acknowledged.

Cover design: Tijs Rovers

Printed by: Ridderprint B.V, Ridderkerk, NL